TECHNISCHE UNIVERSITÄT WIEN
Vienna | Austria

Diploma Thesis

DESIGN AND OPTIMIZATION OF A MULTIENZYMATIC CASCADE TOWARDS FRAGRANCE ALDEHYDES

Conducted to obtain the academic degree: **Master of Science (MSc.)**

Under the supervision of:

ASSOC. PROF. DIPL.-ING. DR.TECHN. FLORIAN RUDROFF

Institute of Applied Synthetic Chemistry

Submitted at:

TU WIEN

Faculty of Technical Chemistry

By:

MAXIMILIAN WUTSCHER

[redacted]

Some smart citation

-Author

Acknowledgements

Acknowledgements

Table of content

Abstract

Aromatic aldehydes bear many applications in industry, such as utilization as flavourings or as fragrance ingredients for perfumes and cosmetics. They also show valuable properties as intermediates for chemical synthesis of pharmaceuticals. Some prominent examples are Vanillin, which is the main ingredient in vanilla extract, or benzaldehyde which is used to produce almond or cherry flavourings. However, industrial production of fragrance aldehydes often involves the use of petrochemicals or toxic chemicals as precursors. Furthermore, the processes associated have a high energy demand and thus a high carbon footprint. Green processes towards the production of fragrance have not been yet widely adopted due to lack of competitiveness or applicability. Herein an expansion of the applicability of a previously developed enzymatic cascade towards the synthesis of aromatic fragrance aldehydes from phenylpropenes is presented.

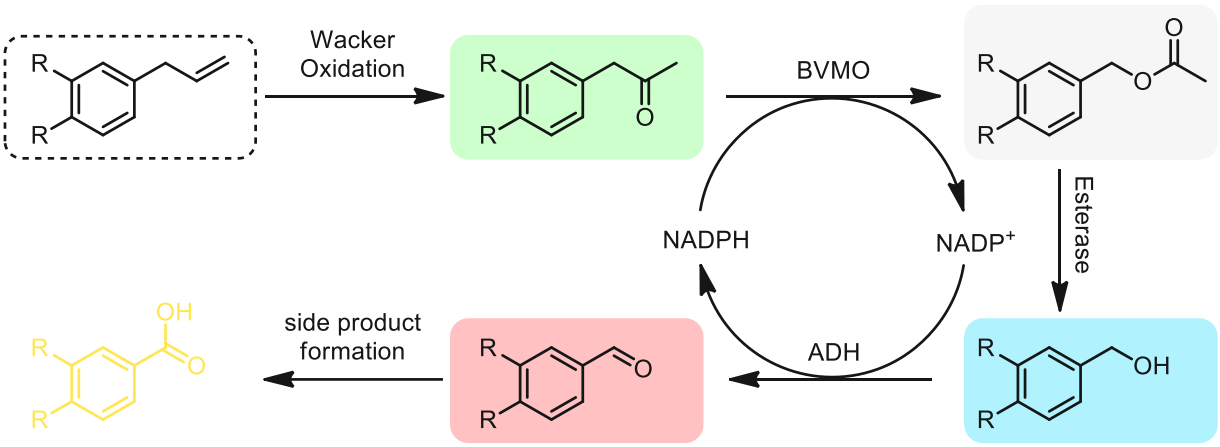

Figure 1: Bioenzymatic cascade from phenylpropenes towards aromatic aldehydes, BVMO: Baeyer Villiger monooxygenase, ADH: alcohol dehydrogenase

The previously *in vivo* established chemoenzymatic cascade uses a Wacker oxidation to transform naturally occurring phenylpropenes into ketones, then in a series of enzymatic transformations, including a Baeyer Villiger monooxygenase (BVMO), an esterase and an alcohol dehydrogenase (ADH), affords the corresponding aldehydes. Unfortunately, it was majorly affected by side product formation due to over oxidation of the aldehydes towards the carboxylic acids. To mitigate the formation of carboxylic acids the enzymes for the cascade were extracted and to do so a suitable ADH was screened out of possible candidates. Further, a shift towards the product side was achieved by addition of an auxiliary substrate. The scope of the reaction sequence was demonstrated on eight natural and non-natural 2-propenylbenzenes, yielding varying amounts of the respective aldehydes.

Kurzfassung

Aromatische Aldehyde finden in der Industrie zahlreiche Anwendungen, z. B. als Aromastoffe, als Duftstoffe für Parfüms und Kosmetika. Sie weisen auch wertvolle Eigenschaften als Zwischenprodukte für die chemische Synthese von Arzneimitteln auf. Einige prominente Beispiele sind Vanillin, der Hauptbestandteil von Vanilleextrakt, oder Benzaldehyd, das zur Herstellung von Mandel- oder Kirscharomen verwendet wird. Bei der industriellen Herstellung von Duftstoffaldehyden werden jedoch häufig Petrochemikalien oder giftige Chemikalien als Ausgangsstoffe verwendet. Darüber hinaus haben die damit verbundenen Prozesse einen hohen Energiebedarf und damit einen großen CO_2-Fußabdruck. Umweltfreundliche Verfahren zur Herstellung von Duftstoffen werden aufgrund mangelnder Wettbewerbsfähigkeit oder Anwendbarkeit noch nicht in großem Umfang eingesetzt. In dieser Arbeit wird eine Erweiterung der Anwendbarkeit einer zuvor entwickelten enzymatischen Kaskade für die Synthese aromatischer Duftaldehyde aus Phenylpropenen vorgestellt.

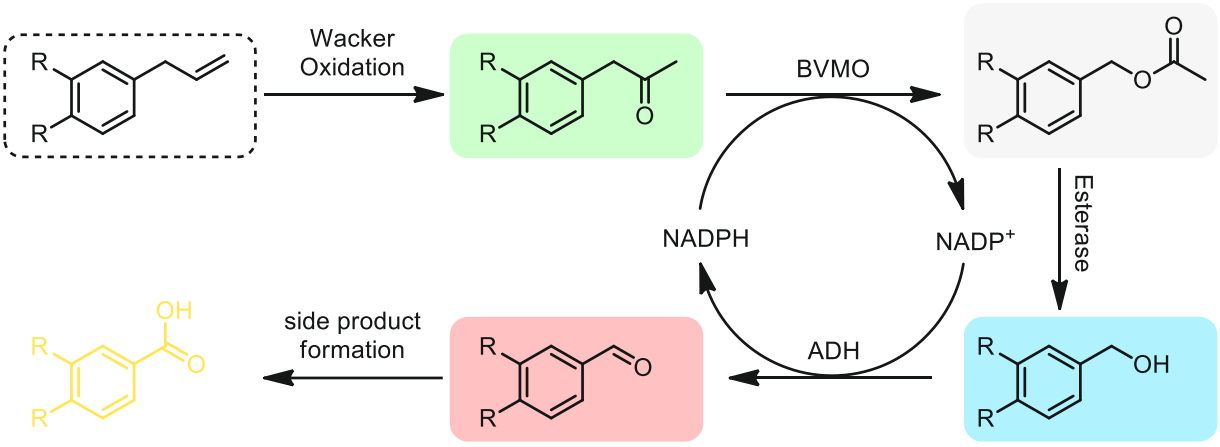

Figure 2: Bioenzymatische Kaskade von Phenylpropenen zu aromatischen Aldehyden, BVMO: Baeyer Villiger Monooxygenase, ADH: Alkohol Dehydrogenase

Die zuvor *in vivo* etablierte chemoenzymatische Kaskade nutzt eine Wacker-Oxidation, um natürlich vorkommende Phenylpropene in Ketone umzuwandeln, aus denen dann in einer Reihe von enzymatischen Transformationen, durch eine Baeyer Villiger Monooxygenase (BVMO), eine Esterase und eine Alkohol Dehydrogenase (ADH), die entsprechenden Aldehyde entstehen. Leider wurde sie durch die Bildung von Nebenprodukten aufgrund der Überoxidation der Aldehyde zu Carbonsäuren stark beeinträchtigt. Um die Bildung von Carbonsäuren abzuschwächen, wurden die Enzyme für die Kaskade extrahiert und dazu eine geeignete Alkoholdehydrogenase aus möglichen Kandidaten gescreent. Des Weiteren wurde durch Zugabe eines Hilfssubstrats eine Verschiebung des Reaktionsgleichgewichts zur Produktseite erreicht. Die Anwendungsreichweite der Reaktionssequenz wurde an acht natürlichen und nicht natürlichen 2-Propenylbenzolen getestet, welche unterschiedliche

Ausbeuten der jeweiligen Aldehyde ergaben.

Abbreviations

µg	microgram
µl	microliter
µM	micromolar
abs.	absolute
ACN	acetonitrile
ADH	alcohol dehydrogenase
amp	ampicillin
APS	ammonium persulfate
BCA	bicinchoninic acid
bp	basepair
BSA	bovine serum albumin
BVMO	Baeyer Villiger monooxygenase
cAMP	cyclic adenosine monophosphate
CFE	cell free extract
DNA	deoxyribonucleic acid
dNTPs	deoxynucleotide triphosphates
ds	double stranded
E. coli	*Escherichia coli*
EDTA	ethylenediaminetetraacetic acid
etc.	et cetera
EtOAc	ethyl acetate
EtOH	ethanol
FAD	flavin adenin dinucleotide
fwd	forward
g	gram
GC	gas chromatography
GDH	glucose dehydrogenase
GST	glutathione S-transferase
h	hours
His	histidine
HLADH	horseliver alcohol dehydrogenase
HPLC	high performance liquid chromatography
IMAC	immobilized metal affinity chromatography

IPTG	isopropyl-β-d-1-thiogalactopyranoside
KAN	kanamycin
kDa	kilodalton
KLD	kinase, ligase, dpnI enzymes
L-Ara	L-arabinose
LB	lysogeny broth
L-Rha	L-rhamnose
m	multiplet
mg	milligram
MHz	megahertz
min	minutes
ml	milliliter
mM	millimolar
mmol	millimole
MOPS	3-(N-morpholino) propanesulfonic acid
Mut	Mutation
NAD^+ (NADH)	nicotinamide adenine dinucleotide (reduced)
$NADP^+$ (NADPH)	nicotinamide adenine dinucleotide phosphate (reduced)
ng	nanogram
nm	nanometer
NMR	nuclear magnetic resonance
NTA	Nitriloacetic acid
OD_{590}	optical density at 590 nm
ORI	origin of replication
PAGE	polyacrylamide gel electrophoresis
PAMO	phenylacetone monooxygenase
PBS	phosphate buffer saline
PCR	polymerase chain reaction
PDH	polyol dehydrogenase
pH	potential of hydrogen
PMSF	phenylmethylsulfonyl fluoride
PTFE	polytetrafluoroethylene
R	organic residue
RCF	relative centrifugal field
rev	reverse
rpm	revolutions per minute

RT	room temperature
s	singlet
SDS	sodium docecyl sulfate
SEC	size exclusion chromatography
SOC medium	super optimal broth medium with catabolite repression
T_a	annealing temperature
TAE	tris-acetate EDTA
TB	terrific broth
TEMED	N, N, N', N', Tetramethylethylenediamine
TFA	Trifluoroacetic acid
TLC	thin layer chromatography
T_m	melting temperature
TU	technical university
UV	ultraviolet
v	volume
w	weight
x g	relative centrifugal force

Compound Library

1a-8a: 2-propenylbenzenes (substrates for Wacker oxidation)

1b-8b: Phenylpropanones (substrates for BVMOs)

1c-8c: Benzylacetates (substrates for esterases)

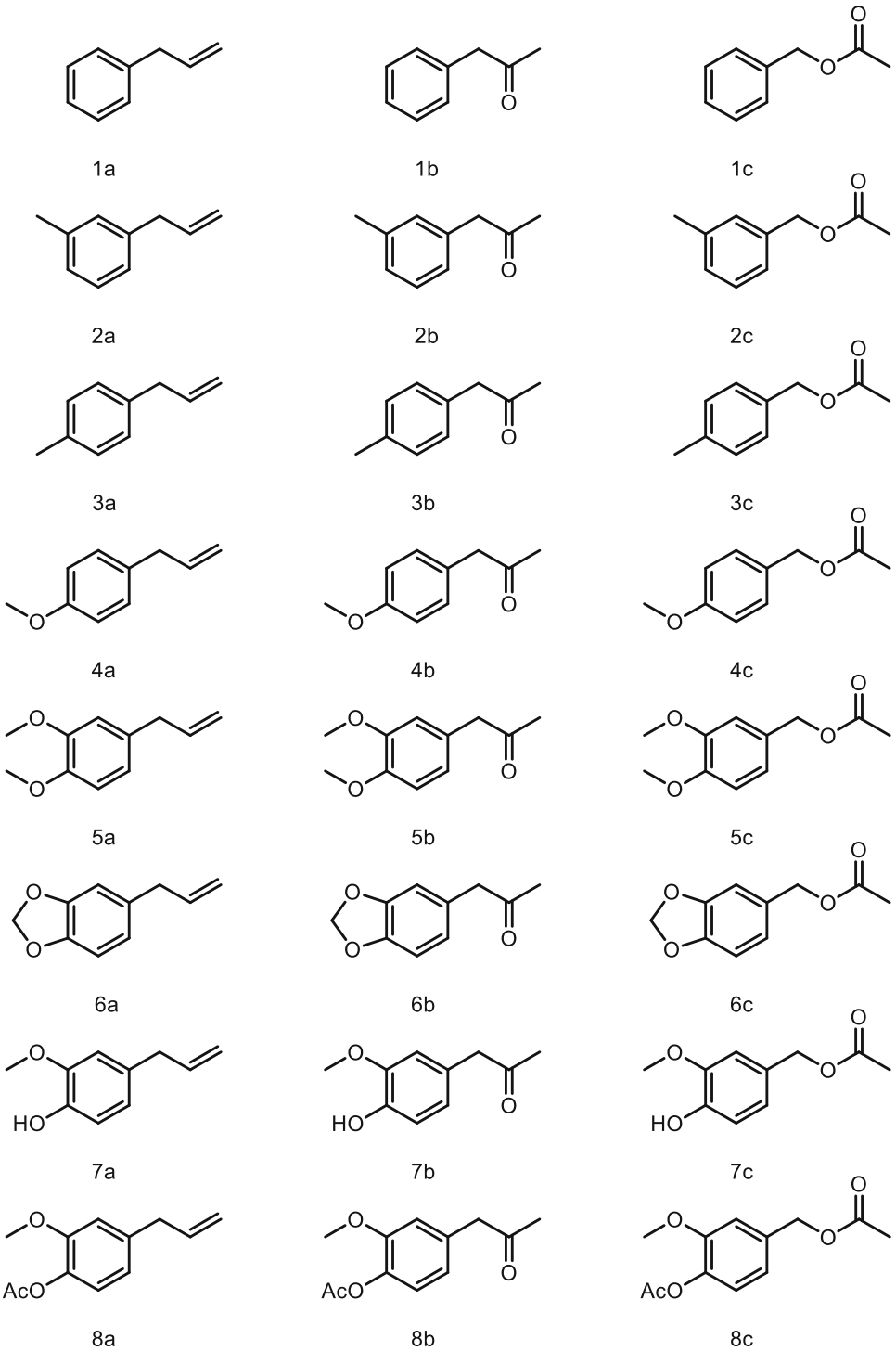

1d-8d: Benzylalcohols (substrates for ADHs)

1b-8b: Benzaldehydes (products of biocatalytic cascade)

1c-8c: Benzoic acids (sideproducts of biocatalytic cascade)

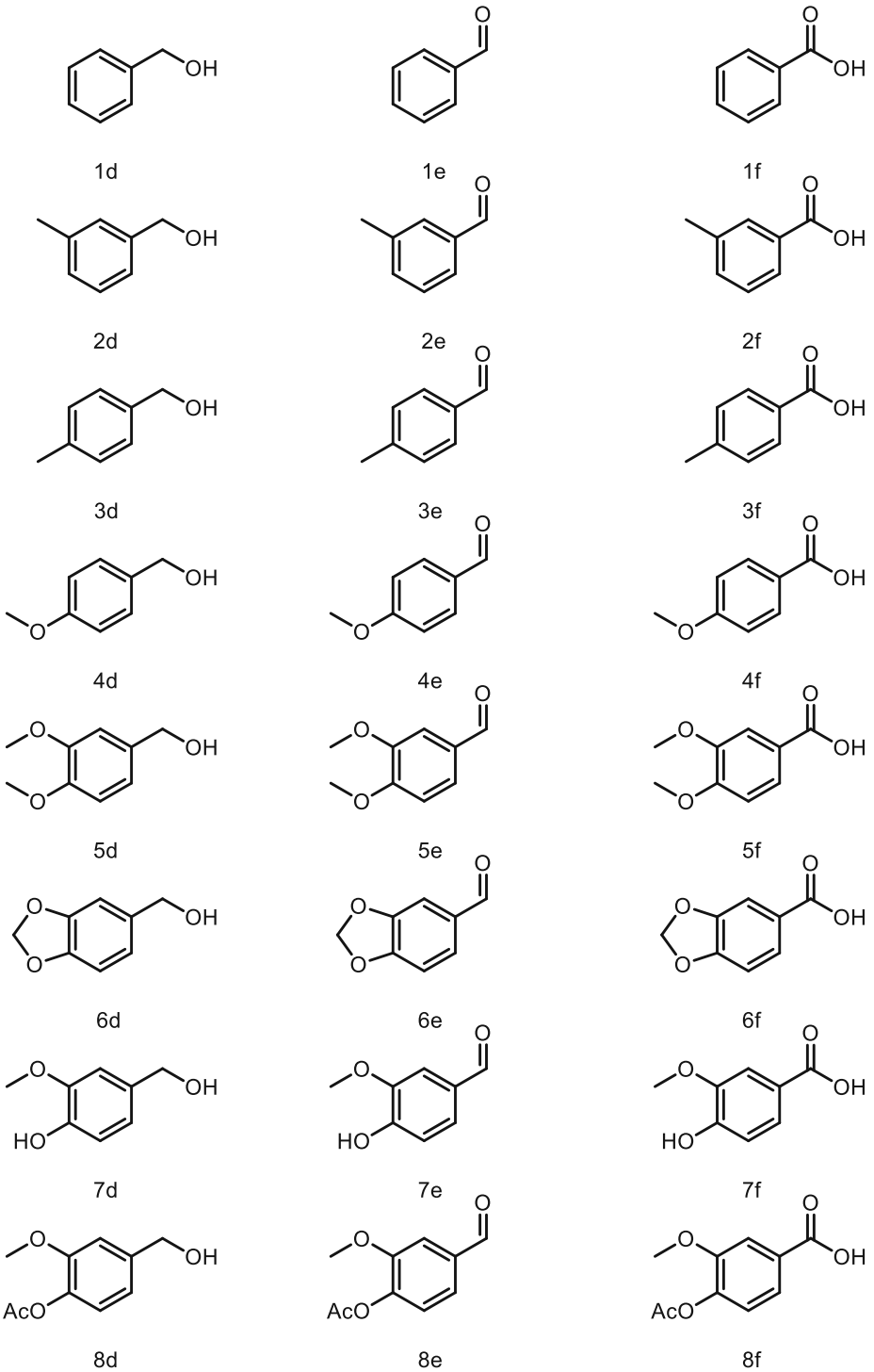

A. Introduction

A.1. The evolution of biocatalysis

Biocatalysis can be defined as the application of enzymes in their purified form, in the form of a cell lysate or whole cells to transform a molecular substrate into a product.[1] It has found its first utilizations as early as in the ancient Mesopotamia, China and Japan for the production of food and alcoholic beverages. This commonly known fermentation process was state of the art until the early 19th century one of the first observations was made by Kirchhoff who discovered a glutinous wheat component capable of transforming starch into sugar.[2] This discovery lead to the insight that not the whole living cell is needed to be applied for a useful biocatalytic transformation, but rather single components of the cells. Further investigations lead to the identification of a new class of isolated active components which was named by Kühne: Enzymes. One of the key characteristics of enzymes was discovered to be specificity by Emil Fischer in the late 19th century who also deduced the well-known picture of "lock and key". Furthermore, he stated that enzymes were in fact proteins, but his hypothesis could not be proven until the early 20th century when Sumner showed proof by the crystallization of Urease.[3] With industrial production progressing at fast pace soon an economic question arose: can enzymes be re-used? To be able to answer that we have to apply two of the most important accomplishments for enzyme research: the exploration and understanding of the protein-structure, but also the comprehension of nucleic acids as hereditary units and carriers of biological information.[2] A viable approach to this economic endeavour was started in the 1950s by several groups who developed methods to immobilize enzymes onto solid supports. This approach offers all the advantages of classical heterogenous catalysis such as separation by filtration or centrifugation, application in continuous processes, in fixed beds, fluidized beds, stirred tanks etc.[2] Combined with the advanced biocatalysts yield, such as lack of energy intensive processing, biodegradability, low toxicity, and low production costs a powerful a renewable class of catalysts was born. This era in the history of enzymatic transformations is known as the "first wave of biocatalysis".[4]

A.2. Modern biocatalysis

From the 1980s onwards, in the so called "second wave of biocatalysis", the substrate range of enzymes could be vastly expanded allowing the (asymmetric) synthesis of unusual and synthetic intermediates for valuable compounds such as pharmaceuticals, herbicides, wax esters, and many more.[4,5] This can be accounted to the advancements made in deoxyribonucleic acid (DNA) sequencing, recombinant DNA technology, bioinformatics and protein engineering which make it possible to identify and synthesize the enzymes with the

most suitable reactivity and selectivity for a given synthetic task.[4,6,7] Further advances were made in biotechnology which allowed the cheap production of enzymes by overexpression implementing recombinant DNA technology in microbial expression hosts.[8] With the work of Pim Stemmer and Frances Arnold in the 1990s the "third wave of biocatalysis" was initiated. With their seminal work on modifying biocatalysts via an *in vitro* version of Darwinian evolution new molecular biology methods were given life to, now commonly known as directed evolution.[4,5] Wildtype enzymes are often not suitable for industrial applications due to unfavourable properties such as substrate specificity, stability, selectivity as well as catalytic efficiency. Directed evolution is a powerful tool to optimize these enzymes towards new functions.

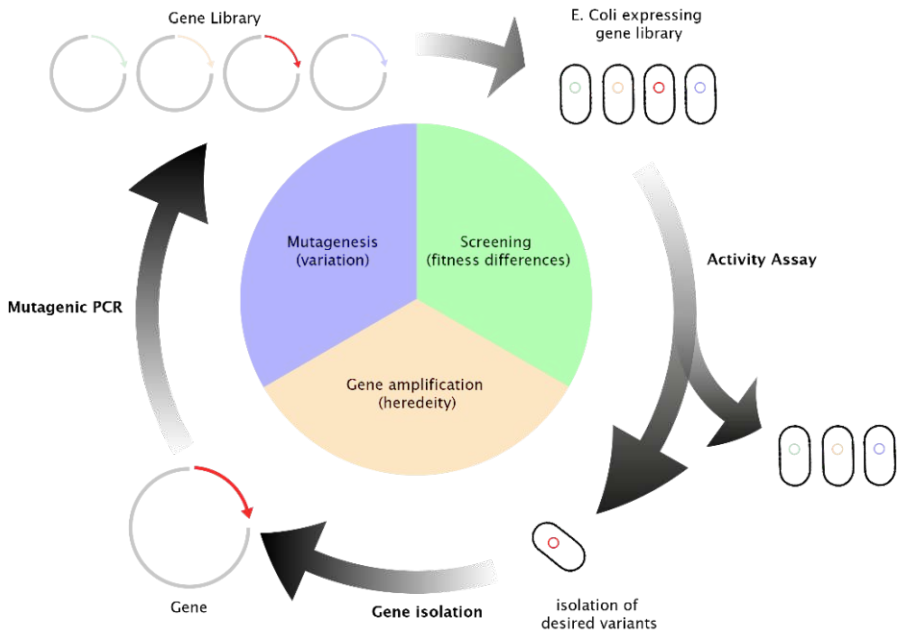

Figure 3: Directed evolution cycle – creation of genetic libraries by random mutagenesis, screening of variants (selection citeria: temperature, pH, solvent, substrates, enantioselectivity, stability), gene amplification

The directed evolution cycle (**Figure 3**) consists of multiple iterations of DNA library design involving random amino acid mutations (mut), gene expression and screening of enzymes in a library. It is possible to optimize multiple properties in parallel and optimized variants can be isolated, characterized and used as starting point for further optimization.[9] Today plenty of methods are available to aid this technology enabling rapid tailored design of enzymes for targeted reactions by combining sequence information and structure databases with modern molecular biology tools and high throughput screening. Furthermore the implementation of novel non-natural reactions into protein scaffolds could be achieved, leading to the emergence of new classes of enzymes all together paving the way for the "fourth wave of biocatalysis" currently in progress.[10]

A.3. Recombinant proteins

With the aforementioned development of recombinant DNA technology and the introduction of PCR scientists had the right tools in hand to explore and understand essential life processes in an easy and straightforward way.[11] For the first time it was possible to propagate eukaryotic DNA in *E. coli* and subsequently active proteins were successfully synthesized from heterologous genes cloned into bacterial plasmids.[12,13] These discoveries opened the door for a plethora of possibilities. While the process seems straightforward, cloning any gene into any given vector and obtaining a functional product is not always an easy task. Many different factors have to be taken into consideration.

The first question that appears is what organism to choose. Available hosts from the reign of microorganisms include bacteria, yeast, filamentous fungi and unicellular algae. They all bring their own repertoire of advantages and disadvantages; the decision has to be made depending on the task. However, the most established organism used for heterologous expression of proteins is still *E. coli*. Thanks to its fast growth kinetics, high density cultures, cheap growth media and rapid easy transformation of exogenous DNA it has been one of the most popular expression hosts over the last decades.[14-16] Although it is a quite remarkable organism, it has its limitations. Shortcomings can be due to high metabolic burden but also aggregation and subsequent denaturation of protein structures can be problematic. Furthermore, since *E. coli* is a prokariotic organism, it is only able to express prokariotic genes. When the gene of interest is of eukariotic nature, the better choice for an expression host would be a yeast.[17]

The second question that arises is the selection of a plasmid. To be able to choose the most suitable plasmid it is crucial to understand the basic building blocks of expression vectors.

(**Figure 4**). The units which make up a plasmid will be discussed in the next sections in detail.

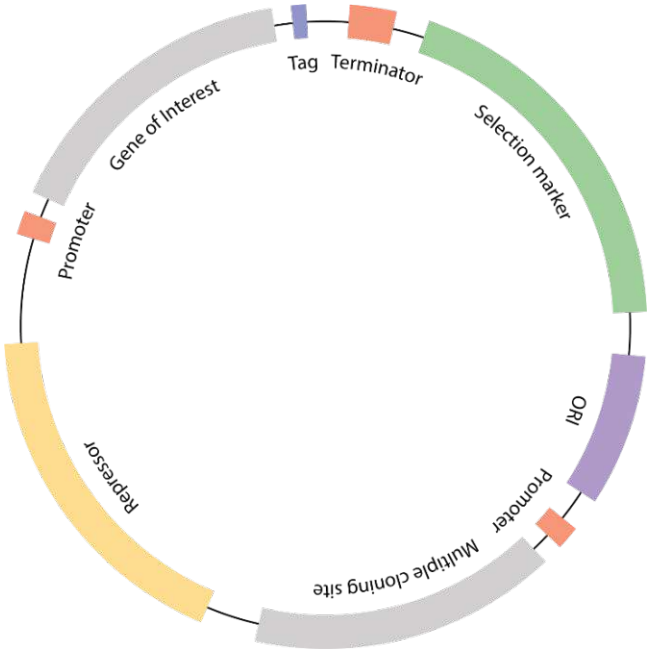

Figure 4: Typical building blocks of an expression vector

A.3.1. Replicon

A fragment of DNA or RNA which is replicated starting from an origin of replication (ORI) is called replicon. When choosing an appropriate vector for a given task an important factor to keep in mind is the copy number, which is dictated by the ORI. A logical assumption would be that the higher the copy amount, the higher the amount of expressed protein is, yet this is not always the case. A high plasmid copy number can impose a high metabolic burden onto the host cells, which can lead to a decrease in healthy organisms for protein production.[17,18] Vectors from the pET series, a frequently used vector type, possess the pMB1 ORI with a copy number of 15 to 60 copies. A mutated version of the pMB1 ORI is present in the pUC series, which has a copy number of 500 to 700 copies per cell. These vectors and many other belong to the same incompatibility group, thus they cannot be expressed at the same time in one cell since they are competing with each other over the replication machinery.[18-20] Multiple recombinant protein expression can be achieved by transforming two compatible vectors, bearing the two genes of interest, into one cell, however this leads to a high metabolic burden for the host resulting in low protein production. To overcome this problem a co-expression vector can be applied. These vectors allow to clone two genes into one plasmid diminishing the metabolic burden. A popular system for co-expression is the Duet vector from Novagen. It contains two multiple cloning sites, each preceded by a T7 promoter, a lac operator and a ribosome binding site.[21,22]

A.3.2. Promoter

A genetic sequence located before a gene which by interaction with specific DNA-binding proteins (transcription factors) can regulate the expression is called a promoter. The expression on a promoter can be controlled (induced) by different factors like media composition, inducer compounds, temperature, pH or ionic concentrations. However the most common way of induction is by inducer compounds.[23]

One of the fundamentals of prokaryotic promoter research is the *lac* promoter. Induction is caused by lactose, however in presence of readily metabolizable carbon sources (e.g. glucose) expression is not fully induced until all the glucose is consumed. As soon as low glucose levels are reached cAMP is produced, and the lac operon completely activated. This type of positive control is also called catabolite repression. A mutant of the lac promoter (lacUV5) was introduced, to be able to achieve expression in the presence of glucose. This promoter is rather weak, however it can be combined with other promoters to exploit the positive features of both at the same time.[24]

Another highly popular promoter is the T7 promoter system applied in pET-systems, due to the system being able to generate up to 50% of the total cell protein in successful cases. This promoter is recognized by the phage T7 RNA polymerase (T7 RNAP) which most commonly is placed in the bacterial genome in a prophage (λ-DE3) encoding for the T7 RNAP controlled transcriptionally by a *lac*UV5 promoter. Induction can be initiated by adding the non-hydrolyzable analogon of lactose isopropyl-β-d-1-thiogalactopyranoside (IPTG). To control basal expression *lacI* can be applied, or T7 lysozyme can be co-expressed which binds to T7 RNAP and inhibits transcription initiation from the promoter. If T7 RNAP is produced by leaky expression, the lysozyme will control unintended expression of heterologous genes under the control of the T7 promoter. After induction to much T7 RNAP is produced for the lysozyme to handle, thus transcription of the recombinant gene is initiated.[16,25]

A.3.3. Selection marker

To be able to distinguish between plasmid-bearing cells and plasmid free cells a selection marker is introduced on the plasmid. Different approaches have been done so far, with antibiotic resistance being the most used type. An example is the *bla* gene (resistance against β-lactam antibiotics), which produces β-lactamase, a periplasmatic enzyme that hydrolyses the β-lactam ring resulting in an inactivation antibiotics like Ampicillin (amp).[26] Due to constant secretion of β-lactamase, the concentration of amp decreases drastically in a couple of hours.

Other types of antibiotics like Chloramphenicol which are degraded by Chloramphenicol-Acetyltransferase face the same problem.[27] To overcome this limitations, antibiotics with resistance not based on degradation but on active efflux of antibiotics out of the cells have been applied. Antibiotics of this type comprise tetracycline or kanamycin (KAN).[28]
Due to the concerns of antibiotic resistance in human pathogens and allergic reactions caused by gene therapy plasmids containing β-lactams, also antibiotic free plasmid systems have been developed. The most common way of achieving antibiotic free selection is by implementing an essential gene into an expression vector and transforming it into a strain with a defect or inhibited expression of the same essential gene. This method is called essential gene complementation.[29]

A.3.4. Affinity tags

When using recombinant proteins, often purification is required. To achieve this in a fast and convenient manner different strategies have been developed. A widely used and very efficient way is to fuse the protein genetically to an affinity fusion partner. These fusion-enzymes can often be purified easily by a single affinity-chromatography step. Today many different types of fusion partners are available, ranging from the size of 1 amino acid to whole proteins capable of selective interaction with an immobilized ligand. Such interactions can be enzyme - substrate, bacterial receptor - serum protein, polyhistidines – metal ion, and antibody – antigen.[30] To choose the best affinity tag for a given task, conditions for purification have to be considered, which differ from system to system. The environment that the protein of interest tolerates is crucial when choosing the right affinity fusion partner.[30] When the protein structure has to be investigated or biochemical studies have to be conducted, tag removal has to be considered as well which can be achieved by enzymatic or chemical cleavage.[16]

After looking at all the factors for a choice of expression vector a third question appears: the choice of an appropriate host strain. There are many candidates available however most of them are designed for very specific tasks and are not required for a first expression screening. The most commonly used lines include BL21(DE3) and some derivatives of the K-12 lines. The most prominent feature of B strains is the deficiency of Lon protease which degrades many foreign proteins and the absence of the outer membrane protease OmpT which degrades extracellular proteins. Additionally, the loss of plasmids can be prevented by the *hsdSB* mutation parental to BL21, resulting in the disruption of DNA degradation and methylation.[31,32]

A.4. Enzyme classification

A.4.1. Baeyer Villiger monooxygenases (BVMOs)

The Baeyer-Villiger reaction was discovered in 1899 by Adolf Baeyer and Victor Villiger. During this oxidation reaction carboxylic compounds are transformed into their corresponding esters or lactones. The Baeyer-Villiger oxidation has proven itself in synthetic organic chemistry as a useful tool for many years. Despite being frequently applied, it comes with limitations such as the lack of selectivity of catalysts and harsh conditions of chemical transformations. Thus, the enzymatic counterparts, Baeyer-Villiger Monooxygenases (BVMOs, EC 1.14.13.x) pose an attractive alternative for synthetic organic chemistry.[33]
BVMOS were first isolated in the 1960s, the first BVMO encoding gene (CHMO) was cloned in 1988. Almost all of the known BVMOs are sequence related to type 1 BVMOs and belong to the subclass B of flavoprotein monooxygenases. They carry flavin adenin dinucleotide (FAD) cofactor as a prosthetic group and use nicotinamide adenine dinucleotide phosphate (reduced) (NADPH) as electron donor.[34]

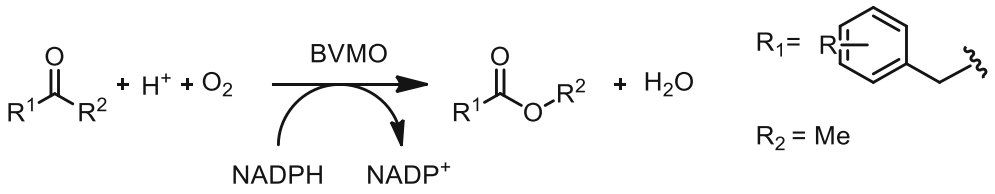

Figure 5: Baeyer-Villiger oxidation of carboxylic compounds catalysed by BVMOs

In the last years many new BVMOS have been discovered by genome mining, most of them present in prokaryotes and some unicellular organisms such as filamentous fungi. Often the natural role of BVMOs is not yet uncovered, usually it is the production of secondary metabolites. BVMOs are known for their low storage and operational stability, most of them operate at neutral pH and room temperature. Nevertheless, in recent years some thermostable examples of BVMOs have been discovered.[35,36]The mechanism for the Baeyer Villiger oxidation catalyzed by BVMOs can be found in **figure 6.**

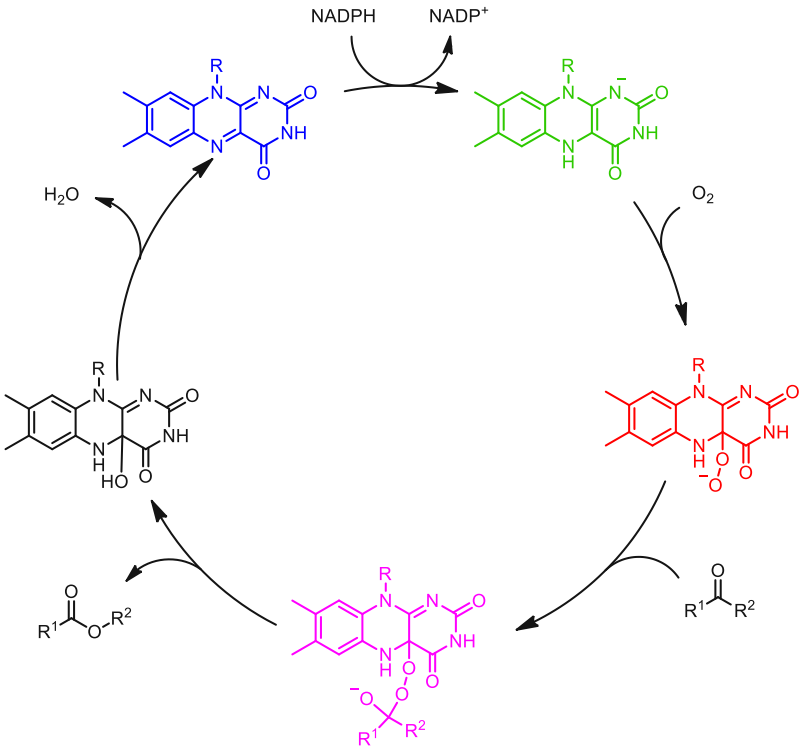

Figure 6.Catalytic cycle of BVMOs, blue oxidized FAD, green reduced FAD, pink Criegee intermediate, red stable peroxyflavin species

BVMO catalysis is initiated by NADPH binding and subsequent reduction of the flavin moiety in its oxidized form (blue) to its reduced form (green). By addition of oxygen the catalytically active species is formed, which consists of a stable peroxyflavin (red). The negatively charged peroxyflavin can now attack a carbonyl and form the tetraedric Criegee intermediate with a weak O-O bond. After heterolytic cleavage of the O-O bond, an alkyl group shifts to an oxygen atom; an ester is formed. Finally, H_2O is cleaved off, the flavin is again in its oxidized form ready to start the cycle again.[33,37]

The tendency of substituents to migrate can generally be predicted by the rules of synthetic Baeyer-Villiger oxidation. Typically, the carbon atom that can best stabilize a cationic charge (the most nucleophilic carbon) will have the highest potential for migration. The outcome of the reaction can also be influenced by stereoelectronic and steric factors. Specifically, the migrating group positioned antiperiplanar to the dissociating O-O of the peroxide bond in the reaction intermediate exhibits the strongest tendency for migration. This orientation allows the best overlap of the C-R_m σ bond with the O – O σ* orbital. Thus, as documented experimentally many times, the following migratory tendency has been established: tert-Bu > Phe ~ iso-Pr > Et > Me. In chemical synthesis, such a tendency is almost never observed, which makes this a valuable feature of BVMOs.[38-40]

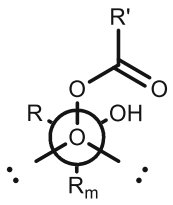

Figure 7: Anti-periplanar orientation of migrating group (R_m) to dissociating O-O bond

A.4.2. Esterases

Carboxylester hydrolases (EC 3.1.1.1) comprise a diverse and extensive group of enzymes that can catalyze the cleavage and formation of carboxyl ester bonds. These enzymes have proven to be useful as biocatalysts due to their stability, high selectivity in terms of chemo-, regio-, or stereoselectivity, and ability to function without organic cofactors. Traditionally, these enzymes have been categorized as either (carboxyl)esterases or lipases based on uncertain experimental data and theoretical hypotheses. Lipases have generally been considered as lipolytic carboxylester hydrolases capable of hydrolyzing water-insoluble esters, releasing long-chain fatty acids (at least 8 carbon atoms), while esterases have been thought to primarily act on water-soluble esters with short-chain acyl residues (less than 8 carbon atoms). In recent years structural insights to the differentiation between the two enzyme classes have been achieved. The main differences lie within the binding sites of the enzymes. Lipases possess a hydrophobic lid, which interacts with the substrate and only changes conformation to an open form when a critical micelle concentration is reached. Esterases do not have this feature, furthermore they differ in shape, deepness and physico-chemical properties of their binding pocket. [41,42]

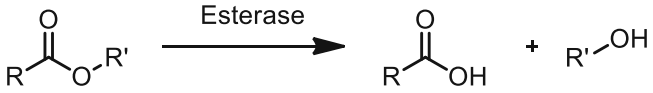

Figure 8: Hydrolysis of carboxylic esters catalysed by esterases

The abilities of esterases have been employed in synthetic organic chemistry for many years. Especially the stereoselective properties are a valuable approach to generate chiral synthons by performing a kinetic racemic resolution.[43] By Kazlauskas rule it is possible to predict which enantiomer of a racemic secondary alcohol reacts faster (for some esterases).[44]

The active site of esterases consists of a combination of acidic and basic amino acid sidechains which is called the Ser-His-Asp catalytic triade and part of the substrate binding site. The catalytic triade occurs in several protein folds such as subtisilin, chymotrypsin and of course the α/β-hydrolase-fold superfamily. The arrangement of residues, typically consisting

of Ser-Asp-His amino acids, facilitates efficient intramolecular hydrogen bond transfer. This arrangement not only stabilizes the transition states but also activates the nucleophile, thereby accelerating the reaction. Most commonly, the oxyanion hole is formed by hydrogen bonds from two main chain N−H's. These bind the carbonyl oxygen and stabilize the oxyanion of the tetrahedral intermediates. The proposed mechanism for the reaction of the catalytic triade is illustrated in **figure 9** and elaborated in the following section.[45]

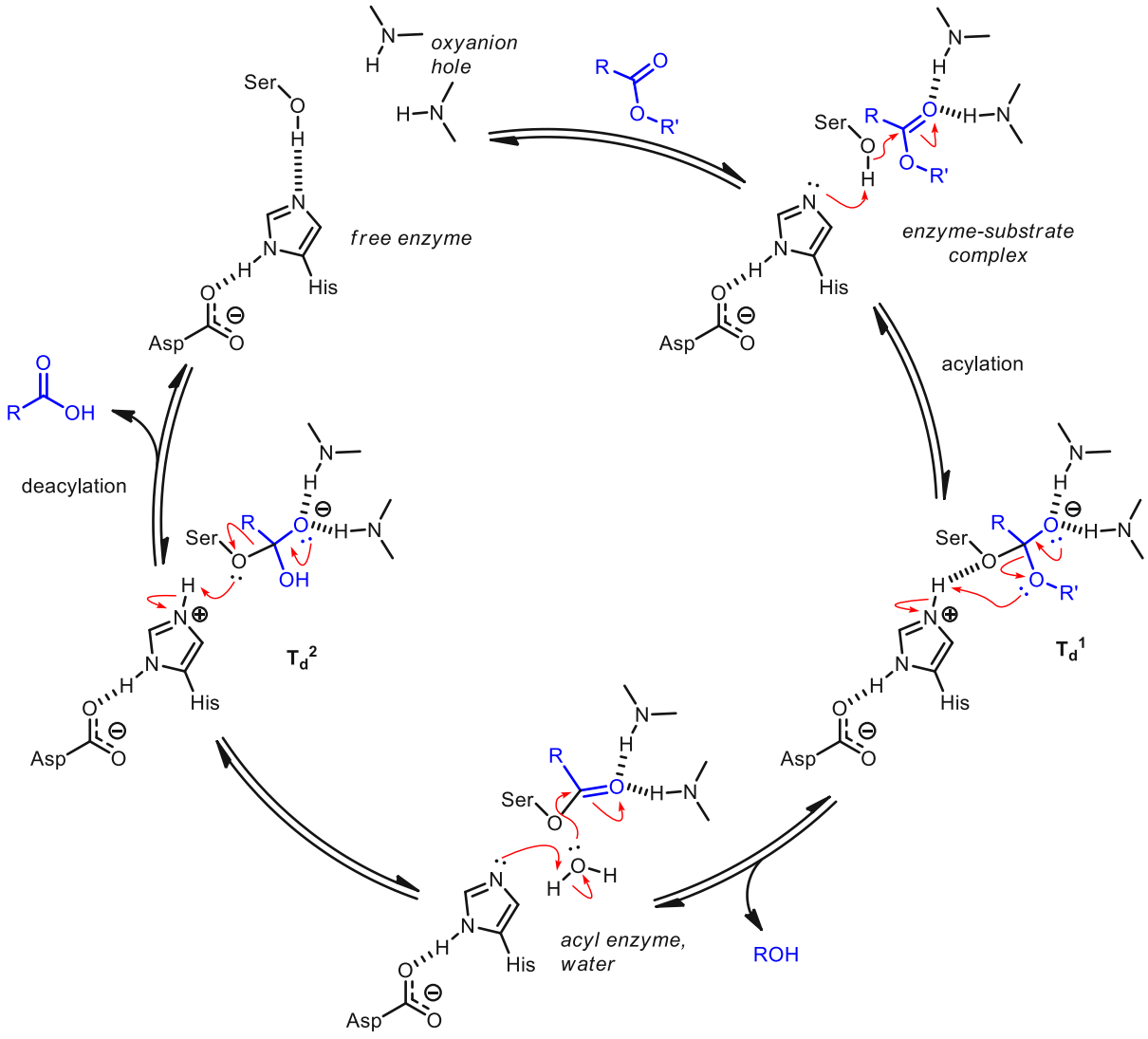

Figure 9: Catalytic mechanism of esterase catalyzed carboxylic ester hydrolysis (adapted image from Rauwerdink et al.[45])

The free enzyme can be seen in the top left structure, the active site contains the catalytic triade (Asp-Ser-His) and the oxyanion hole. In the first step the substrate (a carboxylic ester) is bound in the active site by the oxyanion hole. A nucleophilic attack of serine to the carbonyl carbon affords the first tetrahedral intermediate (T_d^1). The serin is deprotonated by the histidine (his) which acts as a base during this step. By reformation of the carbonyl double

bond, alcohol is released, and the acyl enzyme intermediate is formed. During this step his acts as an acid leading to the release of alcohol instead of the alkoxide. In the next step water binds to the acyl enzyme intermediate. His acts as a base again and deprotonates the water enabling it to perform a nucleophilic attack to the carbon of the carbonyl in the acyl enzyme and form the second tetrahedral intermediate (T_d^2). In the last step the carbonyl double bond is reformed and carboxylic acid is released restoring the free enzyme state and the catalytic cycle is closed.[45]

A.4.3. Alcohol dehydrogenases

Both prokaryotic and eukaryotic cells require the interconversion of alcohols, aldehydes, and ketones as essential metabolic processes. A variety of different electron acceptors can be used by the oxidoreductases catalysing these reactions. They can be divided into three groups: (**1**) NAD(P) dependent ADHs, (**2**) NAD(P) independent ADHs and (**3**) FAD dependent alcohol oxidases. The first group is the best characterized, since it was discovered first, the second uses PQQ or F_{420} as cofactors and the last one catalyses the irreversible oxidation of alcohols.[46]

In synthetic organic chemistry the oxidation of alcohols to carbonyls is one of the most fundamental and significant chemical transformations. Many chemical reactions have been developed, yet they all suffer from the same basic problem: the difficulty to transport redox equivalents between reactants and oxidants. Traditionally such transformations are carried out by using heavy metals mostly in molar some in catalytic amounts.[47] Metal-free alcohol oxidation was made possible by using dimethyl sulfoxide in the presence of an ''activating'' reagent such as an acid anhydride or acid halide. The methods mentioned all have detrimental environmental impacts by using environmentally unfriendly reaction media, toxic chemicals and a catastrophic atom economy.[47] Thus it is of great interest to apply ADHs in the transformation of alcohols to carbonyls since they offer the possibility to mitigate the effects mentioned before.

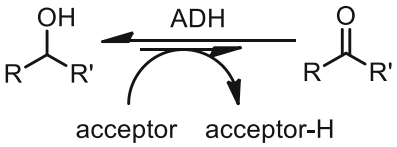

Figure 10: Oxidation of alcohols to carbonyls catalyzed by ADHs

A.4.3.1. NAD(P) dependent ADHs

This ADH superfamily can be subdivided into again three groups: the zinc dependent long-chain ADHs (~350 residues per subunit), zinc independent short-chain ADHs (~250 residues

per subunit) and ''iron activated'' ADHs (~385 residues per subunit. Group one is the best studied out of all the groups and is represented by Horse Liver ADH (HLADH) and *Saccharomyces cerevisiae* ADH (SADHI). Group two ADHs are represented by *Drosophila spp*. ADHs and group three are represented by *Zymomonas mobilis* ADH (ZMADHII).[46]

In the following section HLADH (EC 1.1.1.1) as the most prominent member of the superfamily NAD(P) dependent ADHs will be described.

The reaction catalysed by HLADH is reversible, the enzyme can oxidize alcohols to form carbonyls but also reduce carbonyls to form alcohols. The Zn^{2+} ion contained in the active site, acts as a Lewis acid and activates the carbonyl.

In the following section the catalytic reaction mechanism of HLADH will briefly be described.

As mentioned above HLADH can catalyse the oxidation of alcohols but also the reduction of carbonyls. The oxidative cycle starts after both substrates (cofactor and alcohol) bind to the active site. A hydride transfer from the alcohol carbon to the oxidized nicotinamide moiety affords the Zn-coordinated carbonyl product and NAD(P)H. Both can dissociate leaving APO-ADH. However, if NAD(P)H does not dissociate the reduced ADH can undergo a reductive conversion by binding a carbonyl and transferring a hydride yielding again the alcohol. (**figure 11**).

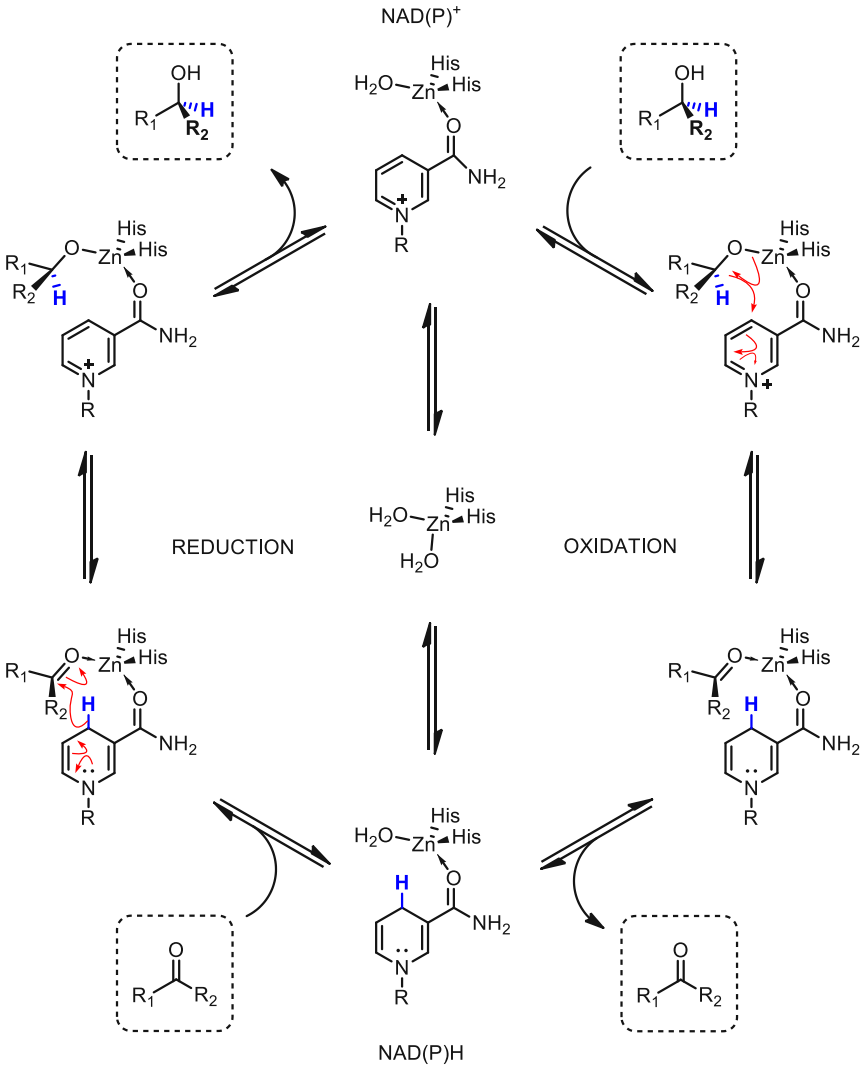

Figure 11: Catalytic reaction mechanism of NAD(P)+ dependent Group 1 ADHs. The right cycle depicts the oxidation of alcohols from top to bottom. The left cycle depicts the reduction of ketones from top to bottom. The hydride transfer can be seen in blue. Picture adapted from de Miranda et al.[48]

Another very important factor to investigate is the enantioselectivity of ADH-catalysis. The selectivity is predominantly determined by the geometry of the active site as well as the structure of the starting material which are responsible for the binding of the substrate relative to the nicotinamide cofactor.[48] When observing the structure of a carbonyl we can make out a front and a back side. The front side is called *re*-face and the back side is called *si*-face. If the hydride transfer occurs on the *re*-face the S-enantiomer of the alcohol is formed. However, if the attack happens on the *si*-face the R-enantiomer of the alcohol is formed. (**Figure 12**)

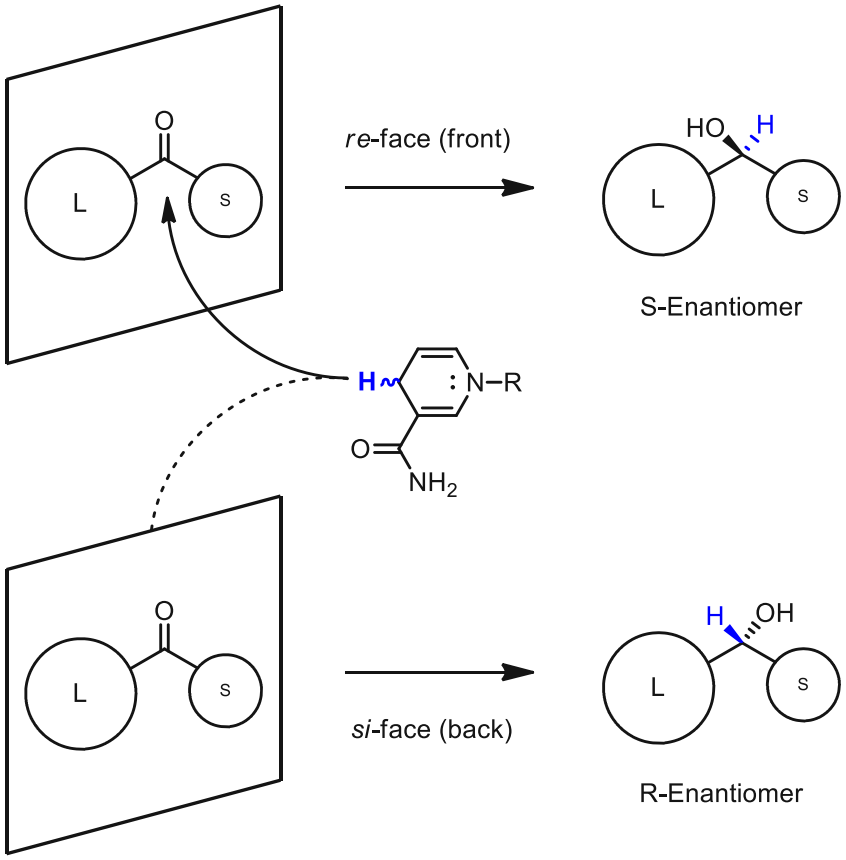

Figure 12:Stereochemical considerations of hydride transfer in ADH-catalysis. Hydride ttacks from the *re*-face (front) result in S-enatiomers whereas attacks from the *si*-face (back) result in R-enantiomers.

Control of the binding and resulting reactivity is nowadays done by protein-engineering however several other factors have an influence on stereochemistry as well. Keinan et al. investigated the influence of the reaction buffer and pH on stereoselectivity of ADH-catalysed reactions in 1986. By using a thermostable ADH from *Thermoanaerobium brockii* as model enzyme to reduce 2-pentanone they observed different reactivity with different buffer systems at different pH values.[49] Additionally ADHs have two different optimal pH values one for the reductive direction and one for the oxidative direction. In general aldehyde/ketone reductions are favoured in acidic media, the oxidation of alcohols is favoured in alkaline media.[48]

Pham et al. investigated the dependence of stereoselectivity on temperature in 1990. They used a secondary ADH from *Thermoanaerobacter ethanolicus* for the oxidation of 2-butanol among other secondary alcohols and observed a temperature dependent reversal of enantiospecifity.[50] In general ADHs have an optimal reaction temperature at the intersection of the (decreasing) curve for thermal stability and the (increasing) curve for activity.[48]

A.5. Biocatalytic cascade reactions

Cascade reactions have proven to pose many advantages in comparison to classical step-by-step synthesis. Via this type of reaction labour intensive isolation and purification of intermediates is made obsolete directly plummeting the costs of the reaction. Further benefit include higher yields, better atom economy, handling of possibly unstable intermediates and control of reaction equilibria.[51,52]Additionally low-cost DNA sequencing and synthesis together with the aforementioned advances in the biocatalytic field the design and optimization of such enzymatic systems has been made readily accessible.[53]

Recombinant proteins can be applied in a cascade reaction directly in their cellular expression host. Either by multiple expression in a single host or single expression in multiple hosts. This approach allows enzymatic cascades with incorporated cofactor regeneration, high regio- and stereo-selectivity. Enzymes are very susceptible to changes in pH, temperature, and media composition, by leaving the cell-host intact they are in a protected vessel. Furthermore, high catalytic efficiency can be achieved under mild and environmentally friendly conditions. Drawbacks of this method include substrate or product inhibition, metabolic side-products and the membrane acting as a mass transport barrier.[54,55]

A.5.1.1. Cofactor recycling

In the following section only nicotinamide cofactors are described, since their recycling was of great interest for the completion of this thesis.

Cell-free or *in vitro* systems can be afforded by lysing the cell host and optionally further purifying the enzyme via an affinity tag. By doing so, the complexity of the cellular host background can be eliminated, and control and maximization of the synthetic process is simplified.[56] A major drawback of *in vitro* enzymatic catalysis is the necessity for expensive cosubstrates such as nicotinamide cofactors. To make a process economically viable the efficient recycling of those cosubstrates is critical.

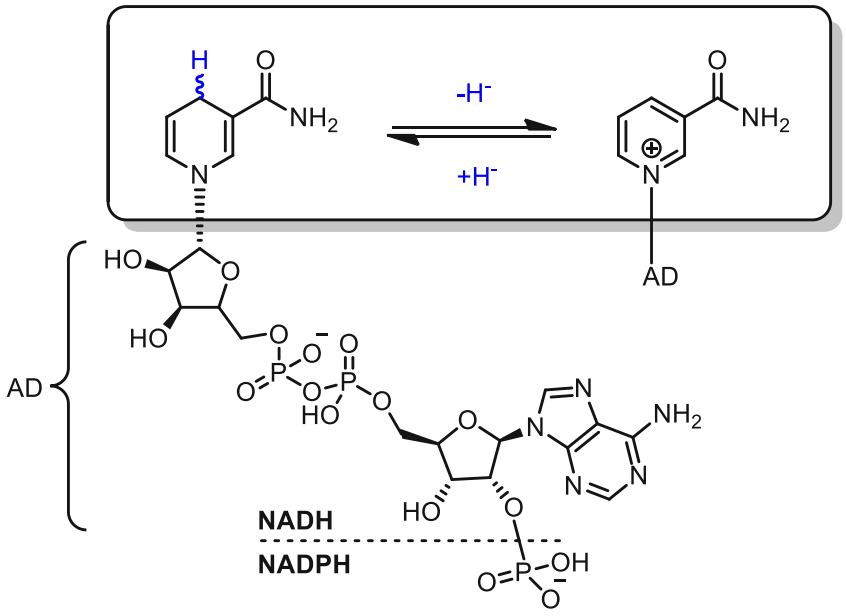

Figure 13: Structure and basic redox chemistry of nicotineamide cofactors. Oxidation of NAD(P)H to NAD(P)$^+$. Adenin is depicted as AD. Picture adapted from de Miranda et al.[48]

To regenerate NAD(P)$^+$ from NAD(P)H an oxidation reaction involving the transfer of two electrons and a hydrogen from the cofactor onto a suitable acceptor has to take place. The most commonly applied methods for NAD(P)$^+$ regeneration are the so called “coupled enzyme” and the “coupled substrate” strategies, which require a carbonyl as a cosubstrate/acceptor. The coupled substrate approach proved to be the less laborious approach, since only one enzyme is applied which is responsible for product formation and cofactor regeneration at the same time. However, to achieve a shift towards the product site, away from the equilibrium, the coupled substrate (generally a carbonyl moiety) has to be applied in vast excess, which can be problematic on a preparative scale.[47,57]

Within the “coupled enzyme” approach, the regeneration of nicotinamide cofactors is decoupled from substrate oxidation by using a second dehydrogenase. A second enzyme in the system brings drawbacks such as different optimal reaction conditions, also exclusive enzyme specificities for substrate and cosubstrate are crucial.[47]

A much more efficient method of nicotinamide cofactor regeneration is to design a self-sufficient one-pot cascade with a so called “closed loop” cofactor recycling system, which promises a high molecular selectivity and atom economy. By doing so product generating enzymes with inverse cofactor demand are chosen, eliminating the need for non-product generating enzymes to recycle the cofactors.(**figure 14**)[53,58-62]

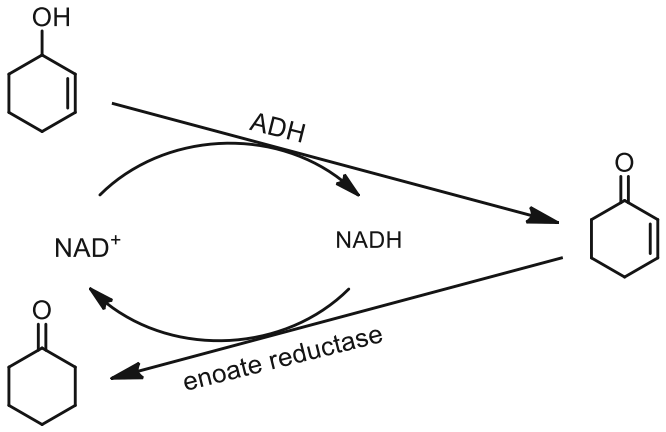

Figure 14: Cascade with closed loop cofactor recycling system with an ADH and an enoate reductase for the synthesis of cyclohexanone.[62]

Another great way of recycling cofactors efficiently are “convergent” enzymatic cascades. Hereby a closed loop cofactor system is applied with to different substrates and two different enzymes coupled by their inverse hydrogen-borrowing cofactor need, however both enzymes yielding the same product. (**figure 15**)[63,64]

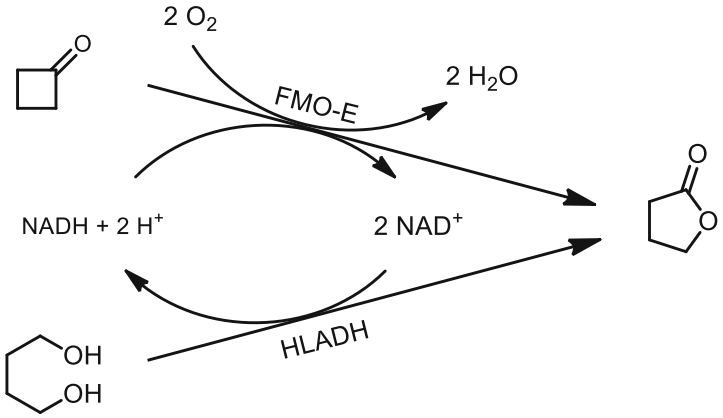

Figure 15: Convergent cascade between FMO-E and HLADH for the synthesis of γ-butyrolactone.

A.5.1.2. By-products

When ADHs such as HLADH are applied in the generation of aldehydes by oxidation of primary alcohols, there is a side reaction which can significantly lower the total product yield. In general, as described in **section A.4.3.1,** the reaction catalysed by ADHs is in an equilibrium between oxidation and reduction. During oxidation $NAD(P)^+$ and the alcohol bind to the active site, a hydride is transferred from the alcohol to the cofactor, and both are released. If NAD(P)H and the formed aldehyde stay bound to the active site, a reduction can happen, and the hydride is transferred back to the aldehyde affording the alcohol. However, if the aldehyde stays in the active site and NAD(P)H is exchanged for a $NAD(P)^+$ a second

oxidation step can happen. After a hydrate is formed by the nucleophilic attack of water the hydride is again transferred to the cofactor and the carboxylic acid released from the active site.[65]

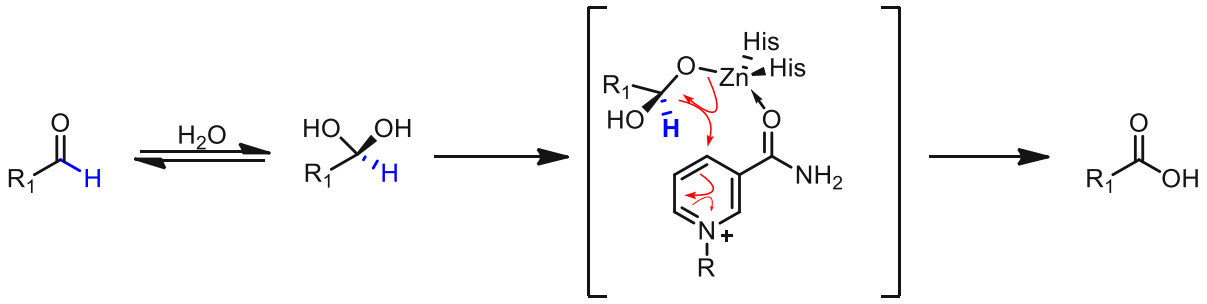

Figure 16: Oxidation of aldehydes to carboxylic acids catalyzed by ADHs

This oxidation can be a problem when pursuing a whole-cell approach, since the host cell background can contain ADHs capable of accepting the substrate but also susceptible to aldehyde oxidation, thus diminishing the final product yield. Furthermore, cross reactivity, inhibition and mutation can impair the enzymes themselves of working properly. To overcome such problems carbon flux has to be balanced throughout the host organism. This can be achieved by removing bottlenecks through systems metabolic engineering which combines the knowledge of metabolic and genetic engineering together with systems and synthetic biology.[60,66]. However, the same problem can arise with purified ADHs, thus the right biocatalyst has to be chosen carefully to avoid side-reactions.[67]

A.6. Aim of the thesis

The goal of this research is to enhance the versatility of the previously developed chemo-enzymatic cascade towards the synthesis of aromatic fragrance aldehydes from phenylpropenes. In **figure 14** the retrosynthetic approach is depicted, starting with chemical transformation from phenylpropenes, followed by the formation of a ketone, an ester, an alcohol and finally the aldehyde by biocatalytic conversions.

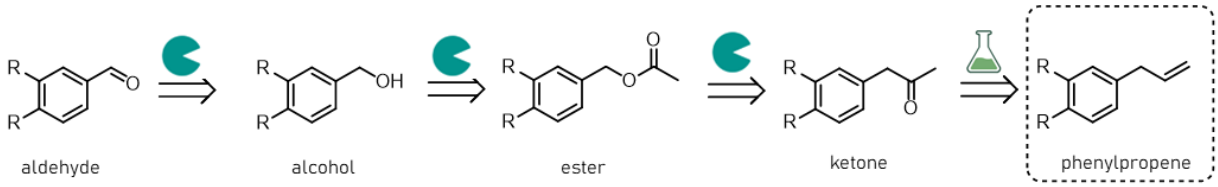

Figure 17: Retrosynthetic approach towards the biocatalytic synthesis of aromatic fragrance aldehydes

To mitigate the side-product formation the enzymes should be purified. For this objective a screening of suitable ADHs should be conducted to be applied in a closed-loop cofactor recycling system. In such a system ADHs have to be $NADP^+$ dependent, since BVMOs generally do not accept NADH as a hydrogen-borrowing cofactor. Furthermore, different methods of purification should be evaluated.

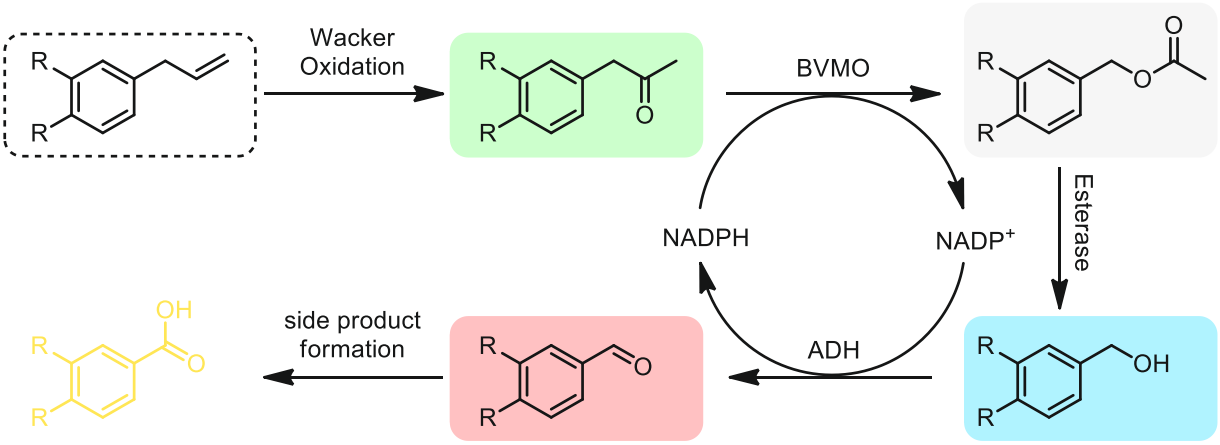

Figure 18: Enzymatic cascade: 1. Wacker oxidation towards ketone, 2. Baeyer-Villiger oxidation towards ester, 3. Diacylation towards alcohol, 4. Oxidation towards aldehyde, 5. Side-product formation.

B. Results and Discussion

B.1. Verification of biocatalytic activity

To proceed with the implementation of enzymes into the biocatalytic cascade, it was necessary to validate the previously reported activity of the BVMO (PAMO from *Thermobifida fusca*) and the esterase (PfeI from *Pseudomonas fluorescens*).[35,68]

B.1.1. BVMO (PAMO)

After sequence confirmation by sequencing of the plasmid bearing the PAMO gene, cultivation of the *E. coli* strain containing the specific gene (PAMO) was conducted, and optimized enzyme production was carried out, following the guidelines provided in **Table 18** of **section D.1**. The standard reaction conditions for biotransformations using cell free extracts (CFEs) were followed, as described in **section C.3.12**.

The oxidating activity of PAMO was confirmed with CFEs through the conversion of ketone **1b**, as explained in **section D.4.1**. Ketone **1b** was successfully transformed into the ester **1c** and subsequently hydrolysed by PfeI towards the benzylic alcohol **1d** in full conversion within 2 hours. The reaction was carried out with stoichiometric amounts of NADPH.

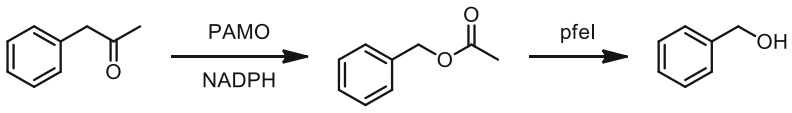

Figure 19: Model reaction catalyzed by PAMO and PfeI. Phenylacetone **1b** was converted to benzylester **1c** and directly hydrolyzed to benzylalcohol **1d**.

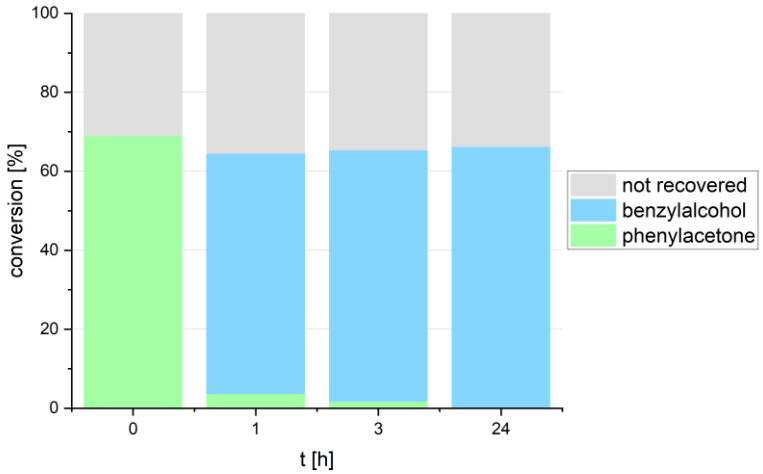

Figure 20: Oxidation and Hydrolysis of Phenylacetone with stoichiometric amounts of NADPH catalysed by PAMO and pfeI

B.1.2. Esterase (PfeI)

After sequence confirmation by sequencing of the plasmid bearing the PfeI gene, cultivation of the *E. coli* strain containing the specific gene (PfeI) was conducted, and optimized enzyme production was carried out, following the guidelines provided in **Table 18** of **section D.1** and **section D.4.2**. The standard reaction conditions for biotransformations using CFEs were followed, as described in **section C.3.12**.

The oxidating activity of the PfeI enzyme was confirmed with lyophilized CFEs through the conversion of ester **1c**, as explained in **section D.4.1**. Ester **1c** was successfully transformed into the alcohol **1d** at full conversion within less than 1 hour.

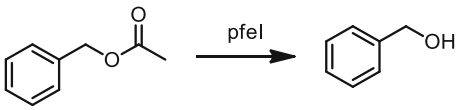

Figure 21: Model reaction catalyzed by PfeI. Benzylester **1c** was converted to benzylalcohol **1d**.

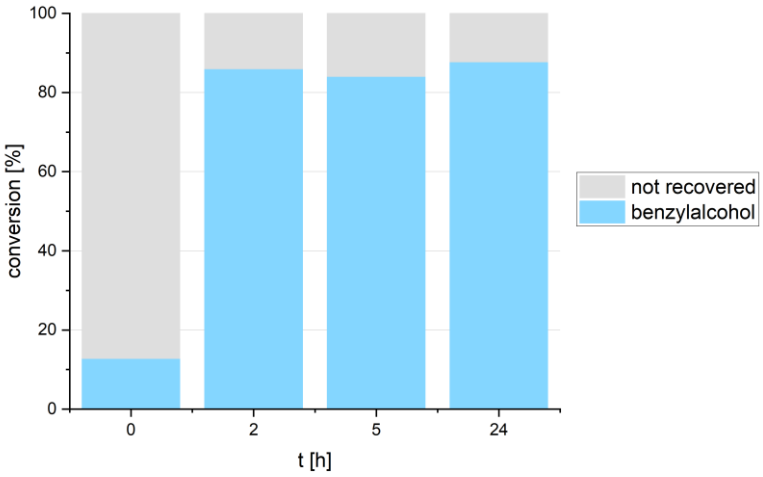

Figure 22: Hydrolysis of Benzylester catalyzed by PfeI, starting material was not plotted due to a technical error.

B.2. Screening for suitable ADHs

For the purpose of finding a suitable ADH for the aforementioned chemo-enzymatic cascade depicted in section **A.6. figure 18** a few parameters had to be taken into consideration. Since the selected BVMO (PAMO) is NADPH dependent, the ADH had to be $NADP^+$ dependent to be able to regenerate the cofactor in a closed loop cycle. Furthermore, the substrate scope chosen consists of aromatic compounds and the alcohol being generated is a secondary alcohol, thus these factors also had to be taken into account. With all of the mentioned aspects regarded a selection of ADHs was chosen to perform a preliminary screening on. The selection can be seen in **table 1**. The preliminary screening was done with stoichiometric amounts of cofactor with biotransformation conditions as described in **section C.3.12**.

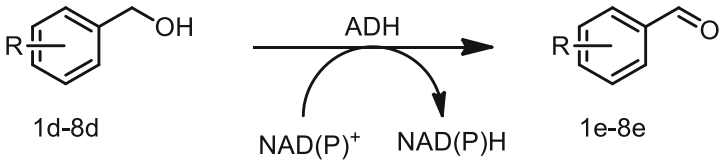

Figure 23: General reaction catalyzed by ADHs

Table 1: Selection of NAD(P)$^+$ dependent, secondary aromatic ADHs

Enzyme	Primary host	Reference
HLADH	*Equus caballus*	Uniprot: P00327[69]
plK10 (YCR107w)	*Saccharomices cerevisiae*	Uniprot: P25612[70]
plK25 (YMR318c)	*Saccharomices cerevisiae*	Uniprot: Q04894[71]
plK32 (YCR105w)	*Saccharomices cerevisiae*	Uniprot: P25377 [72]
SDR B6	*Cupriavidus necator*	Uniprot: Q0K517[73]
SDR B3	*Cupriavidus necator*	Uniprot: Q0K1N7[73]
His6-SDR B3	*Cupriavidus necator*	Uniprot: Q0K1N7[73]
PDH_loopN	*Deinococcus geothermalis*	Uniprot: Q1J3W1[74]
ChnD	*Acinetobacter sp.*	Uniprot: Q7WVD0[75]

A point mutation (deletion) was discovered in the plK25 plasmid, leading to a frameshift and an early stop codon. In order to remove the mutation site directed mutagenesis was performed on the gene as described in **section D.3.** Original and mutated gene sequences can be seen in **figure 24.**

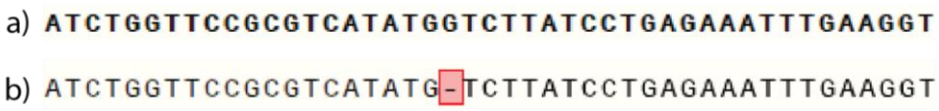

Figure 24: Point mutation (deletion) in the plK25 gene a) correct sequence b) mutated sequence

A point mutation (insertion) was discovered in the plK32 plasmid, leading to a frameshift and an early stop codon. In order to remove the mutation site directed mutagenesis was performed on the gene as described in **section D.3.** Original and mutated gene sequences can be seen in **figure 25.**

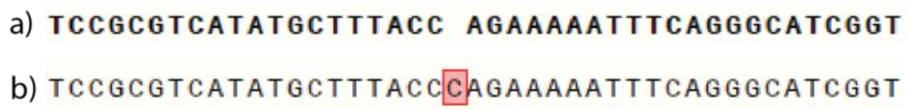

Figure 25: Point mutation (insertion) in the plK32 gene a) correct sequence b) mutated sequence

The mutations in the plK 25 and plK32 genes were successfully rectified using the Q5® Site-Directed Mutagenesis Kit from New England Biolabs Inc. The process involved three main steps: PCR for exponential amplification, kinase, ligase, dpnI enzyme (KLD) reaction for intramolecular ligation and template removal, and transformation directly into *E. coli* BL21 (DE3) cells. Verification of successful mutagenesis was done by sequencing. (**section D.3**)

Some of the substrates were mostly over oxidized to the carboxylic acid, as described in **section A.5.1.2**. This can be attributed to the ability of ADHs being able to oxidize aldehydes to their corresponding carboxylic acids, host background enzymes and above all lots of residual NAD^+ cofactor still being present within the CFEs. During the oxidation of Vanillin acetate, the acetate is lost, the aldehyde depicted corresponds to vanillin. Some loss of mass is observed which can be accounted to the volatility of the compounds or incomplete mixing before a sample was taken.

B.2.1.1. HLADH

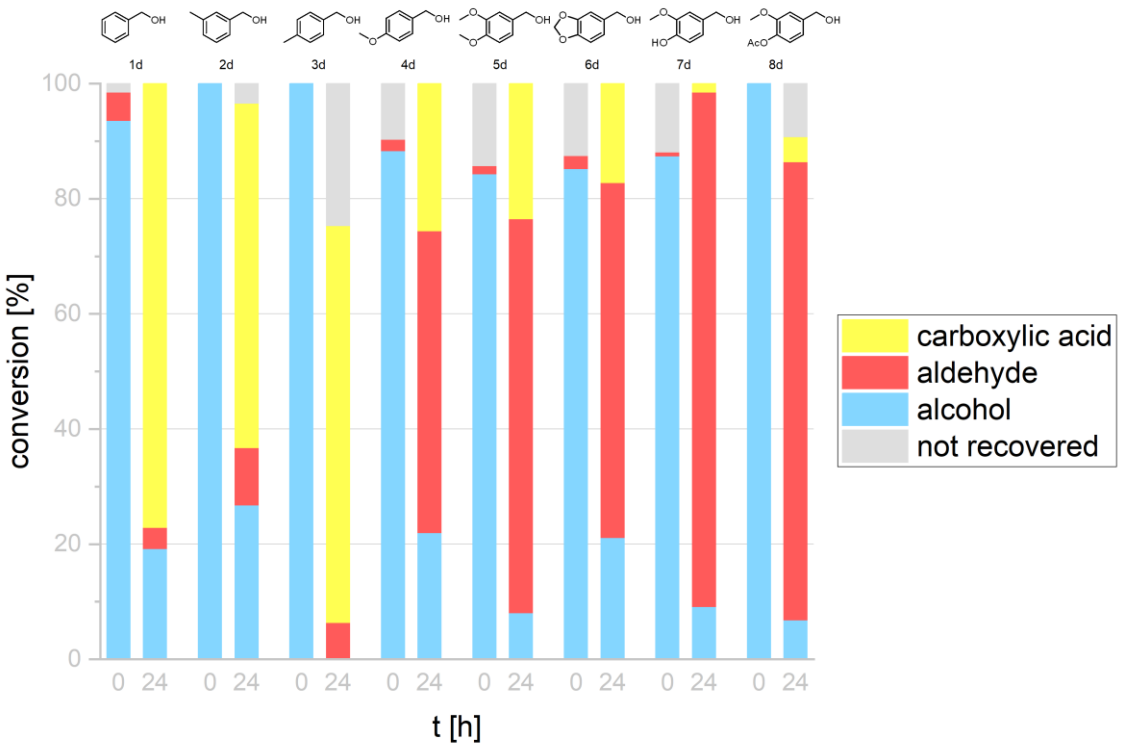

Figure 26: Oxidation of alcohols **1d-8d** catalysed by HLADH, analysis via HPLC

HLADH was heterologous expressed in *E. coli* as described bei Huang et al.[76] and in **section C.3.9**. Additionally, 250 µM of $ZnSO_4$ were added during expression of the enzyme to aid correct folding of the protein.

Horse liver ADH (EC 1.1.1.1) is an NAD(P)-dependent enzyme that possesses a wide range of substrate specificity. It exhibits activity towards diverse types of alcohols, including primary, secondary, branched, and cyclic alcohols. The enzyme is composed of two identical subunits, forming a dimer, with a molecular weight of 80,000. Each subunit consists of a coenzyme-binding domain and a catalytic domain. The structure of the coenzyme-binding domains is

similar to that of other NAD-dependent dehydrogenases. These domains contribute to the central core of the dimer and are characterized by a 12-stranded ß-pleated sheet structure.[77] Substrates **1d** to **8d** all showed a reasonable amount of conversion within 24 hours, however less polar substrates showed lots of over oxidation towards the carboxylic acid. Results depicted in **figure 26.**

B.2.1.2. plK10

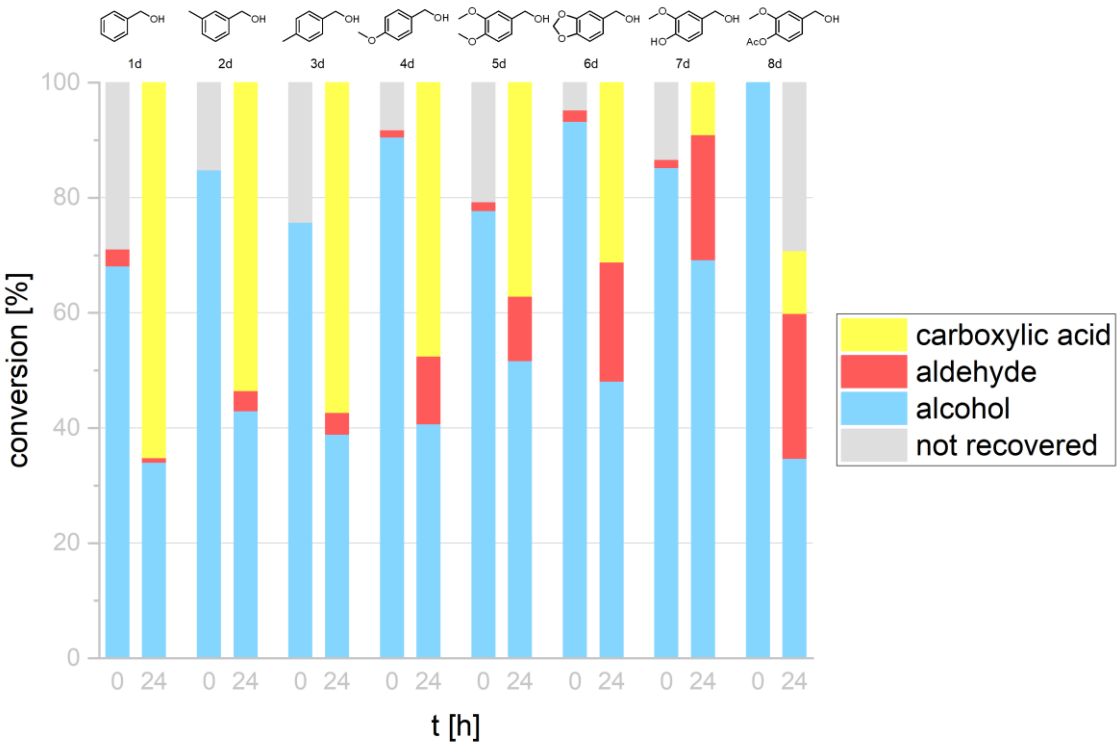

Figure 27: Oxidation of alcohols **1d-8d** catalysed by plK10, analysis via HPLC

plK10 was heterologously expressed in *E. coli* as described by Orskie-Ritchie[78] and in **section C.3.9**. Additionally, 250 µM of $ZnSO_4$ were added during expression of the enzyme to aid correct folding of the protein.

All of the plK ADHs are derived from *Saccharomyces cerevisiae* as the primary host. They all have a high degree of amino-acid sequence identity to the aryl-ADH of the lignin-degrading, filamentous fungus, Phanerochaete chrysosporium. The enzymes display strict specificity for NADPH as their coenzyme and exhibit activity with a diverse range of substrates. These substrates include aliphatic primary alcohols and aldehydes, both linear and branched-chain, as well as aromatic primary alcohols and aldehydes.[70-72]

Results obtained by this catalyst were unsatisfactory. As depicted in **figure 27** within 24 hours mostly less than 60% conversion were achieved, also most of the product formed was the

carboxylic acid.

B.2.1.3. plK25

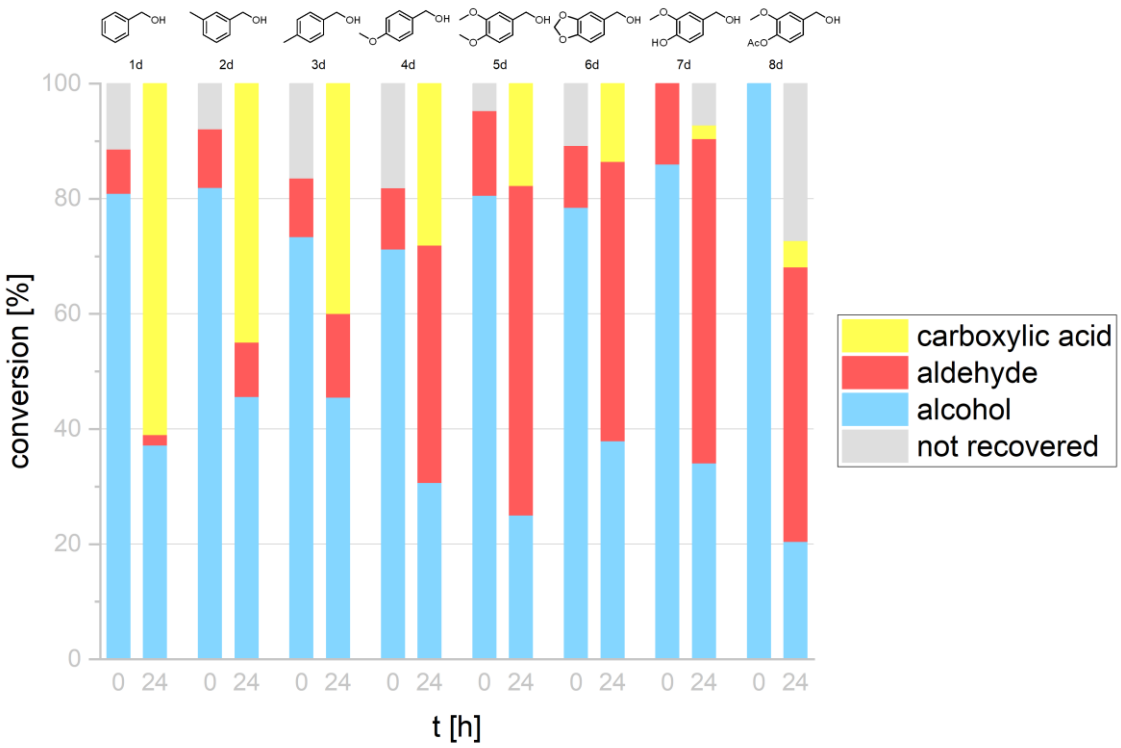

Figure 28: Oxidation of alcohols **1d-8d** catalysed by plK25, analysis via HPLC

plK25 was heterologously expressed in *E. coli* as described by Orskie-Ritchie[78] and in **section C.3.9**. Additionally, 250 µM of $ZnSO_4$ were added during expression of the enzyme to aid correct folding of the protein. The conversion after 24 hours was the best out of the three yeast enzymes (plK10, plK25 and plK32), however a lot of side product was still being generated, especially for the less polar compounds. A maximum of 61% aldehyde was obtained with Vanillyl alcohol **7d**. Results can be seen in **figure 28**.

B.2.1.4. plK32

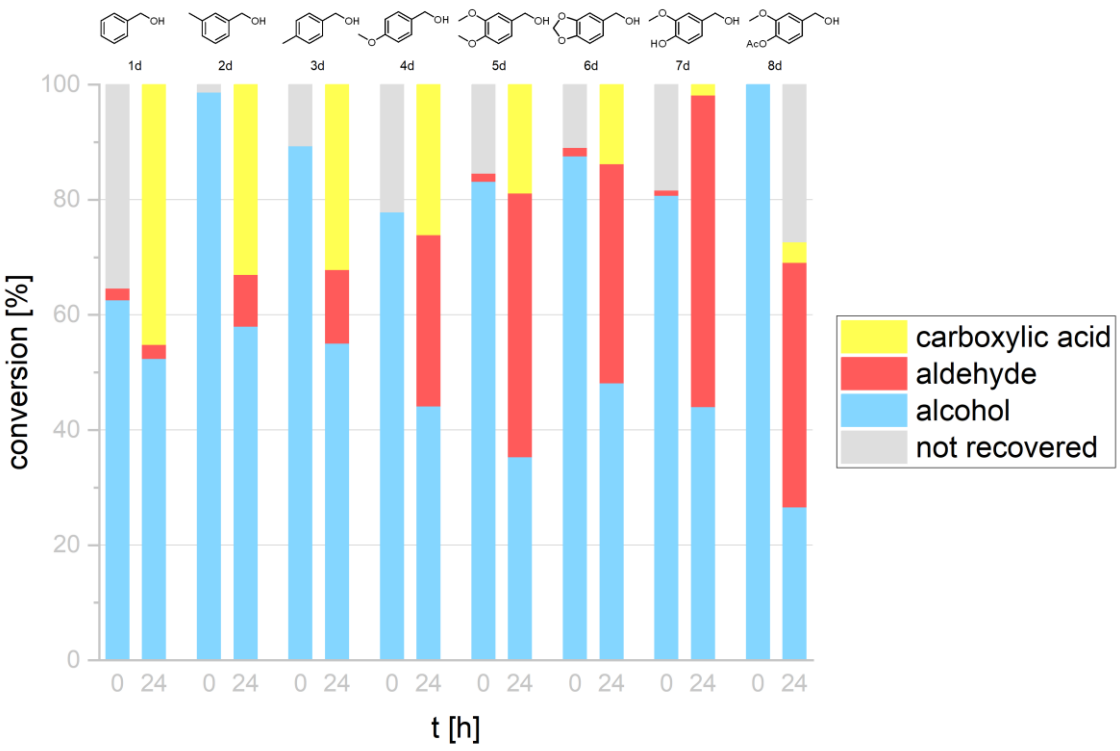

Figure 29: Oxidation of alcohols **1d-8d** catalysed by plK32, analysis via HPLC

plK32 was heterologously expressed in *E. coli* as described by Orskie-Ritchie[78] and in **section C.3.9**. Additionally, 250 µM of $ZnSO_4$ were added during expression of the enzyme to aid correct folding of the protein. Overall aldehyde production of this catalyst was similar to the conversion of plK25, however in total the conversion was less compared to plK25. A maximum of 54% aldehyde was obtained with vanillinalcohol **7d**. Results can be seen in **figure 29**.

B.2.1.5. SDR-B6

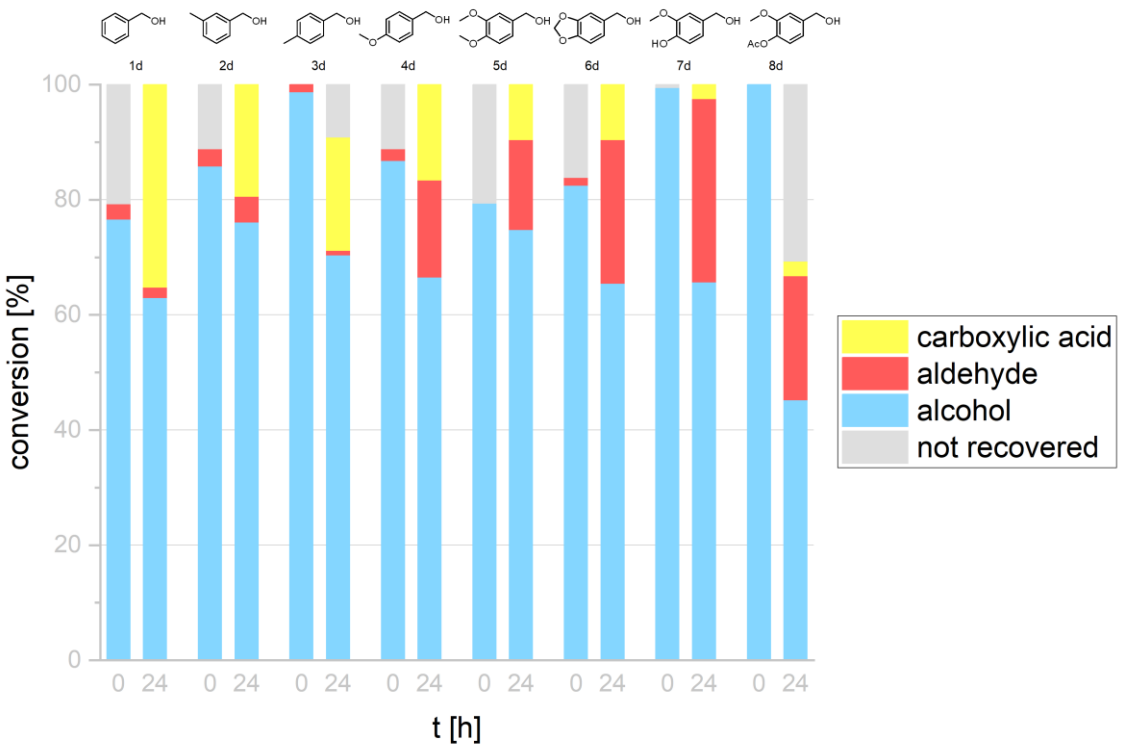

Figure 30: Oxidation of alcohols **1d-8d** catalysed by SDR-B6, analysis via HPLC

SDR-B6 was heterologously expressed in *E. coli* as described by Magomedova[79,80] and in **section C.3.9**. This SDR from *Cupriavidus necator* was obtained together with SDR-B3 from Prof. Margit Winkler.

Cupravidius necator (*Ralstonia eutropha H16*), a hydrogen-oxidizing lithoautotrophic bacterium, is known for its remarkable metabolic versatility. It can sustain itself in the absence of organic growth substrates by utilizing H2 and CO2 as its exclusive sources of energy and carbon. This bacterium garnered significant biotechnological attention almost half a century ago when researchers recognized its potential to produce and store substantial quantities of poly[R-(–)-3-hydroxybutyrate] and other polyesters, which could be utilized for the production of biodegradable plastics.

Unfortunately, all of the SDR-ADHs showed less activity than HLADH. A maximum of 25% aldehyde was obtained with piperonylalcohol **6d**. Results can be seen in **figure 30**.

B.2.1.6. SDR-B3

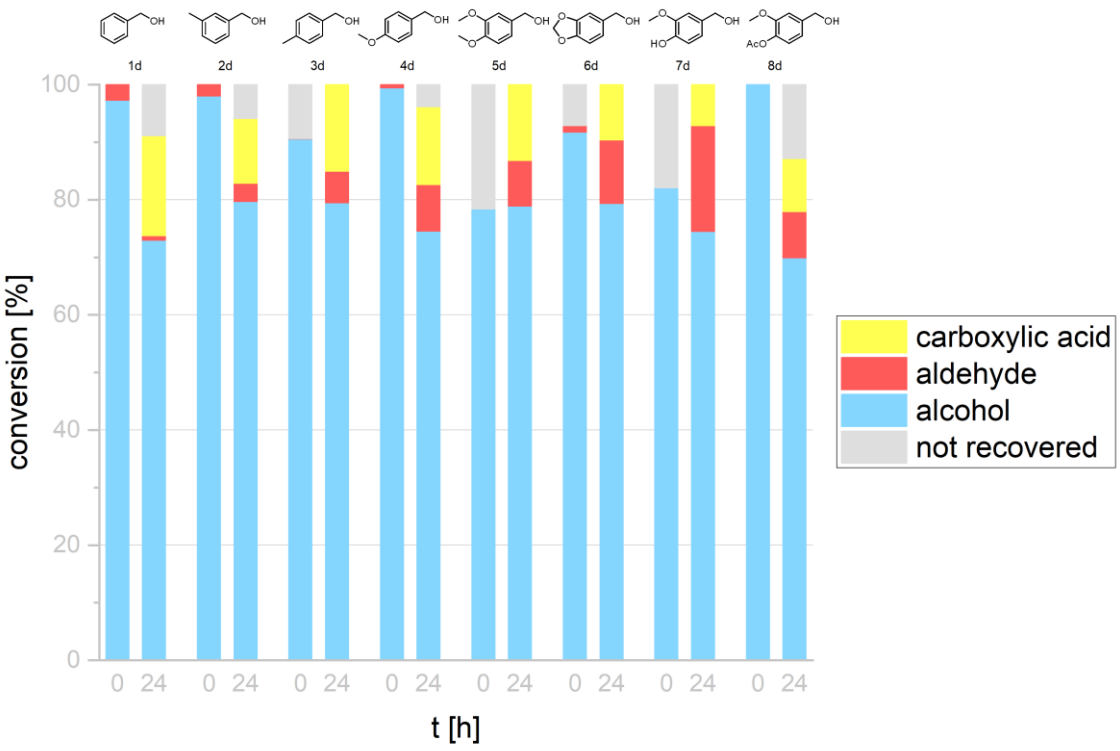

Figure 31: Oxidation of alcohols **1d-8d** catalysed by SDR-B3, analysis via HPLC

SDR-B3 was heterologous expressed in *E. coli* as described by Magomedova[79,80] and in **section C.3.9**. This enzyme had worst performance of all ADHs tested. As depicted in **figure 31** less than 30% overall conversion and a maximum of 18% aldehyde production with vanillinalcohol **7d** could be observed.

B.2.1.7. 6His-SDR-B3

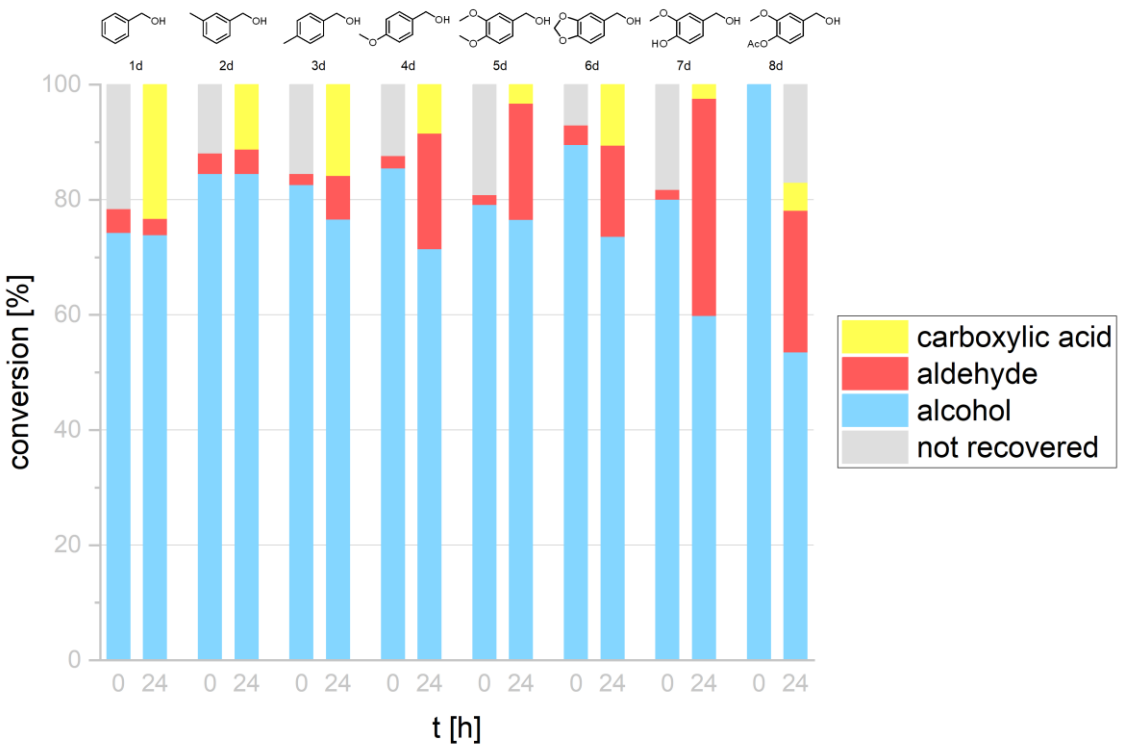

Figure 32: Oxidation of alcohols **1d-8d** catalysed by 6His- SDR-B3, analysis via HPLC

6His-SDR-B3 was heterologously expressed in *E. coli* as described by Magomedova[79,80] and in **section C.3.9**. Out of all ADHs from *Cupriavidus necator* this had the best ratio of aldehyde production, however compared to the other ADHs mentioned before this group of ADHs performed much worse. A maximum of 37% aldehyde was obtained with piperonyl alcohol (**6d)**. Results can be seen in **figure 32**.

B.2.1.8. PDH_loopN

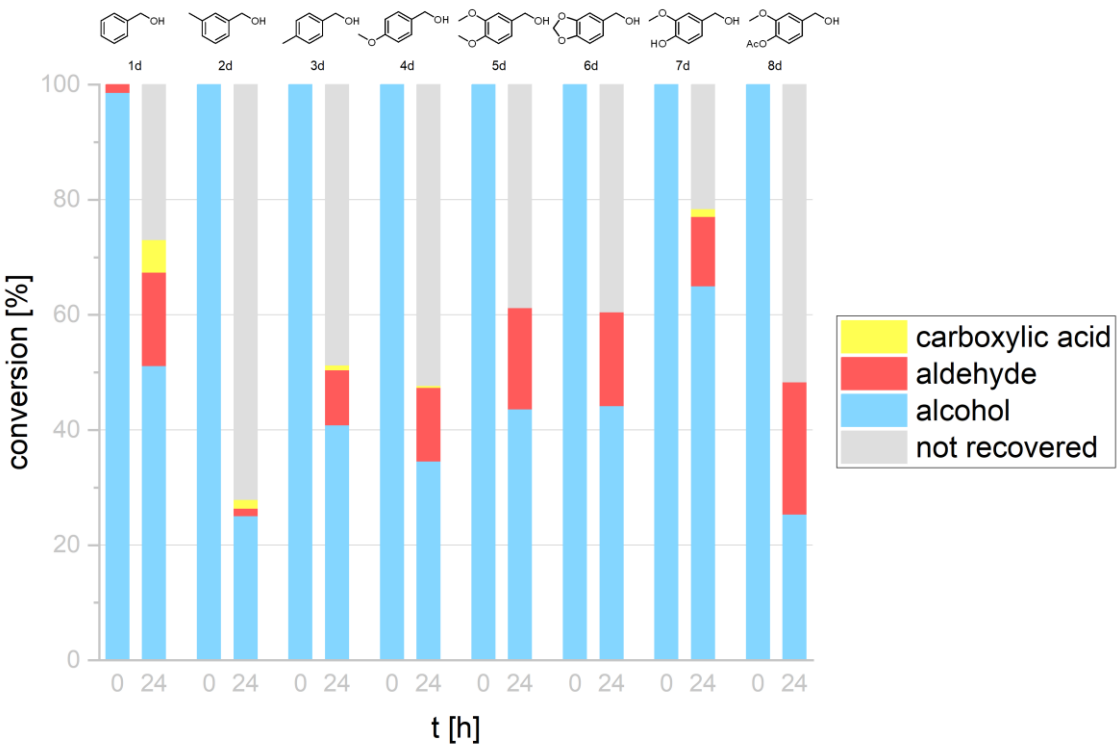

Figure 33: Oxidation of alcohols **1d-8d** catalysed by PDH_loopN at **pH 7.4**, analysis via HPLC

PDH_loopN was heterologous expressed in *E. coli* as described by Wulf et al.[74] and in **section C.3.9**. This enzyme was engineered by the group of Bornscheuer out of the polyol dehydrogenase PDH-11300 from *Deinococcus geothermalis.* To improve thermal stability a chimeric enzyme was formed together with the loop region of a homolog enzyme (PDH-158 from *Rhodobacter sphaeroides*), furthermore the cofactor specificity was altered from NADH to NADPH by an Asp55Asn mutation at the NAD^+ binding cleft. Due to its thermal stability it is possible to express this enzyme at the optimal growing temperature of *E. coli* (37°C) and harvest it already after 4-6 hours of main culture. The optimal temperature of this enzyme lies at 45° and the optimal pH at 11. Since the optimal pH for BVMOs is much lower, the enzyme was tested at pH 7.4 (**figure 33**) and pH 11 (**figure 34**). The results at pH 11 were quite interesting, since the enzyme did not catalyse the over oxidation towards the carboxylic acid, however maximum aldehyde yield was only around 38% for **5d**. The results at pH 7.4 looked less promising, since also carboxylic acid was being formed and much less conversion was observed.

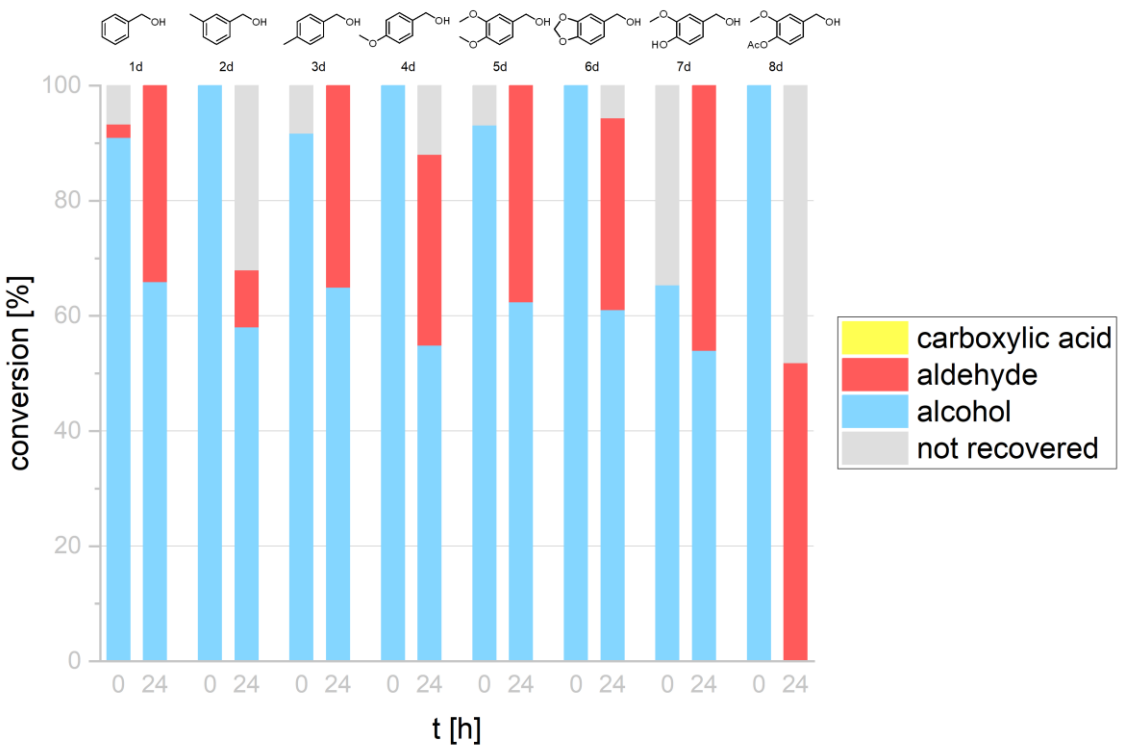

Figure 34: Oxidation of alcohols **1d-8d** catalysed by PDH_loopN at **pH 11**, analysis via HPLC

B.2.1.9. ChnD

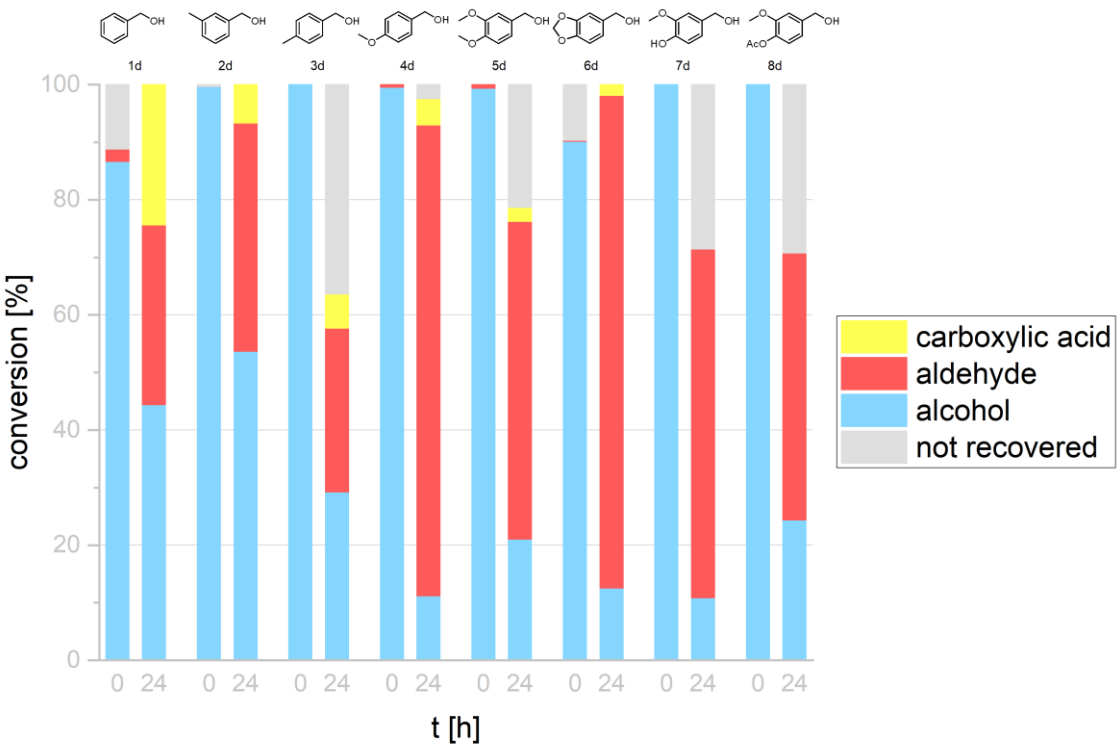

Figure 35: Oxidation of alcohols **1d-8d** catalysed by ChnD, analysis via HPLC

ChnD[75] was heterologous expressed in *E. coli* as described by Wu[81] and in **section C.3.9**. Additionally, 250 µM of $ZnSO_4$ were added during expression of the enzyme to aid correct folding of the protein. This ADH from *Acinetobacter sp.* accepts both NADH and NADPH as cofactor as will be shown later. The optimal substrate for this enzyme is 6-Hydroxyhexanoic acid and the optimal reaction temperature lies at 30°C, which is much closer to the optimal temperature of BVMOs than the optimal temperature of PDHloopN mentioned before. Out of all enzymes tested this ADH had shown by far the best performance on our chosen substrate scope within 24 hours (86% aldehyde production on piperonylic alcohol **6d**). Furthermore, when compared to HLADH, the second-best performer, much less carboxylic acid was being formed.

B.2.1.10. Overview

To be able to compare all the enzymes and choose the most suitable one two values from experimental data were analysed. The first value, displayed in **table 2**, consists of the overall conversion of alcohols **1d-8d** to aldehydes and carboxylic acids after 24 hours. After summing up the conversion for every substrate, it was clear that the best overall conversion was

achieved by HLADH and ChnD.

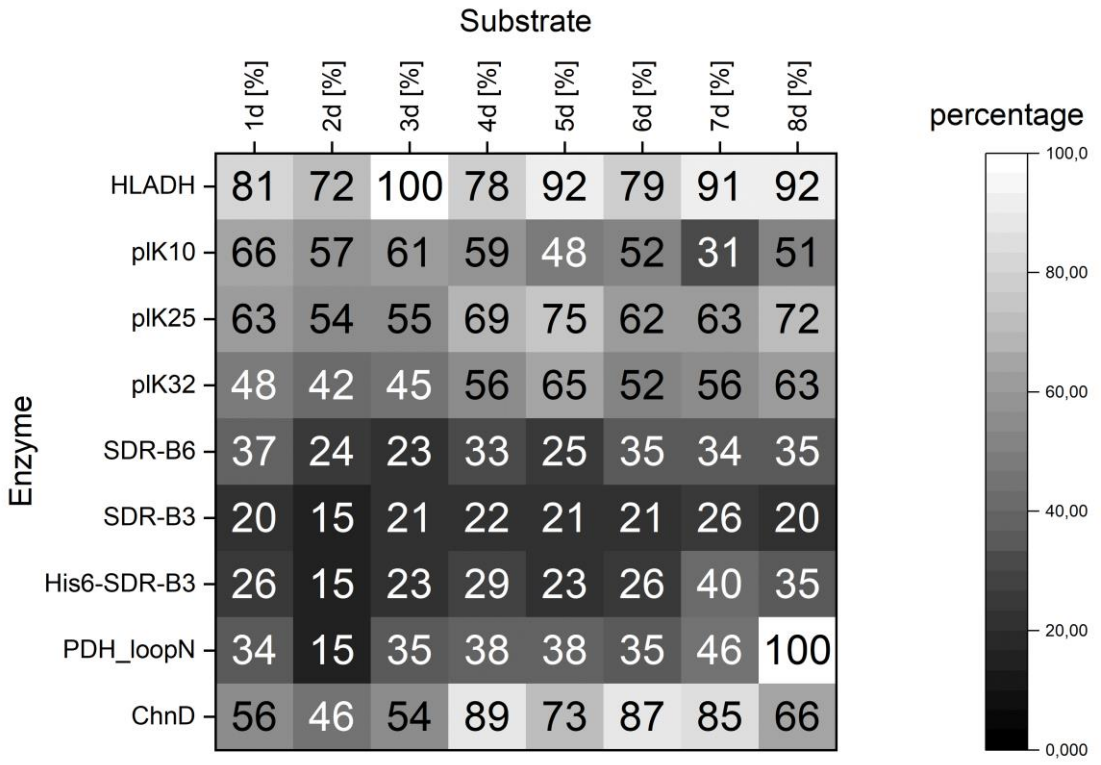

Figure 36: Overall conversion of alcohols **1d-8d** to aldehydes and carboxylic acids after 24 hours

The second value investigated is the ratio of aldehyde to carboxylic acid after 24 hours. As mentioned before PDH_loopN had the best results for this value, since it did not produce any carboxylic acid at all, however since the total conversion was by far not as good as with ChnD or HLADH, PDH_loopN was ruled out for the cascade. When comparing the value of HLADH and ChnD, ChnD has more tha n 1.6-fold the ratio of aldehyde to carboxylic acid compared to HLADH. Thus, ChnD was chosen as the most fitting ADH for the multienzymatic cascade. (**Figure 36, table 3**)

Table 2: Ratio of aldehyde to carboxylic acid after conversion of alcohols **1d-8d** after 24 hours

Enzyme	**1d [%]**	**2d [%]**	**3d [%]**	**4d [%]**	**5d [%]**	**6d [%]**	**7d [%]**	**8d [%]**	**sum [%]**
HLADH	5	14	8	67	74	78	98	95	440
PDH_loopN	100	100	100	100	100	100	100	100	800
ChnD	56	85	83	95	96	98	100	100	713

B.3. Assembly of biocatalytic cascade

B.3.1.1. BVMO GDH recycling system

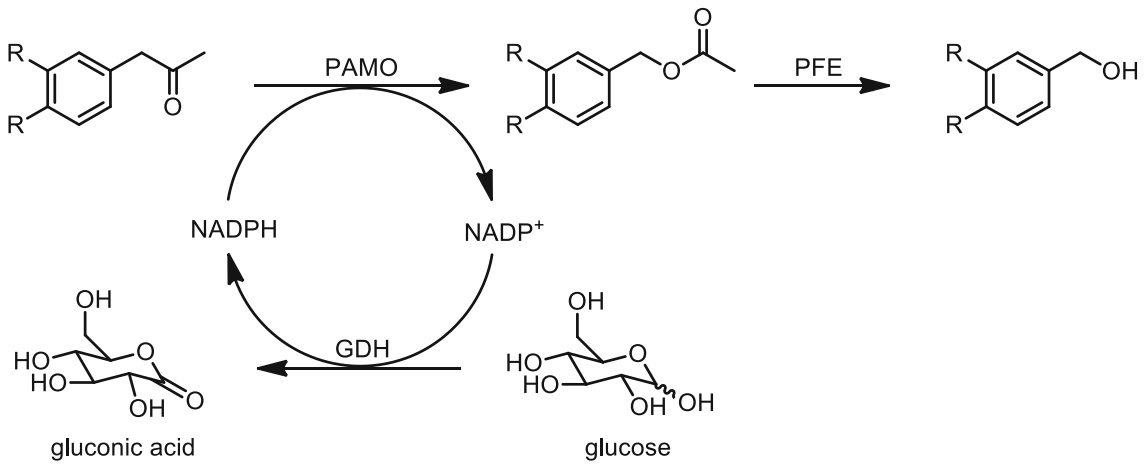

Figure 37: Reaction scheme of cofactor recycling for PAMO done by *GDH*

Before assembling all the enzymes into the cascade, it was important to evaluate if PAMO and PfeI are able to function in CFEs together with a cofactor recycling enzyme. As a recycling enzyme *Glucose dehydrogenase* (*GDH*) was chosen, since it is very common and uses glucose as a substrate to recycle NAD(P)$^+$ to NAD(P)H. This experiment was conducted as described in **section C.3.12.** with catalytic amounts of NADPH and more than 10 equivalents of glucose. As pictured in **figure 38**, full conversion was observed in less than an hour.

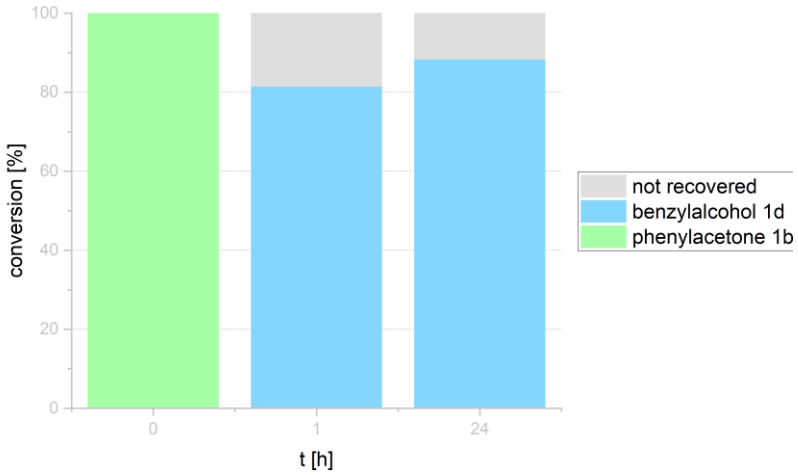

Figure 38: PAMO and PfeI tested together with a cofactor recycling enzyme *GDH* and glucose

B.3.1.2. Cascade assembly

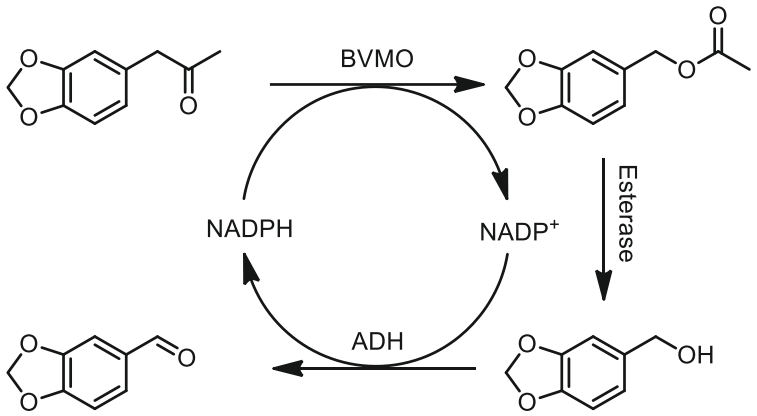

Figure 39: Reaction scheme for first experiment with fully assembled cascade and different amounts of cofactor

After confirming that PAMO indeed is able to work together with a recycling system, the completely assembled cascade was tested on substrate **6b** which seemed to have the best results based on experimental data. The enzymes were normalized to 1 mg/ml in the reaction mixture, as a reaction temperature 33.5 °C was chosen (the mean between the optimal temperature of PAMO and ChnD). First experiments with catalytic amounts of cofactor were unsuccessful, however with stoichiometric amounts the cascade seemed to work. Therefore, an experimental setup was designed to determine at which concentration of NADPH the cascade stops working due to the K_m value of the enzymes. NADPH concentrations between 1 and 4 mM were applied.

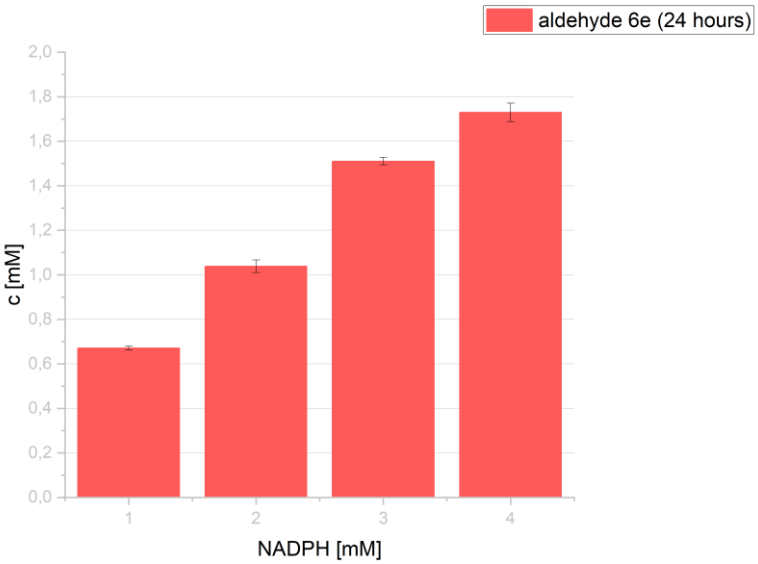

Figure 40: Cascade tested with piperonylmethylketone **6b** and different amounts of cofactor (5 mM substrate)

The results depicted in **figure 40** were different than expected. In theory, if the cascade is

working properly, either almost full conversion should be observed (due to the system recycling the cofactor) or almost no conversion (when the amount of cofactor is too low for the enzymes to work in a reasonable time frame). Thus, the issue had to be further investigated.

B.4. Determination of cofactor acceptance

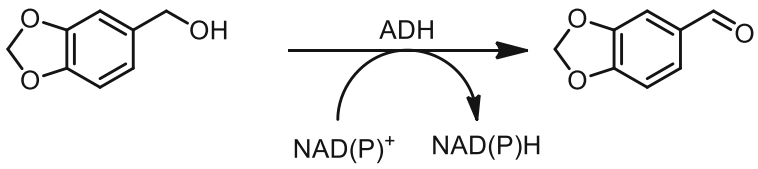

Figure 41: Reaction scheme for determination of cofactor acceptance

From experimental data and from the structure of the enzyme it was clear the enzyme accepts $NADP^+$ as cofactor. However, in the literature multiple publications state that the ADH ChnD is in fact NAD^+ dependent.[75,81,82] Thus, an experiment was designed to investigate if ChnD in fact can accept NAD^+ as well. Biotransformations were conducted as described in **section C.3.12** with NAD^+ in stoichiometric amounts and $NADP^+$ in stoichiometric amounts as control experiment. This experiment was conducted on substrate **6d** which is the intermediate for the experiment described in **section B.4.1.2**.

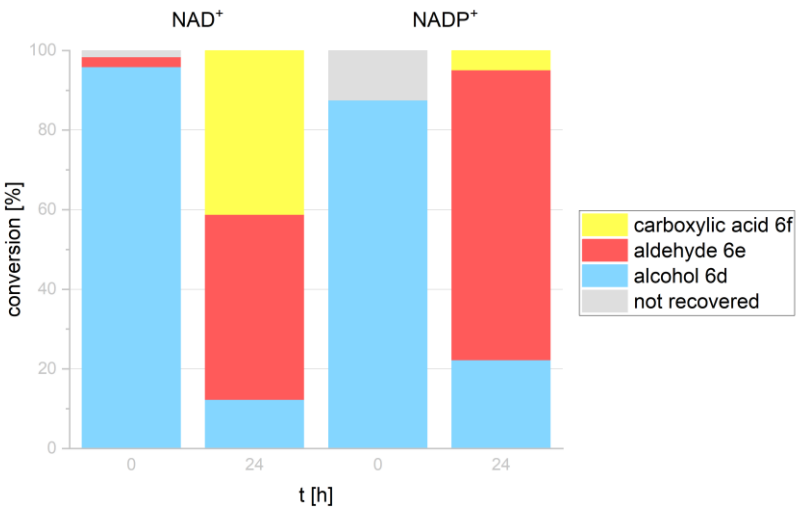

Figure 42: Comparison between biotransformation with NAD^+ or $NADP^+$

As expected, ChnD accepts both NAD^+ and $NADP^+$, although with NAD^+ much more carboxylic acid is generated. This observation could be an explanation for the unsatisfactory results obtained from early experiments with the cascade and catalytic cofactor. Since the experiments where all conducted in CFEs, which means that the enzymes are not purified and there are still residual cofactors in the mixture, those native cofactors can interfere with the

recycling of the desired cofactor $NADP^+$.

B.5. Purification of Enzymes

To ensure that the recycling system works properly without the interference of residual cofactors the enzymes had to be purified. Unfortunately, classic methods such as Ni-NTA (Nitriloacetic acid) immobilized metal affinity chromatography (IMAC) or Zn-NTA IMAC lead to the inactivation of ChnD. This is attributed to the fact that the enzyme is zinc-dependent, and the ions immobilized on the purification column interact with the active centre leading to inactivation of the enzyme. Thus, another method had to be applied.

A viable approach appeared to be the application of centrifuge filtration tubes with a cutoff of 10 kilodalton (kDa). The cofactors and various smaller components of the extract can pass through the filter, while the enzymes will be retained and washed with buffer. While this method was not perfect, since a lot of background enzymes would still be present in the reaction mixture, it showed quite promising results regarding the removal of cofactor.

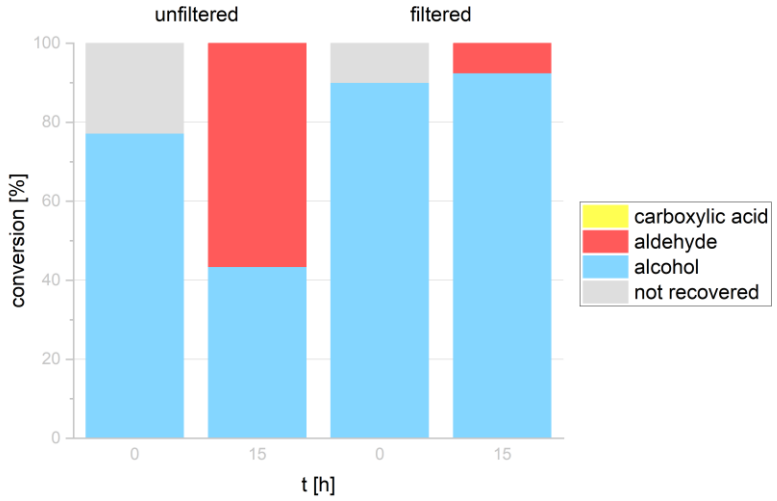

Figure 43: Comparison between filtered and unfiltered CFE of ChnD

The experiment was conducted again with piperonylic alcohol **6d** but this time no additional cofactor was added to the reaction. In the experiment filtered ChnD was compared to unfiltered ChnD. As expected, unfiltered CFE contained a lot of residual cofactor which can be seen in **figure 43**. Without adding cofactor more than 50% conversion towards the aldehyde can be observed. After filtration the formation of aldehyde drops down to less than 10%. To ensure that in the assembled cascade no cofactor is present, this method of purification was applied to PAMO and PfeI as well. Additionally, PAMO was semi-purified by heatshock, as described in **section C.3.10.1** since it is thermally stable enzyme. However,

with all the measures taken into account, the cascade was still not functional.

B.6. Verification of recycling activity

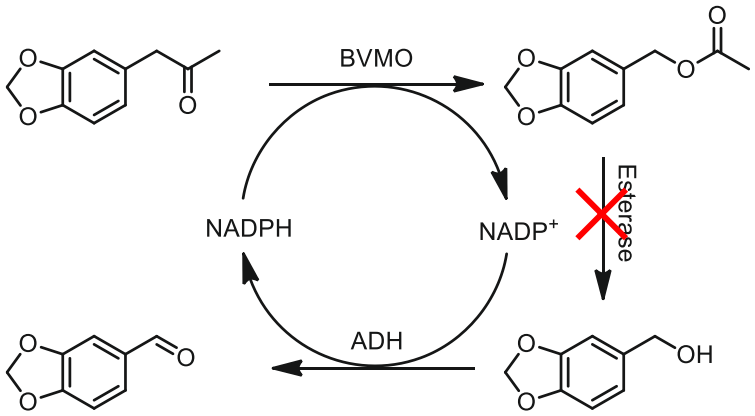

Figure 44: Reaction scheme for evaluation of cofactor recycling

Now that interference of cofactors was ruled out, we wanted to find out what was impeding the cascade to function properly. Thus, we decided to evaluate if both the BVMO and ADH are able to recycle catalytic amounts of cofactor when enough substrate is present. To achieve this, an experiment was conducted as depicted in **figure 44**. Both reactions (from the ketone to the ester and from the alcohol to the aldehyde were decoupled by removing the esterase from the reaction system. The reaction was carried out using catalytic amounts of NADPH, filtered CFEs of the enzymes and 5 mM of each substrate (ketone **6b** and alcohol **6d**).

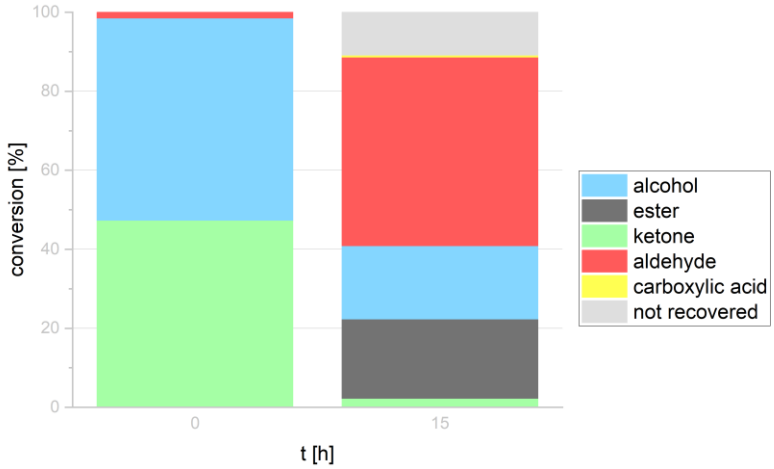

Figure 45: Evaluation of recycling system with catalytic amounts of NADPH, no esterase, 5 mM of ketone **6b** and alcohol **6d**

The results can be seen in **figure 45**, quite remarkably almost 5 mM of the aldehyde were

obtained after 15 hours, which meant that NADPH had successfully been converted to $NADP^+$ and recycled back to NADPH. Since the reaction was decoupled, this meant that in theory 50% aldehyde and 50% ester should be observed, however the ester formed by PAMO was partially hydrolysed to the alcohol as well. The results of this experiment lead to the hypothesis that the problem, was that the ADH needs enough substrate to be able to recycle the cofactor efficiently.

B.7. Equilibrium shift by auxiliary substrate

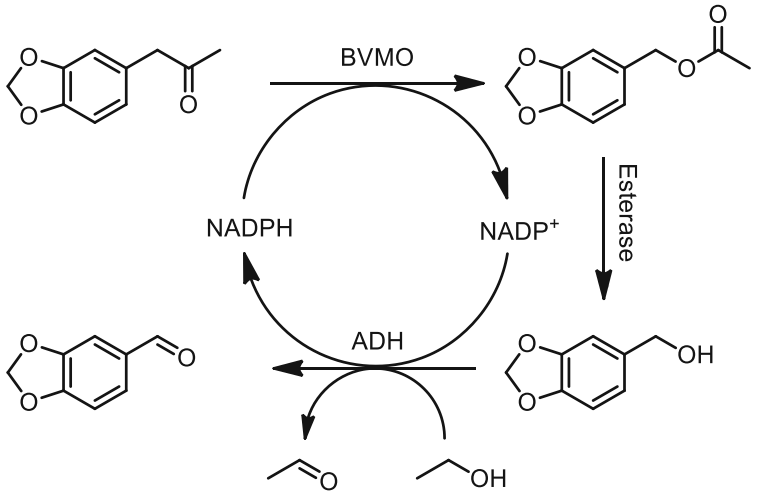

Figure 46: Reaction scheme for equilibrium shift towards desired aldehyde by addition of auxiliary substrate ethanol

By adding a second substrate to the reaction mixture the ADH should be able to recycle the cofactor for the BVMO more efficiently, since when added in excess there is never a lack of substrate for the ADH.[83] However, the amount of cosubstrate has to be chosen carefully, since when the excess is too high, the conversion of the desired substrate might suffer. As a cosubstrate ethanol (EtOH) was chosen, since it is readily available and known to be converted easily to acetaldehyde by ADHs such ChnD. To determine the right amount of EtOH, a series of experiments was conducted with different volumetric amounts of cosubstrate.

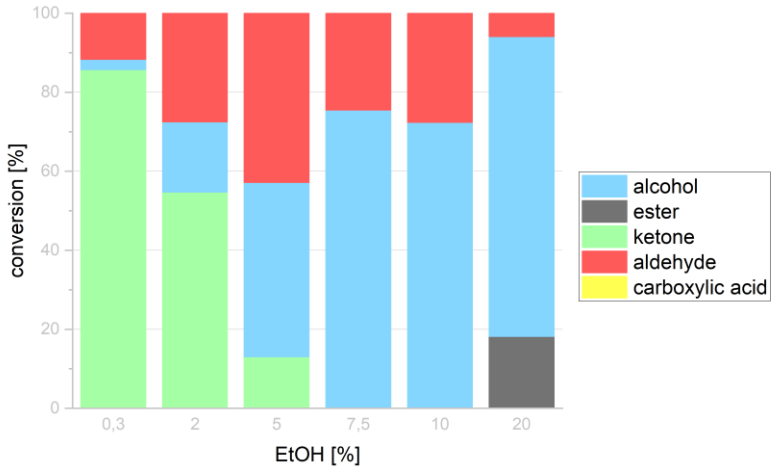

Figure 47: Determination of proper EtOH concentration as cosubstrate for enzymatic cascade after 24 hours

The results (**figure 47**) showed that at a concentration of 5% (v/v) EtOH more than 40% of the desired aldehyde were generated when catalytic amounts of cofactor were applied to the system. Thus, the equilibrium was successfully shifted towards the side of the products, with the compromise of a lot of alcohol **6d** being formed as well. However, formation of carboxylic acid was completely eliminated.

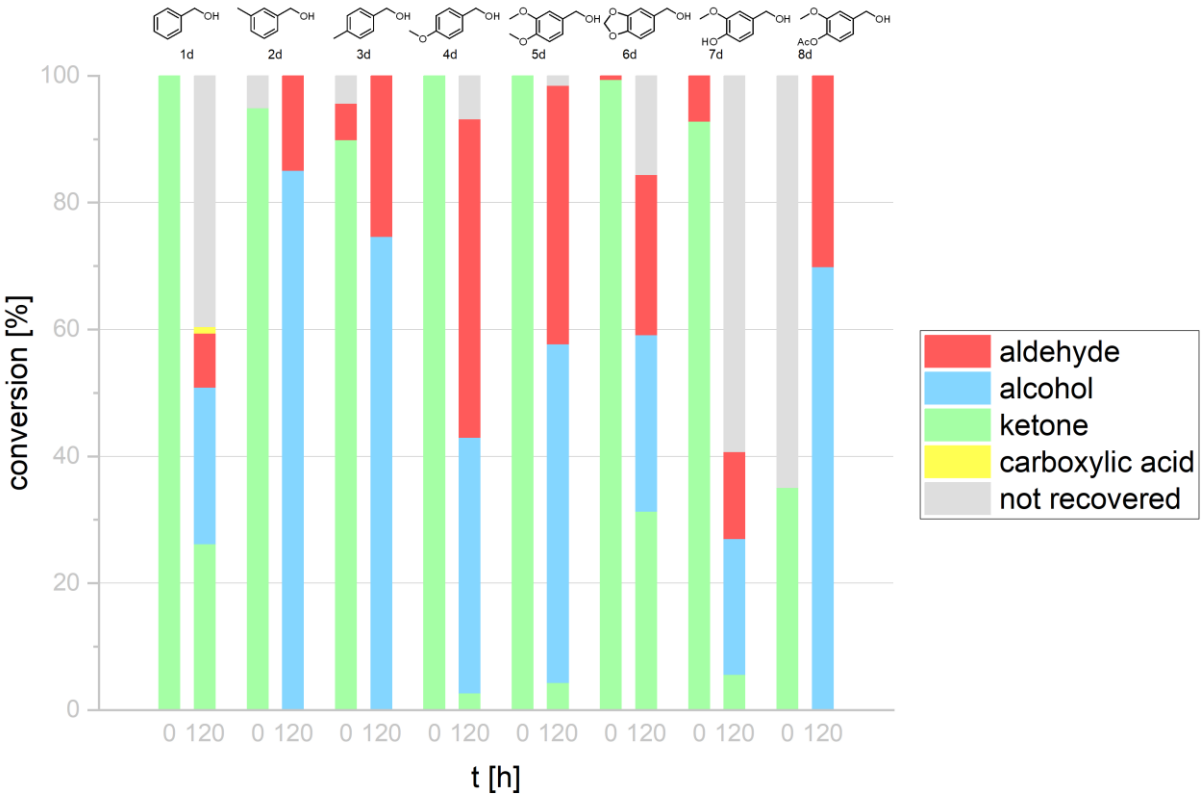

Figure 48:Final results of complete catalytic cascade on all substrates with 5% EtOH applied

B.8. Conclusion and outlook

In conclusion, the successful expansion of the applicability of the previously developed biocatalytic cascade, which consisted of the BVMO PAMO, esterase PfeI and ADH AlkJ was achieved through the exchange of AlkJ with ChnD.

To ensure the success of the biocatalytic cascade reactions, several factors needed careful consideration and attention. Initially, the genetic sequences of the pathway enzymes had to undergo validation and, if required, corrections. Subsequently, suitable biocatalysts had to be chosen, and their biocatalytic activity had to be thoroughly verified.

A purification method was developed, despite problems regarding the catalytic center of the selected ADH. By implementing the new ADH and purifying, carboxylic acid formation could be mitigated.

To shift the equilibrium towards the product side an auxiliary substrate was selected and implemented into the cascade. This helped product formation and made it possible to test the cascade on the whole substrate scope.

To increase the final product yield, a few different strategies can be applied.

First of all, the concentration of the auxiliary substrate can be further optimized, a possible different substrate could be applied.

The concentration of enzyme in the reaction mixture can be varied to find the optimal working concentration.

A different method of purification can be used to make sure no other enzymes or cofactors interfere with the cascade. For example, a different tag could be implemented into the sequence of the enzyme, such as Glutathione S-transferase (GST), which also increases solubility, or streptavidin tags.

C. Materials and Methods

C.1. General Comments

Following practices were applied before every procedure unless otherwise stated.

All the glass equipment used for biological experiments was sterilized (121°C, 20 min, > 15 psi) or was purchased sterile.

Antibiotics for *E. coli* culture were applied in a concentration of 0.1% v/v.

C.2. Preparation of reagents

C.2.1. Stock Solutions

Stock solutions were sterilized by filtration with 0.2 µm PTFE syringe filters and stored at -20°C.

Table 3: Commonly used stock solutions

reagent	*concentration in dH_2O*	*working concentration*
Amp	100 mg/ml	100 µg/ml
Kan	50 mg/ml	50 µg/ml
IPTG	0.1 M	var.
L-Ara	20% (w/v)	var.
L-Rha	20% (w/v)	var.
PMSF	0.1 mM (in abs. iPrOH)	0.1 µM
$ZnSO_4$	0.1 M	25 µM

C.2.2. Standard Media

Quantity of reagents refers to 400 ml of final volume unless stated otherwise. All the media were sterilized by autoclavation and stored at RT. The media were visually inspected before use for possible contamination.

Table 4: Media preparation

component	*LB Medium*	*TB Medium*	*LB Agar*
bacto-peptone	4 g	-	4 g
bacto-tryptone	-	4.8 g	-
yeast extract	2 g	9.6 g	2 g
NaCl	4 g	-	4 g
K_2HPO_4	-	5 g	-
KH_2PO_4	-	0.91 g	-
Agar No. 1	-	-	6 g

C.2.3. Buffers

Quantity of reagents refers to 1 l of final volume unless stated otherwise. All the buffers were sterilized by autoclavation and stored at RT. The buffers were visually inspected before use for possible contamination.

Table 5: Buffer preparation

component	*50 mM Na-PBS (pH 7.4)*	*100 mM K-PBS (pH 8.0)*	*50 mM Tris HCl (pH 7.5)*	*50 mM Glycin-NaOH (pH 11)*
$Na_2HPO_4.7H_2O$	10.10 g	-	-	-
$NaH_2PO_4.H_2O$	1.69 g	-	-	-
K_2HPO_4	-	16.28 g	-	-
KH_2PO_4	-	0.89 g	-	-
Tris	-	-	6.06 g	-
glycine	-	-	-	3.75 g

Buffers were sterilized by autoclavation and stored at RT. The pH was adjusted with 2M HCl or 2M NaOH.

C.3. Standard molecular biology techniques

C.3.1. SDS-PAGE

C.3.1.1. Buffers and reagents

Table 6: SDS-PAGE buffers preparation

component	*10 x running buffer*	*resolving gel buffer*	*stacking gel buffer*	*sample buffer*
Tris	30.3 g	18.15 g	6 g	-
glycine	144 g	-	-	-
SDS	10 g	-	-	-
dH_2O	fill up to 1L	fill up to 100ml	fill up to 100ml	7.1 ml
stacking buffer	-	-	-	2.5 ml
glycerol	-	-	-	5.0 ml
10% SDS	-	4.0 ml	4.0 ml	4.0 ml
1% bromophenolblue	-	-	-	0.2 ml
β-mercaptoethanol	-	-	-	1 ml

Buffers were sterilized by autoclavation and stored at RT. Quantity of reagents refers to 1000 ml of final volume for the 10x running buffer and 100 ml for the resolving and stacking gel buffers. The sample buffer was stored at 4°C after the addition of β-mercaptoethanol. SDS-running buffer was diluted 1:10 with dH_2O before use.

Table 7: Reagents for SDS-PAGE

component	*30 % acrylamide*	*10 % SDS*	*1 % bromophenolblue*	*10 % APS*
acrylamide	29.2 g	-	-	-
N',N'-bis-methylene acrylamide	0.8 g	-	-	-
SDS	-	1 g	-	-
bromophenol blue	-	-	1 g	-
APS	-	-	-	1 g

Reagents were sterilized by filtration and stored at 4°C. Quantity of reagents refers to 100 ml of final volume for the 30 % acrylamide and 10 ml for the other reagents.

C.3.1.2. Gel preparation

Table 8: Gel preparation

component	resolving gel	stacking gel
dH_2O	3.2 ml	3.2 ml
resolving buffer	2.5 ml	-
stacking buffer	-	1.3 ml
30% acrylamide	5.25 ml	625 µl
1% bromphenolblue	-	30 µl
10% APS	50 µl	25 µl
TEMED	8 µl	8 µl

The volumes account for the preparations of 2 sodium docecyl sulfate-polyacrylamide gel electrophoresis (SDS-PAGE) gels. Upon addition of N, N, N', N', Tetramethylethylenediamine (TEMED) and ammonium persulfate (APS) in the end, the gels were poured immediately.

C.3.1.3. Gel electrophoresis

The samples were prepared by adding protein-solution (8 µl) to sample buffer (64 µl). The samples were denatured for 5 min at 95°C before loading onto a gel (6 µl). The first lane was loaded with prestained protein ladder (6 µl, PageRuler™ Prestained Protein Ladder 26616, Thermo Scientific). Gel electrophoresis was performed at 90-120V in SDS-running buffer.

C.3.1.4. Gel staining

After a gel-electrophoresis was performed, the gel was carefully removed from the chamber and added into a staining box. After rinsing and covering with dH_2O it was incubated in the microwave at 750W for 1 min and shaken for 2 min. The gel was rinsed and covered again in dH_2O, incubated in the microwave at 500W for 1 min and shaken for 2 min. The water was discarded, the gel was covered in staining solution (SimplyBlue™ SafeStain;LC6065,Novex®), incubated at 500W for 40 sec. and shaken for 5 min. After discarding the staining solution the gel was rinsed and covered in dH_2O, shaken for 10 min, stored in 20% (w/v) NaCl and scanned for documentation.

C.3.2. Site directed mutagenesis

C.3.2.1. Polymerase Chain Reaction

The Q5® High-Fidelity DNA Polymerase (M0491) was used to repair mutations found in

plasmid DNA. All reaction components were assembled on ice, spun down and quickly and transferred to a thermocycler preheated to the denaturation temperature (98°C). Primers were designed using NEBbaseChanger (https://nebasechanger.neb.com/) and SnapGene® software. A list of primers is attached in the appendix. Annealing temperatures (T_a) were calculated using the NEBtmCalculator (https://tmcalculator.neb.com/#!/main#!%2F).

Table 9: PCR reagents mix

component	*50 µl reaction*	*final concentration*
5X Q5 reaction buffer	10 µl	1x
10 mM dNTPs	1.0 µl	200 µM
10 µM forward primer	2.5 µl	0.5 µM
10 µM reverse primer	2.5 µl	0.5 µM
template DNA (50-100 ng/µl)	1.0 µl	1-2 ng/µl
Q5 High-Fidelity DNA polymerase	0.5 µl	0.02 U/µl
5X Q5 high GC enhancer	10 µl	1x
nuclease-free water	31.5 µl	

Table 10: General thermocycling conditions

step	*temp*	*time*	*cycles*
initial denaturation	98°C	30 sec	1
denaturation	98°C	5-10 sec	25-30
annealing	50-72°C	10-30 sec	
extension	72°C	20-30 sec/kb	
terminal extension	72°C	2 min.	1
hold	4°C	∞	

C.3.2.2. KLD Reaction

For circularization and template removal the KLD-reaction was performed on the PCR-products. The reaction was assembled as shown in the table below following the kit-protocol (M0554).

Table 11: KLD reagents mix

component	
PCR product	1 µl
KLD reaction buffer (2x)	5 µl
KLD reaction mix (10x)	1 µl
nuclease-free water	3 µl
total volume	10 µl

The reaction was mixed thoroughly by pipetting, incubated at room temperature (25°C) for 5 minutes and placed on ice. The transformation was performed by adding the KLD-reaction (5 µl) to chemocompetent *E. coli* cells (50 µl) and further by following the procedure for transformation mentioned in **section C.3.6.**.

C.3.3. Agarose gel electrophoresis

Agarose gel was prepared by the following procedure: Agarose (0.8g) were dissolved in tris-acetate EDTA (TAE) buffer (80 ml, 1% w/v) by heating the solution in a microwave for about 3 minutes. The solution was then cooled in a water bath until it was safe to touch, and SYBR Safe DNA Gel Stain (8 µl) were added. The mixture was then poured into an appropriate agarose gel tray, and a comb was inserted to create wells. After the gel had solidified, the tray was placed in an electrophoresis chamber and covered with TAE buffer. For sample preparation, 6 x purple DNA loading dye (NEB B7024S) was mixed with PCR product at a ratio of 1:5 and loaded into the wells. A DNA ladder (10 µl, Thermo Scientific SM01313) was used as a reference. Electrophoresis was carried out at 100 V for 40-45 minutes, and DNA visualization was performed under UV light using an Analytic Jena UVP UVsolo touch.

Table 12: TAE-buffer 50X preparation

component	
Tris	2 M
Acetic acid	5.71% (v/v)
EDTA[a]	50 mM

[a] From 0.5 M stock solution adjusted to pH 8

C.3.4. Gel purification of PCR products

The target DNA band was visualized under UV-Light and then excised with a scalpel. The slices were weighed and placed into 2ml Eppendorf tubes. Purification was performed with the GeneJET gel extraction kit from Thermo Scientific, following the enclosed instructions. An

equal volume of binding buffer was added to the gel slices, and the resulting gel mixtures were incubated at 50 °C for 10 minutes until the gel had dissolved. The solubilized gel solution was then transferred to the GeneJET purification column, centrifuged for 1 min at 16000 RCF and the flow-through was discarded. The column was washed twice with wash solution (700 µl), centrifuged for 1 min at 16000 RCF and the flow-through discarded. The empty column was centrifuged again at 16000 RCF for 1 minute, then transferred into a clean 1.5 ml Eppendorf tube and placed into a heat block for evaporation of residual EtOH. Pre-warmed nuclease-free water (35 µl) was added to the center of the purification column, incubated for 10 min, and then centrifuged at 16000 RCF for 2 minutes. The purified plasmid-DNA was quantified using a NanoDrop® (NanoDrop™ OneC Microvolume UV-Vis Spectrophotometer, Thermo Scientific) in the measurement mode “dsDNA” using 1.0 µl of the sample. Finally, the purification columns were discarded, and the samples were stored at -20 °C.

C.3.5. Preparation of $RbCl_2$ competent Cells

To prepare the desired *E. coli* strain, a single colony was cultured overnight in lysogeny broth (LB) medium (5 ml, 37°C, 180 rpm). Then fresh LB medium (100 ml) was inoculated with 1% (v/v) of the overnight culture and grown until reaching an optical density at 590 nm (OD_{590}) of 0.3-0.4. The cells were then harvested via centrifugation (4000 RCF, 4°C, 10 min), resuspended in 1/5 volume of the main culture of RF1 buffer (20ml) and incubated for 15 min. After centrifugation, the cells were resuspended in in 1/5 volume of RF1 suspension (4 ml). The cells were dispensed into 1.5 ml tubes in 50 µL aliquots, snap-frozen in liquid nitrogen, and stored at -80°C.

Table 13: RF1 buffer (pH 5.8) and RF2 buffer (pH 6.8)

reagent	*RF1 buffer*	*RF2 buffer*
RbCl	1.21 g (100 mM)	0.12 g
$MnCl_2$	0.6292 (50 mM)	-
KOAc	0.294 (30 mM)	-
$CaCl_2$	0.1109 (10 mM)	0.83 g
glycerol	15 (15% w/v)	7.5 g
MOPS	-	0.21 g

C.3.6. Transformation into *E. coli*

Chemically competent cells preserved at -80°C were thawed on ice for 5 minutes. Plasmid

DNA (1 µl, 50-100 ng/µl) was added to the cell suspension (50 µl) and allowed to incubate on ice for 30 minutes. The cells were then subjected to a heat shock at 42°C for 1 minute and immediately placed on ice for 2 minutes. Super optimal broth medium with catabolite repression (SOC) (400 µl), pre-warmed to 37°C, was added, and the cells were incubated at 37°C, 1000 rpm for 1 hour. The cell suspension was plated onto an LB-Agar plate supplemented with the appropriate antibiotic and incubated upside down at 37°C over night.

C.3.6.1. Preparation of SOC medium

Table 14: SOC medium

reagent	
yeast extract (0.5% w/v)	2.5 g
tryptone (2% w/v)	10 g
NaCl (10 mM)	0.29 g
KCl (2.5 mM)	0.09 g
$MgSO_4$ (10 mM)	0.60 g
$MgCl_2$ (10 mM)	0.48 g

After adjusting the pH to 7.5 with NaOH the medium was filled up to 490 ml with dH_2O and sterilized by autoclavation. After it cooled down to RT 10 ml of filter-sterilized 20% glucose was added. Quantity of reagents refers to 500 ml of final volume.

C.3.7. Plasmid DNA isolation and quantification

Plasmid DNA isolation was performed according to the GeneJET Plasmid Miniprep Kit (K0503) by Thermo Scientific, following the instructions provided with the kit. The entire procedure was carried out at room temperature.

A single colony of *E. coli* containing the desired plasmid was incubated in LB-Miller medium (5 ml) with the appropriate antibiotic at 37°C and 180 rpm overnight. The cells were harvested into a pellet by centrifugation of the overnight culture (4ml) in a 2 ml Eppendorf tube, using two consecutive centrifugation steps (6000 RCF, 10 min). After discarding the supernatant, the pellet was resuspended in cold resuspension solution (250 µl) containing RNase A, followed by addition of lysis solution (250 µl), and thorough mixing by inversion. Next neutralization solution (350 µl) was added and mixed by inversion. Cell debris and chromosomal DNA were removed by centrifugation (>16000 RCF, 5 min), and the supernatant

decanted into a supplied spin column without disturbing the precipitate. The column was centrifuged at >16000 RCF for 1 min, and then washed twice with washing solution (500 µl) containing EtOH. The flowthrough was discarded, and the column was centrifuged for 1 min to remove residual washing solution. The spin column was transferred to a fresh 1.5 ml Eppendorf tube and incubated for 5 min at 60°C to evaporate residual EtOH. Finally, plasmid DNA was eluted with nuclease-free water (50 µl) by centrifugation at >16000 RCF for 2 min. The purified plasmid-DNA was quantified using a NanoDrop® (NanoDrop™ OneC Microvolume UV-Vis Spectrophotometer, Thermo Scientific) in the measurement mode "dsDNA" using 1.0 µl of the sample.

Sequencing was performed by Microsynth AG via Sanger Sequencing. To afford optimal results plasmid concentrations should be between 40 and 100 ng/µl.

C.3.8. Preparation of cryostocks

A single colony of the desired strain was incubated overnight in LB-Miller medium (5 ml) at 37°C and 180 rpm. Subsequently the culture (500 µl) was combined with 60% glycerol (500 µl) in a cryogenic vial and stored at -80°C.

C.3.9. Enzyme expression

C.3.9.1. Cultivation

LB medium (5 ml) was supplemented with the appropriate antibiotic (0.1 % v/v), inoculated with the desired strain, and incubated in an orbital shaker at 37 °C, 180 rpm over-night. Pre-cultivated bacteria (1 % v/v) were transferred to an Erlenmeyer-flask filled to 1/5 of the volume with terrific broth medium (TB) containing the same concentration of antibiotic as before. They were incubated at 37 °C, 180 rpm for 2- 3 hours to reach an OD_{590} of 0.6-0.8. Then IPTG, L-Arabinose (L-Ara) or L-Rhamnose (L-Rha) were added to the respective final concentration and the flask was transferred to an orbital shaker and incubated for 18-22 h at 180 rpm (temperature depending on expressed enzyme).

C.3.9.2. Preparation of CFEs

All further steps were carried out at 4 ºC to protect the enzyme against inactivation. The overnight culture containing expressed recombinant cells was centrifuged at 4000 RCF, 4 ℃ for 10 min, and cells were collected. Cell pellets were washed once with buffer, after centrifugation resuspended in buffer and PMSF (100 µM) was added. The crude cell extract was sonicated by a Bandelin KE76 sonotrode connected to a Bandelin Sonoplus HD 3200 in

9 cycles (5s pulse, 55s break, amplitude 50 %). Cell debris and aggregates were removed by centrifugation (15000 g, 25 min, 4 ºC).

C.3.10. Protein purification

Cultivation of the desired strain was conducted as described in **section C.3.9.**

C.3.10.1. Partial purification by heat shock

Protein purification by heat shock could be performed on thermostable proteins such as BVMOs from *Thermobifida fusca*.[84] After cell-disruption the samples were incubated at 50°C for 1 hour. Subsequently the samples were centrifuged for 25 minutes at 14000 RCF to remove denatured proteins.

C.3.10.2. Purification by Ni-NTA-Agarose IMAC

To purify the protein, 1 ml HisTrapTM FF prepacked Ni SepharoseTM columns (17-5255-01, GE Healthcare) were used, following these steps: The precharged column was washed with dH2O (5 ml) and equilibration buffer (5 ml). The CFEs were prepared according to **section C.3.9** and filtered through a 0.2 µm cellulose acetate syringe filter. CFEs were slowly loaded onto the column and washed with equilibration buffer (10 ml). Elution was performed with elution buffer (10 ml) and fractions were collected in 2 ml tubes. The flow-through during sample loading and washing was collected and analysed as well. Analysis was done via SDS-PAGE. Eluates containing the target protein were pooled and concentrated with a centrifugal membrane concentrator (UFC901024, Millipore) with a molecular weight cutoff of 10 kDa. After five rounds of purification, the column was stripped and recharged. This was done by purging the column with dH_2O (5 ml) and stripping buffer (10 ml), followed by washing with binding buffer (5 ml) and dH_2O (10 ml). For recharging, Ni_2SO_4 solution (0.5 ml, 0.1 M) was applied to the column.

C.3.10.3. Buffers IMAC

Table 15: Buffers for Immobilized Metal Affinity Chromatography

component	equilibration buffer pH 7.2	elution buffer pH 7.2	desalting buffer pH 7.2	stripping buffer pH 7.5	molecular weight g/mol
Na_2HPO_4	3.55 g (25 mM)	3.55 g (25 mM)	1.89 g (33.3 mM)	-	141.96
NaH_2PO_4	3.00 g (25 mM)	3.00 g (25 mM)	0.80 g (16.7 mM)	-	119.98
NaCl	17.53 g (300 mM)	17.53 g (300 mM)	-	2.92 g (500 mM)	58.44
Glycerol	100 ml (10% v/v)	100 ml (10% v/v)	-	-	92.09
Imidazole	2.04 g (30 mM)	27.2 g (400 mM)	-	-	68.08
Tris-HCl	-	-	-	0.606g (50 mM)	121.14
EDTA	-	-	-	20 ml of 250mM EDTA (pH 8)	292.24

C.3.10.4. Purification by SEC

Protein purification via size exclusion (SEC) was performed on an ÄKTA purification system. All samples and buffers were filtrated before use.

Table 16: Running Buffer for SEC

component	
K_2HPO_4	8.14 g
KH_2PO_4	0.44 g
NaCl (200mM)	9.35 g

The components account for 800 ml of total volume. The pH was adjusted to 8.0 with NaOH/HCl.

C.3.11. BCA assay total protein amount

To determine the total protein concentration, a bicinchoninic acid (BCA) assay was performed using a protein standard. The working reagent was prepared by mixing reagent A and reagent B (BCA Protein Assay Kit Thermo Scientific) in a 50:1 ratio. After diluting the protein solution 1:10 in dH_2O 25 µl of the diluted protein solution was transferred to a 96 well plate. The samples were mixed with working reagent (200 µl) by pipetting and incubated at 37°C for 30 minutes. Absorbance was measured at 562 nm using a Tecan Spark® plate reader and the protein concentration was determined using the BSA calibration curve.

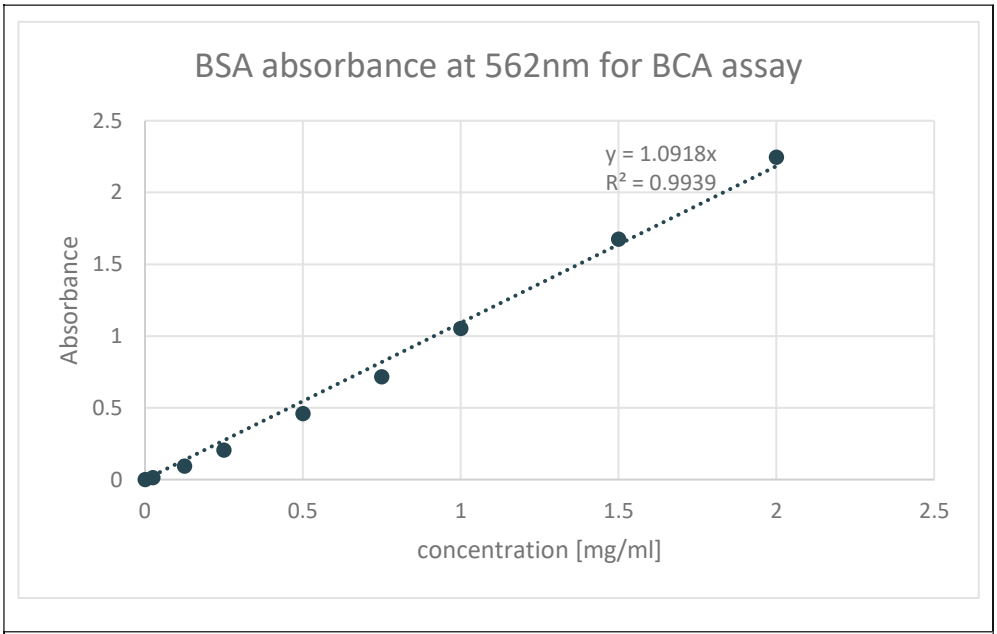

Figure 49. BSA calibration curve

C.3.12. Biotransformations

Optimized enzyme production was performed as described in **section C.3.9**. Expression conditions for single enzymes are summarized in **section D.1.** Total protein concentration was checked prior to biotransformations as described in **section C.3.11.**

The reactions were performed between 25°C and 37°C (220 rpm) depending on the enzymes applied. Biotransformations were carried out in 1.0 ml total volume with 5 mM of substrate applied. Protein concentration of CFE varied between 1.0 and 4.0 mg/ml. For redox enzymes concentrations between 0.5 mM and 5.25 mM of the appropriate cofactor, when needed together with a suitable recycling system, were added from 0.5 M freshly prepared stock solutions. The substrate was added last and after the mixture was briefly vortexed a T_0 sample

was taken and analysed as described in **section C.3.13.** and **C.3.14.** After different time intervals more samples were taken and analysed.

C.3.13. GC analysis

GC-analysis was performed on Thermo Scientific Trace Dual, Restek Rtx-5, 10250. The method applied for GC analysis was equal for every compound. It was performed as described below:

7 min
Initial temperature of 80 °C
hold 0.5 min, ramp 1 at 40 °C
min^{-1} to 220 °C, ramp 2 at 80 °C
min^{-1} to 300 °C, hold 1 min

C.3.13.1. Standard calibration

Standards in concentrations of 0.1, 0.5, 1, 2 and 4 mM were prepared in ethyl acetate (EtOAc) containing 1 mM of internal standard (methyl benzoate) and filtrated with 0.2 µm PTFE syringe filters prior to measurement.

C.3.13.2. Sample preparation

A volume of 150 µl was taken from the reaction vessel and added to a 1.5 ml Eppendorfer tube. Extraction was performed by adding EtOAc (300 µl) containing internal standard (1 mM methyl benzoate) and vigorous vortexing. The organic fraction was dried over Na_2SO_4. Finally, the samples were filtrated with 0.2 µm PTFE syringe filters, filled into glass vials with inlets and fitted with GC caps.

C.3.14. HPLC analysis

HPLC-Analysis was performed on a Jasco-HPLC system equipped with an Eclipse XDB-C18 column. The method applied for HPLC analysis had to be evaluated beforehand and differed for some of the compounds.

C.3.14.1. Standard Calibration

Standards in concentrations of 0.1, 0.5, 1, 2 and 4 mM were prepared in a 1:1 mixture of acetonitrile and dH_2O and filtrated with 0.2 µm PTFE syringe filters prior to measurement.

C.3.14.2. Sample preparation

A volume of 150 µl was taken from the reaction vessel and added to a 1.5 ml Eppendorfer tube. To the sample acetonitrile (150 µl) was added and vigorously vortexed. Finally, the samples were filtrated with 0.2 µm PTFE syringe filters, filled into glass vials equipped with inlets and fitted with HPLC caps.

D. Experimental Part

D.1. Enzyme library

Table 17: Enzyme attributes

Enzyme	Enzyme Class	Primary host	Reference	Gene Size	Amino acids	Molecular mass
PAMO	BVMO	*Thermobifida fusca*	Uniprot: Q47PU3 [35]	1629 bp	542	61 kDa
PfeI	Esterase	*Pseudomonas fluorescens*	Uniprot: P22862[68,85]	1196 bp	272	30 kDa
HLADH [a]	ADH	*Equus caballus*	Uniprot: P00327[69]	1761 bp	375	40 kDa
plK10 (YCR107w)	ADH	*Saccharomices cerevisiae*	Uniprot: P25612[70]	1092 bp	363	40 kDa
plK25 (YMR318c)	ADH	*Saccharomices cerevisiae*	Uniprot: Q04894[71]	1083 bp	360	40 kDa
plK32 (YCR105w)	ADH	*Saccharomices cerevisiae*	Uniprot: P25377 [72]	1086 bp	361	39 kDa
SDR B6 [b]	ADH	*Cupriavidus necator*	Uniprot: Q0K517[73]	750 bp	249	25 kDa
SDR B3 [b]	ADH	*Cupriavidus necator*	Uniprot: Q0K1N7[73]	765 bp	254	26 kDa
His6-SDR B3 [b]	ADH	*Cupriavidus necator*	Uniprot: Q0K1N7[73]	793 bp	260	26 kDa
PDH_loopN [c]	ADH	*Deinococcus geothermalis*	Uniprot: Q1J3W1[74]	1161 bp	386	42 kDa
ChnD [c]	ADH	*Acinetobacter sp.*	Uniprot: Q7WVD0[75]	1059 bp	352	37 kDa

[a] Obtained from Dr. Diederik Johannes Opperman (University of Free State, South Africa)

[b] Obtained from Prof. Margit Winkler (TU Graz, Austria)

[c] Obtained from Prof. Uwe Bornscheuer (University of Greifswald, Germany)

Table 18: Growth and expression parameters

Enzyme	*E. coli strain*	*Vector*	*Resistance*	*Inducer*	*Inducer conc.*	*OD590 induction*	*Temp. [°C]*	***Speed** [rpm]*	*Time [h]*
PAMO	Top 10	pBADNK	AMP	L-Ara	0.02% v/v	0.6-0.8	25	140 rpm	22
PfeI	$DH5_{\alpha}$	pGaston	AMP	L-Rha	0.2% v/v	0.3	37	140 rpm	3
*HLADH**	BL21(DE3)	pET28b	KAN	IPTG	0.5 mM	0.6-0.8	25	140 rpm	22
plK10 (YCR107w)	BL21(DE3)		KAN	IPTG	0.5 mM	0.6-0.8	25	140 rpm	22
plK25 (YMR318c)	BL21(DE3)		KAN	IPTG	0.5 mM	0.6-0.8	25	140 rpm	22
plK32 (YCR105w)	BL21(DE3)		KAN	IPTG	0.5 mM	0.6-0.8	25	140 rpm	22
*SDR B6**	Top 10	pk470	KAN	IPTG	0.1 mM	0.6-0.8	28	140 rpm	22
*SDR B3**	K13 XL1 Blue	pk470	KAN	IPTG	0.1 mM	0.6-0.8	28	140 rpm	22
*His6-SDR B3**	Top 10	pk470	KAN	IPTG	0.1 mM	0.6-0.8	28	140 rpm	22
*PDH_loopN**	BL21(DE3)	pET22b	AMP	IPTG	0.1mM	0.8-1.0	37	140 rpm	6
*ChnD**	BL21(DE3)	pET28a	KAN	IPTG	0.5mM	0.6-0.8	22	140 rpm	22

* $ZnSO_4$ was added after induction at a concentration of 250µM

D.2. Sequencing of enzyme plasmids

Prior to use sequencing was performed on all enzyme plasmids to check for possible mutations.

Point mutations were detected in the constructs plK25 and plK32. These had to be corrected by mutagenesis before being able to continue working with them, since insertion/deletion of basepairs (bp) caused a frameshift resulting into a stop-codon prohibiting the expression of a functional enzyme.

Table 19: Primers used for verification of plasmid sequence

plasmid	*primer*	*sequence*
PAMO	pBAD-for	ATGCCATAGCATTTTTATCC
	pBAD-rev	GATTTAATCTGTATCAGG
PfeI	pG_FW	CTTTCCCTGGTTGCCAATGG
	pG_RV	GCTTCTGCGTTCTGATTTAATC
pET28b_HLADH	T7-probis	TCCCGCGAAATTAATACG
	T7-terbis	AACCCCTCAAGACCCG
plK10	T7-probis	TCCCGCGAAATTAATACG
	T7-terbis	AACCCCTCAAGACCCG
plK25	T7-probis	TCCCGCGAAATTAATACG
	T7-terbis	AACCCCTCAAGACCCG
plK32	T7-probis	TCCCGCGAAATTAATACG
	T7-terbis	AACCCCTCAAGACCCG
pk470_SDRB6	Lac-Op-for	CGGATAACAATTTCACACAG
	LCO-1490	GGTCAACAAATCATAAAGATATTGG
pk470_SDRB3	Lac-Op-for	CGGATAACAATTTCACACAG
	LCO-1490	GGTCAACAAATCATAAAGATATTGG
pk470_6-HisSDRB3	Lac-Op-for	CGGATAACAATTTCACACAG
	LCO-1490	GGTCAACAAATCATAAAGATATTGG
pET22b_PDHloopN	T7-probis	TCCCGCGAAATTAATACG
	T7-terbis	AACCCCTCAAGACCCG
pET28a_ChnD	T7-probis	TCCCGCGAAATTAATACG
	T7-terbis	AACCCCTCAAGACCCG

D.3. Correction of mutations via site-directed mutagenesis

Site-directed mutagenesis was performed with Q5® Site-Directed Mutagenesis Kit as described in section **C.3.2**.

D.3.1. Correction of plK25

Primers used for the mutagenesis of plK25 for removal of insertion of G/C at position 739:
pMAX001: GTCTTATCCTGAGAAATTTGAAGG
pMAX002: ATATGACGCGGAACCAGA

An agarose gel-electrophoresis was performed to evaluate the success of the mutagenesis. Afterwards the mutated plasmid was sequenced.

Table 20:Thermocycling conditions plK25

step	*temp*	*time*	*cycles*
initial denaturation	98°C	30 sec	1
denaturation	98°C	10 sec	
annealing	62°C	30 sec	30
extension	72°C	3 min 15 sec	
terminal extension	72°C	2 min.	1
hold	4°C	∞	

D.3.2. Correction of plK32

Primers used for the mutagenesis of plK32 to removal of insertion of C/G at position 740/741:

pMAX003: CAGAAAAATTTCAGGGCATC
pMAX004: GGTAAAGCATATGACGCG

Thermocycling conditions applied as described in **section D.3.1.**, T_a used for pMAX003 and pMAX004: 58°C

Successful mutation could not be confirmed via gel electrophoresis, so a new primer pair with larger overhangs was designed. The following primers were used:

pMAX005: AGAAAAATTTCAGGGCATCG
pMAX006: GGGTAAAGCATATGACGC

Thermocycling conditions applied as described in **section D.3.1.**, T_a used for pMAX005 and pMAX006: 61°C

An agarose gel-electrophoresis was performed to evaluate the success of the mutagenesis. Afterwards the mutated plasmid was sequenced.

D.4. Characterization of single enzymes

All desired enzymes were already present in appropriate vectors for expression. *E. coli* strains

containing the corresponding vectors were cultured using standard conditions of cultivation as described in **section C.3.9**. The total protein content was assessed through BCA Assay and SDS-PAGE, as described in **sections C.3.11** and **C.3.1** The expression conditions have been summarized in **section D.1, Table 18**. CFEs and cryostocks were prepared as described in **sections C.3.9.1** and **C.3.9.2.** Standard reaction conditions for biotransformations with CFEs are described in **section C.3.12**. Reaction monitoring was performed via calibrated GC and HPLC, as described in **sections C.3.13** and **C.3.14.**

D.4.1. PAMO – Oxidation of phenylpropanones to benzylacetates

Enzyme Expression by L-Ara induction

A preculture was started with the *E. coli* Top10 cells harbouring plasmid PAMO. Optimized enzyme production was performed following the protocol for cultivation in **section C.3.9**. The CFE and cryostocks were prepared. The enzyme AlkJ (60kDa) was used as a reference enzyme.

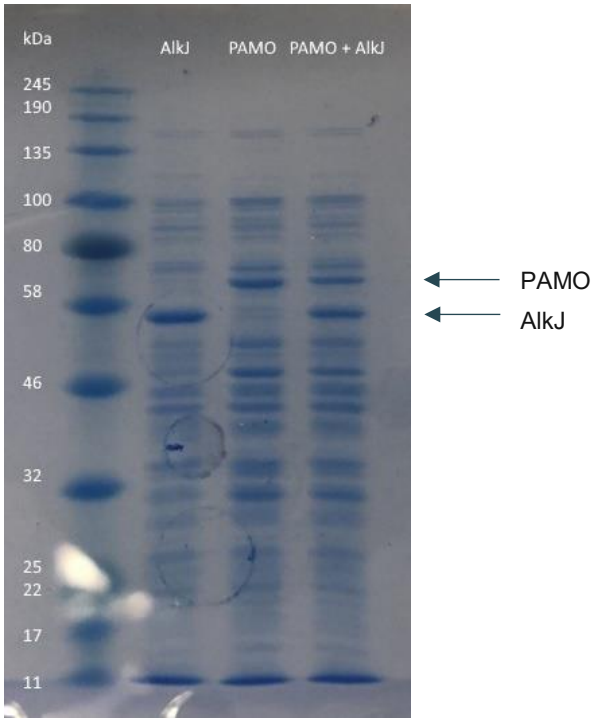

Figure 50: SDS-PAGE of PAMO and AlkJ

Verification of biocatalytic activity

Oxidation activity of the enzyme was verified by the conversion of 5 mM Phenylacetone **1b** to Benzylacetate **1c** in CFE and subsequently to **1d** (by addition of esterase) at 37 °C, 220 rpm. Full conversion to **1d** was observed after 1 hour reaction time **(section B.1.1, figure 20)**.

D.4.2. PfeI – Hydrolysis of benzyl acetates to benzyl alcohols

Enzyme expression by L-Rha induction

A preculture was started with the *E. coli* DH5α cells harbouring plasmid pGaston_PfeI. Optimized enzyme production was performed following the protocol for cultivation in **section C.3.9**. After 3 hours of cultivation the cells were harvested by centrifugation (6000 RCF., 10 min.) and resuspended in 10 ml of sterile water in a 15 ml falcon tube. After snap-freezing the suspension in liquid nitrogen the tube was placed into a 1000 ml round bottom and lyophilized for 24 hours, leading to a dry off-white powder which was stored at -80 °C.

Verification of biocatalytic activity

Hydrolysis activity of the enzyme was verified by the conversion of 5 mM Benzylacetate **1c** to benzyl alcohol **1d** at 37 °C, 220 rpm. Full conversion to **1d** was observed after 1 hour reaction time **(B.1.2, figure 22)**.

D.4.3. HLADH – Oxidation of benzylalcohols to benzaldehydes

Enzyme expression by IPTG induction

A preculture was started with the *E. coli* BL21(DE3) cells harbouring plasmid pET28b_HLADH. Optimized enzyme production was performed following the protocol for cultivation in **section C.3.9**. After induction 250 µM of $ZnSO_4$ were added to ensure correct expression of the protein.

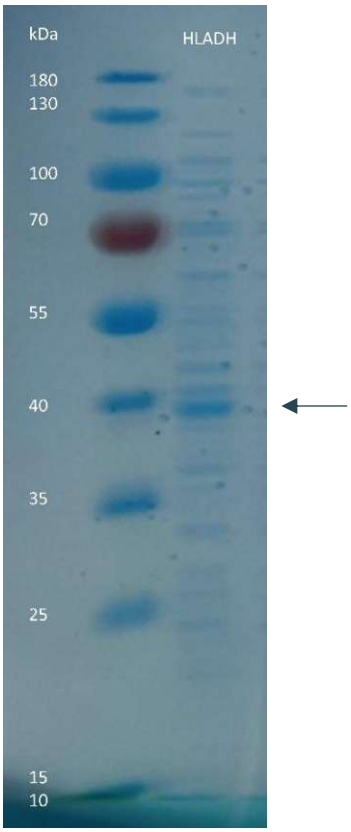

Figure 51: SDS-PAGE of HLADH

Substrate acceptance screening

Oxidation activity of the enzyme was verified by the conversion of 5 mM benzylalcohols **1d-8d** to benzaldehydes **1e-8e** at 28 °C, 220 rpm. **(B.2.1.1, figure 26)**.

D.4.4. plK10 - Oxidation of benzylalcohols to benzaldehydes

Enzyme expression by IPTG induction

A preculture was started with the *E. coli* BL21(DE3) cells harbouring plasmid plK10 and incubated in an orbital shaker at 37 °C, 180 rpm over-night. Pre-cultivated bacteria (1 % v/v) were transferred to an Erlenmeyer-flask filled to 1/5 of the volume with TB medium containing the same concentration of antibiotic as before. They were incubated at 37 °C, 180 rpm for 2-3 hours to reach an OD_{590} of 0.6-0.8. Then IPTG and glucose were added was added to the final concentration of 0.5 mM and 0.25% v/v respectively. After 2 hours of incubation at 37°C and 180 rpm glucose was added to the final concentration of 0.5% v/v overall and incubated overnight under the same conditions.

Substrate acceptance screening

Oxidation activity of the enzyme was verified by the conversion of 5 mM benzylalcohols **1d-**

8d to benzaldehydes **1e-8e** at 28 °C, 220 rpm. **(B.2.1.2, figure 27)**.

D.4.5. pIK25 - Oxidation of benzylalcohols to benzaldehydes

Enzyme expression by IPTG induction

A preculture was started with the *E. coli* BL21(DE3) cells harbouring plasmid pIK25. Optimized enzyme production was performed following the protocol for cultivation of pIK enzymes described in **section D.4.4.**

Substrate acceptance screening

Oxidation activity of the enzyme was verified by the conversion of 5 mM benzylalcohols **1d-8d** to benzaldehydes **1e-8e** at 28 °C, 220 rpm. **(B.2.1.3, figure 28)**.

D.4.6. pIK32 - Oxidation of benzylalcohols to benzaldehydes

Enzyme expression by IPTG induction

A preculture was started with the *E. coli* BL21(DE3) cells harbouring plasmid pIK25. Optimized enzyme production was performed following the protocol for cultivation of pIK enzymes described in **section D.4.4**.

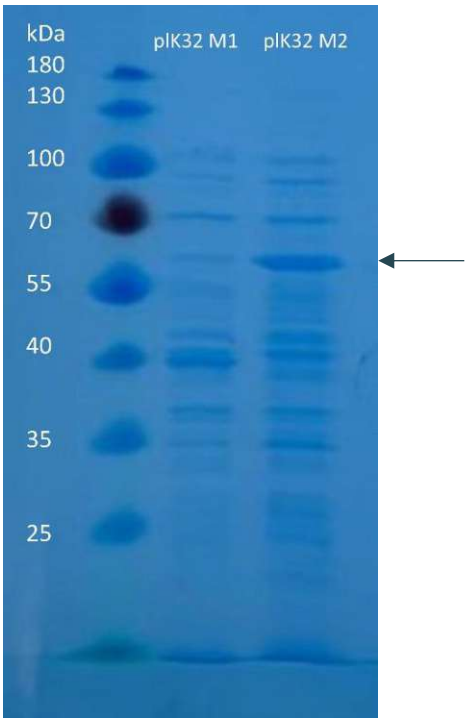

Figure 52: SDS-PAGE of pIK32 Mutant 1 and 2 (GST-fusion protein: 40 kDa + 20 kDa = 60 kDa)

Substrate acceptance screening

Oxidation activity of the enzyme was verified by the conversion of 5 mM benzylalcohols **1d-8d** to benzaldehydes **1e-8e** at 28 °C, 220 rpm. **(B.2.1.4, figure 29)**.

D.4.7. SDR-B6 - Oxidation of benzylalcohols to benzaldehydes

Enzyme expression by IPTG induction

A preculture was started with the *E. coli* BL21(DE3) cells harbouring plasmid pk470_SDRB6. Optimized enzyme production was performed following the protocol for cultivation in **section C.3.9**. After induction 250 µM of $ZnSO_4$ were added to ensure correct expression of the protein.

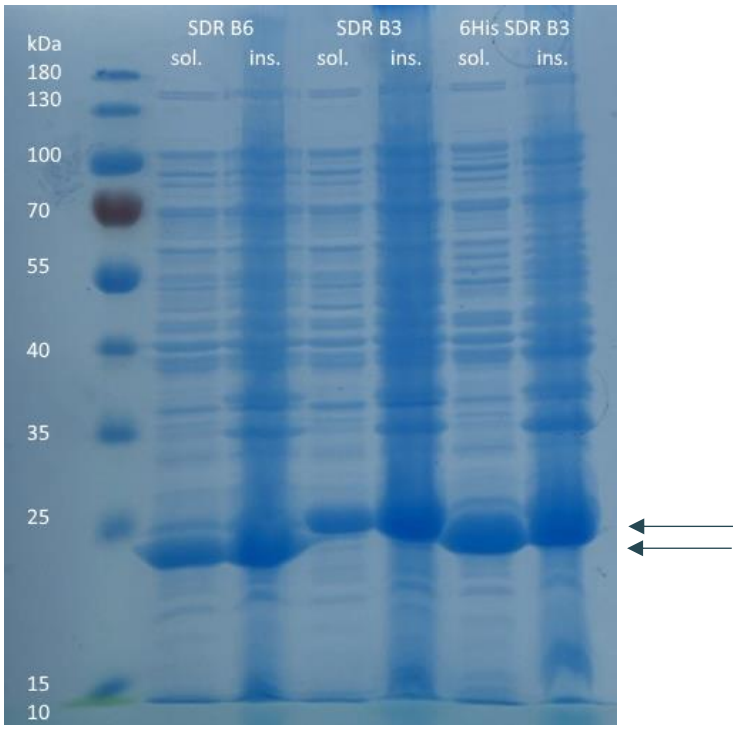

Figure 53: SDS-PAGE of SDRB6, SDRB3 and 6HisSDRB3

Substrate acceptance screening

Oxidation activity of the enzyme was verified by the conversion of 5 mM benzylalcohols **1d-8d** to benzaldehydes **1e-8e** at 28 °C, 220 rpm. **(B.2.1.5, figure 30)**.

D.4.8. SDR-B3 - Oxidation of benzylalcohols to benzaldehydes

Enzyme expression by IPTG induction

A preculture was started with the *E. coli* BL21(DE3) cells harbouring plasmid pk470_SDRB3. Optimized enzyme production was performed following the protocol for cultivation in **section C.3.9**. After induction 250 µM of $ZnSO_4$ were added to ensure correct expression of the

protein. SDS-PAGE of the enzyme can be seen in **section D.4.7. figure 49.**

Substrate acceptance screening

Oxidation activity of the enzyme was verified by the conversion of 5 mM benzylalcohols **1d-8d** to benzaldehydes **1e-8e** at 28 °C, 220 rpm. **(B.2.1.6, figure 31)**.

D.4.9. 6His-SDR-B3 - Oxidation of benzylalcohols to benzaldehydes

Enzyme expression by IPTG induction

A preculture was started with the *E. coli* BL21(DE3) cells harbouring plasmid pk479_6HisSDRB3. Optimized enzyme production was performed following the protocol for cultivation in **section C.3.9**. After induction 250 µM of $ZnSO_4$ were added to ensure correct expression of the protein. SDS-PAGE of the enzyme can be seen in **section D.4.7. figure 49.**

Substrate acceptance screening

Oxidation activity of the enzyme was verified by the conversion of 5 mM benzylalcohols **1d-8d** to benzaldehydes **1e-8e** at 28 °C, 220 rpm. **(B.2.1.7, figure 32)**.

D.4.10. PDHloopN - Oxidation of benzylalcohols to benzaldehydes

Enzyme expression by IPTG induction

A preculture was started with the *E. coli* BL21(DE3) cells harbouring plasmid pET22b_PDHloopN. Pre-cultivated bacteria (1 % v/v) were transferred to an Erlenmeyer-flask filled to 1/5 of the volume with TB medium containing the same concentration of antibiotic as before. Protein expression was induced at an OD_{590} of 0.8–1.0 with 0.1 mM IPTG. 250 µM $ZnSO_4$ were added to ensure correct expression of the protein. After 4–6 h of protein expression at 37°C cells were harvested as described in **section C.3.9.**

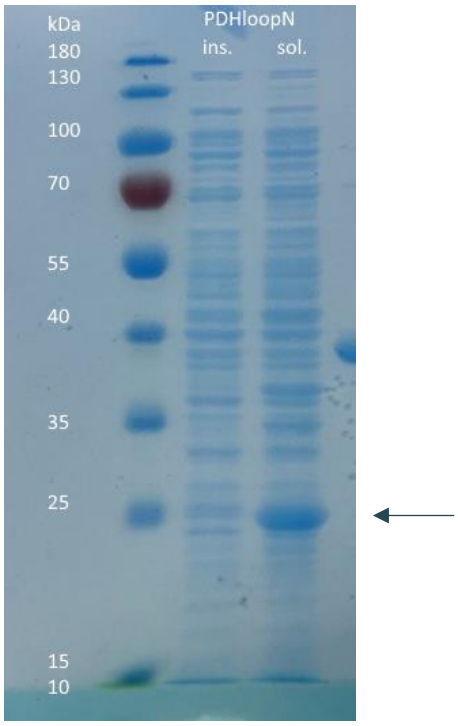

Figure 54: SDS-PAGE of PDHloopN

Substrate acceptance screening

Oxidation activity of the enzyme was verified by the conversion of 5 mM benzylalcohols **1d-8d** to benzaldehydes **1e-8e** at 45 °C, 220 rpm. **(B.2.1.8, figure 33 and 34)**.

D.4.11. ChnD - Oxidation of benzylalcohols to benzaldehydes

Enzyme expression by IPTG induction

A preculture was started with the *E. coli* BL21(DE3) cells harbouring plasmid pET28a_ChnD. Optimized enzyme production was performed following the protocol for cultivation in **section C.3.9**. After induction 250 µM of $ZnSO_4$ were added to ensure correct expression of the protein.

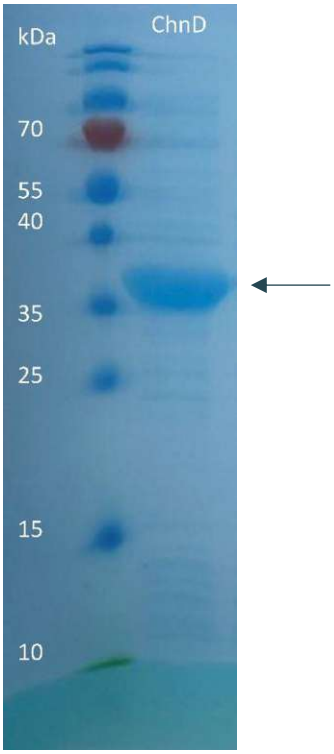

Figure 55: SDS-PAGE of ChnD

Substrate acceptance screening

Oxidation activity of the enzyme was verified by the conversion of 5 mM benzylalcohols **1d-8d** to benzaldehydes **1e-8e** at 30 °C, 220 rpm. **(B.2.1.9, figure 35)**.

D.5. Synthesis of substrates for biotransformations

D.5.1. General procedure for Wacker-Tsuji oxidations

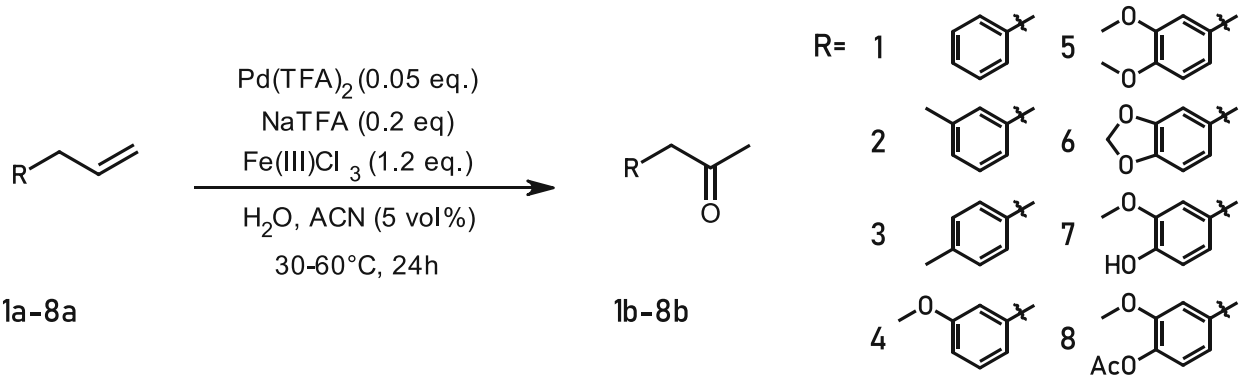

Procedure

To a round bottomed flask, fitted with a septum and a magnetic stirbar, $Pd(TFA)_2$, NaTFA and $FeCl_3$ were added. The vessel was flushed with the standard Schlenk technique. Water was degassed by three freeze-pump-thaw cycles and added via a syringe. A solution of allylbenzene **1a-8a** in ACN was added dropwise. The mixture was stirred for 24 hours at 30°-60°C, reaction control was carried out via TLC. After complete conversion the mixture was extracted with EtOAc, the combined organic phases dried over Na_2SO_4 and the solvent removed under reduced pressure.[86]

D.5.2. Synthesis of 1-phenylpropan-2-one 1b

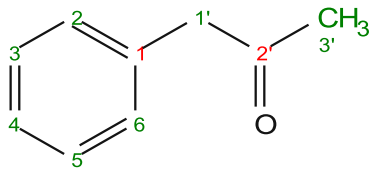

1b

$C_9H_{10}O$

MW: 134.18 g/mol

1b was prepared according to the general procedure for Wacker-Tsuji oxidations (**section E.5.1**). The reaction was carried out at 45 °C with $PdTFA_2$ (4.1 mg, 5 mol%), 1a (44 mg, 0.25 mmol, 1.0 equiv.) and FeCl3 (60 mg, 0.375 mmol, 1.5 equiv.).

Purification: column chromatography (PE/EtOAc 4:1)

Yield: 23% (GC)

Appearance: yellow oil

^{1}H NMR($CDCl_3$, 400 MHz): δ (ppm) 7.41 – 7.26 (m, 4H, 2, 3, 5, 6), 7.26 – 7.20 (m, 1H, 4), 3.72 (s, 2H, 1'), 2.18 (s, 3H, 3')

Spectrum in accordance to literature[87]

D.5.3. 1-(3-methylphenyl)propan-2-one 2b

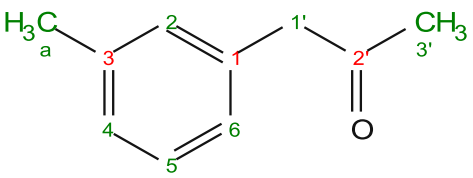

2b

$C_{10}H_{12}O$

MW: 148.20 g/mol

2b was prepared according to the general procedure for Wacker-Tsuji oxidations. The reaction was carried out at 30 °C with $PdTFA_2$ (18.9 mg, 0.055 mmol, 0.05 equiv.), NaTFA (29.9 mg, 0.22 mmol, 0.2 equiv.), 2a (150 mg, 1.1 mmol, 1.0 equiv.) and $FeCl_3$ (214 mg, 1.32 mmol, 1.2 equiv.).

Purification: column chromatography (PE/EtOAc 4:1-1:1)

Yield: 32% (after purification)

Appearance: colorless oil

^{1}H NMR($CDCl_3$, 400 MHz): δ (ppm) 7.23 (t, *J*=7.5 Hz, 1H, 5), 7.09 (d, *J*=7.6 Hz, 1H, 6), 7.04 – 6.98 (m, 2H, 2, 4), 3.66 (s, 2H, 1'), 2.34 (s, 3H, a), 2.16 (s, 3H, 3')

Spectrum in accordance to literature[87]

D.5.4. 1-(4-methylphenyl)propan-2-one 3b

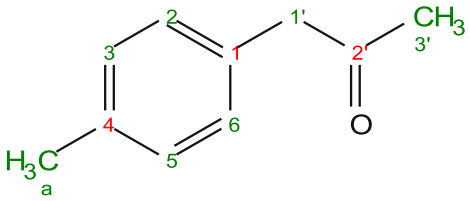

3b

$C_{10}H_{12}O$

MW: 148.20 g/mol

2b was prepared according to the general procedure for Wacker-Tsuji oxidations. The reaction was carried out at 30 °C with $PdTFA_2$ (18.9 mg, 0.055 mmol, 0.05 equiv.), NaTFA (29.9 mg, 0.22 mmol, 0.2 equiv.), 2a (150 mg, 1.1 mmol, 1.0 equiv.) and FeCl3 (214 mg, 1.32 mmol, 1.2 equiv.).

Purification: column chromatography (PE/EtOAc 4:1-1:1)

Yield: 33% (after purification)

Appearance: colorless oil

^{1}H NMR($CDCl_3$, 400 MHz): δ (ppm) 7.15 (d, *J*=8.0 Hz, 2H, 3, 5), 7.09 (d, *J*=8.0 Hz, 2H, 2, 6), 3.66 (s, 2H, 1'), 2.34 (s, 3H, a), 2.15 (s, 3H, 3')

Spectrum in accordance to literature[87]

D.5.5. 1-(4-methoxyphenyl)propan-2-one 4b

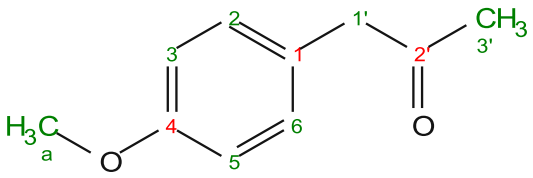

4b

$C_{10}H_{12}O_2$

MW: 164.20 g/mol

4b was prepared according to the general procedure for Wacker-Tsuji oxidations. The reaction was carried out at 45 °C with $PdTFA_2$ (18.9 mg, 0.055 mmol, 0.05 equiv.), **3a** (150 mg, 1.1 mmol, 1.0 equiv.) and $FeCl_3$ (214 mg, 1.32 mmol, 1.2 equiv.).

Purification: column chromatography (PE/EtOAc 4:1-1:1)

Yield: 33% (after purification)

Appearance: colorless oil

^{1}H NMR (400 MHz, $CDCl_3$) δ 7.16 – 7.08 (m, 2H, 3, 5), 6.91 – 6.83 (m, 2H, 2, 6), 3.80 (s, 3H, a), 3.63 (s, 2H, 1'), 2.14 (s, 3H, 3').

Spectrum in accordance to literature[87]

D.5.6. 1-(3,4-dimethoxyphenyl)propan-2-one 5b

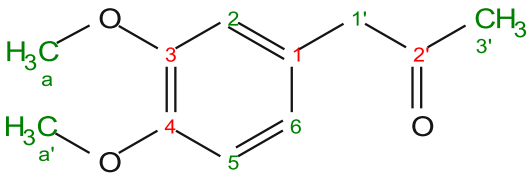

5b

$C_{11}H_{14}O_3$

MW: 194.23 g/mol

5b was prepared according to the general procedure for Wacker-Tsuji oxidations. The reaction was carried out at 60 °C with $PdTFA_2$ (14.3 mg, 0.042 mmol, 0.05 equiv.), NaTFA (22.7 mg, 0.17 mmol, 0.2 equiv.), 5a (150 mg, 0.833 mmol, 1.0 equiv.) and $FeCl_3$ (162mg, 1.00 mmol, 1.2 equiv.).

Purification: column chromatography (PE/EtOAc 4:1-1:1)

Yield: 52% (GC)

Appearance: colorless oil

^{1}H NMR($CDCl_3$, 400 MHz): δ (ppm) 6.84 (d, *J*=8.1 Hz, 1H, 6), 6.75 (dd, *J*=8.1, 2.0 Hz, 1H, 5), 6.71 (d, *J*=2.0 Hz, 1H, 2), 3.87 (s, 6H, a', a), 3.63 (s, 2H, 1'), 2.15 (s, 3H, 3')

Spectrum in accordance to literature[87]

D.5.7. 1-(2H-1,3-benzodioxol-5-yl)propan-2-one 6b

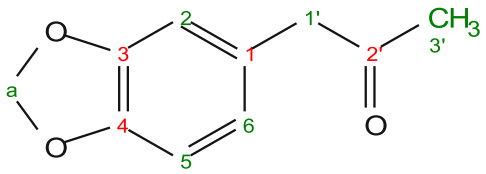

6b

$C_{10}H_{10}O_3$

MW: 178.18 g/mol

6b was prepared according to the general procedure for Wacker-Tsuji oxidations. The reaction was carried out at 60 °C with $PdTFA_2$ (15.8 mg, 0.046 mmol, 0.05 equiv.), NaTFA (25.1 mg, 0.19 mmol, 0.2 equiv.), 6a (150 mg, 0.92 mmol, 1.0 equiv.) and FeCl3 (180mg, 1.11 mmol, 1.2 equiv.).

Purification: column chromatography (PE/EtOAc 4:1-1:1)

Yield: 58% (GC)

Appearance: orange oil

^{1}H NMR($CDCl_3$, 400 MHz): δ (ppm) 6.77 (d, *J*=7.9 Hz, 1H, 6), 6.70 – 6.61 (m, 2H, 2, 5), 5.95 (s, 2H, a), 3.60 (s, 2H, 1'), 2.15 (s, 3H, 3')

Spectrum in accordance to literature[87]

D.5.8. 1-(4-hydroxy-3-methoxyphenyl)propan-2-one 7b

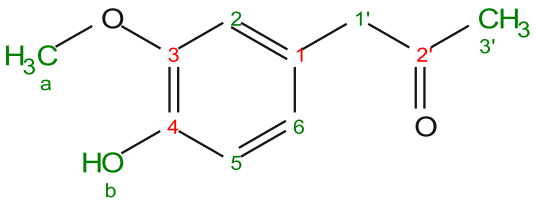

7b

$C_{10}H_{12}O_3$

MW: 180.08 g/mol

7b was prepared according to the general procedure for Wacker-Tsuji oxidations. The reaction was carried out at 45 °C with $PdTFA_2$ (4.28 mg, 0.0125 mmol, 0.05 equiv.), NaTFA (6.8 mg, 0.05 mmol, 0.2 equiv.), 6a (41.5 mg, 0.25 mmol, 1.0 equiv.) and $FeCl_3$ (48.7mg, 0.3 mmol, 1.2 equiv.).

Purification: column chromatography (PE/EtOAc 4:1-1:1)

Yield: 40% (GC)

Appearance: colorless oil

^{1}H NMR($CDCl_3$, 600 MHz): δ (ppm) 6.87 (d, *J*=7.9 Hz, 1H, 2), 6.73 – 6.67 (m, 2H, 5, 6), 5.58 (s, 1H, b), 3.87 (s, 3H, a), 3.61 (s, 2H, 1'), 2.15 (s, 3H, 3')

Spectrum in accordance to literature[88]

D.5.9. 2-methoxy-4-(2-oxopropyl)phenyl acetate 8b

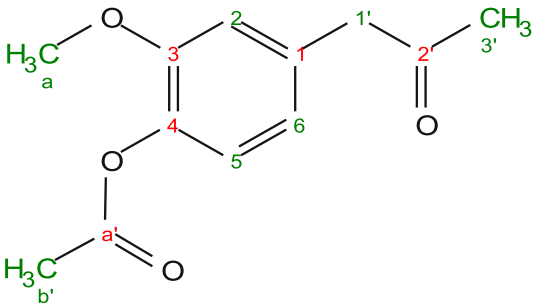

8b

$C_{12}H_{14}O_4$

MW: 222.09 g/mol

After dissolving 1-(4-hydroxy-3-methoxyphenyl)propan-2-one **7b** (1 g, 5.33 mmol, 1.0 equiv.) in aqueous 10% NaOH (3.25 ml, 17.3 mmol, 3.25 equiv.) the solution was cooled by the addition of ice. Acetic anhydride (0.75 ml, 7.85 mmol, 1.5 equiv.) was added to the mixture, which was stirred vigorously for 5 minutes. The heavy oil was separated, and the aqueous layer extracted twice with 10 ml of Diethyl ether. After combining the heavy oil with the organic fractions, they were back extracted twice with 10 ml of 1% NaOH, washed with water, dried over Na_2SO_4 and the solvent removed under reduced pressure.

Purification: column chromatography (PE/EtOAc 4:1-1:1)

Yield: 55% (after purification)

Appearance: colorless oil

^{1}H NMR($CDCl_3$, 600 MHz): δ (ppm) 6.99 (d, *J*=7.9 Hz, 1H), 6.81 – 6.76 (m, 2H), 3.82 (s, 3H, a), 3.67 (s, 2H, 1'), 2.31 (s, 3H, b'), 2.17 (s, 3H, 3')

Spectrum in accordance to literature[89]

E. Appendix

E.1. Primers

Primers which did not afford satisfactory results are highlighted in grey.

Table 21: Primers for mutagenesis

primers for mutagenesis	*sequence*	*T_a [°C]*
pMAX001	GTCTTATCCTGAGAAATTTGAAGG	61
pMAX002	ATATGACGCGGAACCAGA	63
pMAX003	CAGAAAAATTTCAGGGCATC	59
pMAX004	GGTAAAGCATATGACGCG	61
pMAX005	AGAAAAATTTCAGGGCATCG	61
pMAX006	GGGTAAAGCATATGACGC	60

Table 22: Primers used for Sanger-Sequencing (Microsynth AG)

primers for mutagenesis	*sequence*	*T_a [°C]*
LacOp-for	CGGATAACAATTTCACACAG	
LCO-1490	GGTCAACAAATCATAAAGATATTGG	
pBAD-for	ATGCCATAGCATTTTTATCC	
pBAD-rev	GATTTAATCTGTATCAGG	
T7-probis	TCCCGCGAAATTAATACG	
T7-terbis	AACCCCTCAAGACCCG	

E.2. Gene sequences

In this section gene sequences for single enzymes are given. Startcodons are marked in green, possible His-Tags and GST are marked in blue, stop codons are marked in red.

6-His-HLADH

1812 bp

ATGGGCAGCAGCCATCATCATCATCATCACAGCAGCGGCCTGGTGCCGCGCGGCAGCCATATGAGCACAG
CAGGAAAAGTAATAAAATGCAAAGCGGCTGTGCTGTGGGAGGAAAAGAAACCATTTTCCATCGAGGAGGTG
GAGGTTGCACCCCCGAAGGCCCATGAAGTCCGTATAAAGATGGTGGCCACAGGAATTTGTCGCTCAGATGA

CCACGTGGTTAGTGGAACCCTTGTCACACCTCTTCCTGTGATCGCAGGCCATGAGGCAGCGGGCATTGTGG
AGAGCATTGGAGAAGGCGTCACTACAGTAAGACCAGGTGATAAAGTCATCCCACTCTTTACTCCCCAGTGTG
GAAAATGCAGGGTTTGTAAGCACCCTGAAGGCAACTTCTGCTTGAAAAATGATCTGAGCATGCCTCGGGGA
ACCATGCAGGATGGTACCAGCAGGTTCACCTGCAGAGGGAAGCCCATCCACCACTTCCTTGGCACCAGCAC
CTTCTCCCAGTACACCGTGGTGGACGAGATCTCAGTGGCCAAGATCGATGCGGCCTCACCGCTGGAGAAA
GTCTGTCTCATTGGCTGTGGATTTTCTACTGGTTATGGGTCTGCAGTCAAGGTTGCCAAGGTCACCCAGGGC
TCCACCTGTGCCGTGTTTGGCCTTGGAGGAGTGGGCCTGTCTGTTATCATGGGCTGTAAAGCAGCCGGAGC
GGCCAGGATCATTGGGGTGGACATCAACAAAGACAAGTTTGCAAAGGCCAAAGAAGTGGGTGCCACTGAGT
GTGTCAACCCTCAGGACTACAAGAAACCCATCCAGGAGGTGCTGACAGAAATGAGCAATGGAGGTGTGGAT
TTTTCCTTTGAAGTCATTGGTCGGCTCGACACTATGGTGACTGCCTTGTCATGCTGTCAAGAAGCATATGGT
GTGAGCGTCATTGTGGGAGTACCTCCTGATTCCCAAAATCTCTCTATGAATCCTATGTTGCTACTGAGTGGA
CGTACCTGGAAAGGAGCTATTTTTGGCGGTTTTAAGAGTAAAGATTCTGTCCCCAAACTTGTGGCCGATTTTA
TGGCTAAAAAGTTTGCACTGGATCCTTTAATCACCCATGTTTTACCTTTTGAAAAAATAAATGAAGGATTTGAC
CTGCTTCGCTCTGGAGAGAGTATCCGTACCATCCTGACGTTTTGAGACCATACAAATGTCTGCACTTGTAGC
CGTCTTCTGGCTCCTCTATCCTCTGGATCATCAGCCAAACGACATCAATAATTCTGTTCCTCAAAGATGCTAT
TAATAGTTACCGCTGGGAGCTTTCTAAAAGAAACAAAAATTGATGTGAAGTCACTTTTCAAGCAAACGTTTAA
AATCCAAGTGAGAGCTAGAGGAACCATCAGCTGGGTAACTGAGCCCACTAAACTTTCCTTCTTAATCATTCT
CCTCACGTTGAATCCTGTCACCTTTCCCATTGAGGGAAGGCATGTGTTTTGACTTCTTGCATGATTTGTATCT
TGGGCACCCTTAGTATTGAAGCCGGGGGGTGGGGGGTCCTCATGATACTTGCCCCTCAGCATACACGTGATG
GGCTATTGTGCTCTAAGCCTTCTCCTTCTACATGCATTTCCACTGTCTGTATTTGCCTTTTGATGAAGGTAAC
AAGGTCGCACAGTAAAATACAGTCTGTGAAAAGATACTCTCGGATTTATAAGTGGAGAAGGTCTAGAACTTC
TAAATGCAGGGAATTTCTTAGGAAAATGTCATACATCTTTATAAGGTGGAGGGAAATGTCTTTATCGCTTTTAT
ACTGTTGGCAGTGTAA

GST-fusion-pIK10

1776 bp

ATGACCAAGTTACCTATACTAGGTTATTGGAAAATTAAGGGCCTTGTGCAACCCACTCGACTTCTTTTGGAAT
ATCTTGAAGAAAAATATGAAGAGCATTTGTATGAGCGCGATGAAGGTGATAAATGGCGAAACAAAAAGTTTG
AATTGGGTTTGGAGTTTCCCAATCTTCCTTATTATATTGATGGTGATGTTAAATTAACACAGTCTATGGCCATC
ATACGTTATATAGCTGACAAGCACAACATGTTGGGTGGTTGTCCAAAAGAGCGTGCAGAGATTTCAATGCTT
GAAGGAGCGGTTTTGGATATTAGATACGGTGTTTCGAGAATTGCATATAGTAAAGACTTTGAAACTCTCAAAG
TTGATTTTCTTAGCAAGCTACCTGAAATGCTGAAAATGTTCGAAGATCGTTTATGTCATAAAACATATTTAAAT
GGTGATCATGTAACCCATCCTGACTTCATGTTGTATGACGCTCTTGATGTTGTTTTACACATGGACCCAATGT
GCCTGGATGCGTTCCCAAAATTAGTTTGTTTTAAAAAACGTATTGAAGCTATCCCACAAATTGATAAGTACTT
GAAATCCAGCAAGTATATAGCATGGCCTTTGCAGGGCTGGCAAGCCACGTTTGGTGGTGGCGACCATCCTC
CAAAATCGGATCATCTGGTTCCGCGTCATATGATTGGGTCCGCGTCCGACTCATCTAGCAAGTTAGGACGC
CTCCGATTTCTTTCTGAAACTGCCGCTATTAAAGTATCCCCGTTAATCCTAGGAGAAGTCTCATACGATGGAG
CACGTTCGGATTTTCTCAAATCAATGAACAAGAATCGAGCTTTTGAATTGCTTGATACTTTTTACGAGGCAGG
TGGAAATTTCATTGATGCCGCAAACAACTGCCAAAACGAGCAATCAGAAGAATGGATTGGTGAATGGATACA
GTCCAGAAGGTTACGTGATCAAATTGTCATTGCAACCAAGTTTATAAAAAGCGATAAAAAGTATAAAGCAGGT
GAAAGTAACACTGCCAACTACTGTGGTAATCACAAGCGTAGTTTACATGTGAGTGTGAGGGATTCTCTCCGC
AAATTGCAAACTGATTGGATTGATATACTTTACGTTCACTGGTGGGATTATATGAGTTCAATCGAAGAATTTAT
GGATAGTTTGCATATTCTGGTCCAGCAGGGCAAGGTCCTCTATTTGGGTGTATCTGATACACCTGCTTGGGT

TGTTTCTGCGGCAAACTACTACGCTACATCTTATGGTAAAACTCCCTTTAGTATCTACCAAGGTAAATGGAAC
GTGTTGAACAGAGATTTTGAGCGTGATATTATTCCAATGGCTAGGCATTTCGGTATGGCCCTCGCCCCATGG
GATGTCATGGGAGGTGGAAGATTTCAGAGTAAAAAAGCAATGGAGGAACGGAGGAAGAATGGAGAGGGTAT
TCGTTCTTTCGTTGGCGCCTCCGAACAAACAGATGCAGAAATCAAGATTAGTGAAGCATTGGCCAAGATTGC
TGAGGAACATGGCACTGAGTCTGTTACTGCTATTGCTATTGCCTATGTTCGCTCTAAGGCGAAAAATTTTTTT
CCGTCGGTTGAAGGAGGAAAAATTGAGGATCTCAAAGAGAACATTAAGGCTCTCAGTATCGATCTAACGCCA
GACAATATAAAATACTTAGAAAGTATAGTTCCTTTTGACATCGGATTTCCTAATAATTTTATCGTGTTAAATTCC
TTGACTCAAAAATATGGTACGAATAATGTTTAG

GST-fusion-plK25 (Mut)

1767 bp

ATGACCAAGTTACCTATACTAGGTTATTGGAAAATTAAGGGCCTTGTGCAACCCACTCGACTTCTTTTGGAAT
ATCTTGAAGAAAAATATGAAGAGCATTTGTATGAGCGCGATGAAGGTGATAAATGGCGAAACAAAAAGTTTG
AATTGGGTTTGGAGTTTCCCAATCTTCCTTATTATATTGATGGTGATGTTAAATTAACACAGTCTATGGCCATC
ATACGTTATATAGCTGACAAGCACAACATGTTGGGTGGTTGTCCAAAAGAGCGTGCAGAGATTTCAATGCTT
GAAGGAGCGGTTTTGGATATTAGATACGGTGTTTCGAGAATTGCATATAGTAAAGACTTTGAAACTCTCAAAG
TTGATTTTCTTAGCAAGCTACCTGAAATGCTGAAAATGTTCGAAGATCGTTTATGTCATAAAACATATTTAAAT
GGTGATCATGTAACCCATCCTGACTTCATGTTGTATGACGCTCTTGATGTTGTTTTACACATGGACCCAATGT
GCCTGGATGCGTTCCCAAAATTAGTTTGTTTTAAAAAACGTATTGAAGCTATCCCACAAATTGATAAGTACTT
GAAATCCAGCAAGTATATAGCATGGCCTTTGCAGGGCTGGCAAGCCACGTTTGGTGGTGGCGACCATCCTC
CAAAATCGGATCATCTGGTTCCGCGTCATATGTCTTATCCTGAGAAATTTGAAGGTATCGCTATTCAATCACA
CGAAGATTGGAAAAACCCAAAGAAGACAAAGTATGACCCAAAACCATTTTACGATCATGACATTGACATTAAG
ATCGAAGCATGTGGTGTCTGCGGTAGTGATATTCATTGTGCAGCTGGTCATTGGGGCAATATGAAGATGCC
GCTAGTCGTTGGTCATGAAATCGTTGGTAAAGTTGTCAAGCTAGGGCCCAAGTCAAACAGTGGGTTGAAAGT
CGGTCAACGTGTTGGTGTAGGTGCTCAAGTCTTTTCATGCTTGGAATGTGACCGTTGTAAGAATGATAATGA
ACCATACTGCACCAAGTTTGTTACCACATACAGTCAGCCTTATGAAGACGGCTATGTGTCGCAGGGTGGCTA
TGCAAACTACGTCAGAGTTCATGAACATTTTGTGGTGCCTATCCCAGAGAATATTCCATCACATTTGGCTGCT
CCACTATTATGTGGTGGTTTGACTGTGTACTCTCCATTGGTTCGTAACGGTTGCGGTCCAGGTAAAAAAGTT
GGTATAGTTGGTCTTGGTGGTATCGGCAGTATGGGTACATTGATTTCCAAAGCCATGGGGGCAGAGACGTA
TGTTATTTCTCGTTCTTCGAGAAAAAGAGAAGATGCAATGAAGATGGGCGCCGATCACTACATTGCTACATTA
GAAGAAGGTGATTGGGGTGAAAAGTACTTTGACACCTTCGACCTGATTGTAGTCTGTGCTTCCTCCCTTACC
GACATTGACTTCAACATTATGCCAAAGGCTATGAAGGTTGGTGGTAGAATTGTCTCAATCTCTATACCAGAAC
AACACGAAATGTTATCGCTAAAGCCATATGGCTTAAAGGCTGTCTCCATTTCTTACAGTGCTTTAGGTTCCAT
CAAAGAATTGAACCAACTCTTGAAATTAGTCTCTGAAAAAGATATCAAAATTTGGGTGGAAACATTACCTGTT
GGTGAAGCCGGCGTCCATGAAGCCTTCGAAAGGATGGAAAAGGGTGACGTTAGATATAGATTTACCTTAGT
CGGCTACGACAAAGAATTTTCAGACTAG

GST-fusion-plK32 (Mut)

1770 bp

ATGACCAAGTTACCTATACTAGGTTATTGGAAAATTAAGGGCCTTGTGCAACCCACTCGACTTCTTTTGGAAT
ATCTTGAAGAAAAATATGAAGAGCATTTGTATGAGCGCGATGAAGGTGATAAATGGCGAAACAAAAAGTTTG
AATTGGGTTTGGAGTTTCCCAATCTTCCTTATTATATTGATGGTGATGTTAAATTAACACAGTCTATGGCCATC
ATACGTTATATAGCTGACAAGCACAACATGTTGGGTGGTTGTCCAAAAGAGCGTGCAGAGATTTCAATGCTT
GAAGGAGCGGTTTTGGATATTAGATACGGTGTTTCGAGAATTGCATATAGTAAAGACTTTGAAACTCTCAAAG
TTGATTTTCTTAGCAAGCTACCTGAAATGCTGAAAATGTTCGAAGATCGTTTATGTCATAAAACATATTTAAAT
GGTGATCATGTAACCCATCCTGACTTCATGTTGTATGACGCTCTTGATGTTGTTTTACACATGGACCCAATGT
GCCTGGATGCGTTCCCAAAATTAGTTTGTTTTAAAAAACGTATTGAAGCTATCCCACAAATTGATAAGTACTT
GAAATCCAGCAAGTATATAGCATGGCCTTTGCAGGGCTGGCAAGCCACGTTTGGTGGTGGCGACCATCCTC
CAAAATCGGATCATCTGGTTCCGCGTCATATGCTTTACCCAGAAAAATTTCAGGGCATCGGTATTTCCAACG
CAAAGGATTGGAAGCATCCTAAATTAGTGAGTTTTGACCCAAAACCCTTTGGCGATCATGACGTTGATGTTG
AAATTGAAGCCTGTGGTATCTGCGGATCTGATTTTCATATAGCCGTTGGTAATTGGGGTCCAGTCCCAGAAA
ATCAAATCCTTGGACATGAAATAATTGGCCGCGTGGTGAAGGTTGGATCCAAGTGCCACACTGGGGTAAAAA
TCGGTGACCGTGTTGGTGTTGGTGCCCAAGCCTTGGCGTGTTTTGAGTGTGAACGTTGCAAAAGTGACAAC
GAGCAATACTGTACCAATGACCACGTTTTGACTATGTGGACTCCTTACAAGGACGGCTACATTTCACAAGGA
GGCTTTGCCTCCCACGTGAGGCTTCATGAACACTTTGCTATTCAAATACCAGAAAATATTCCAAGTCCGCTA
GCCGCTCCATTATTGTGTGGTGGTATTACAGTTTTCTCTCCACTACTAAGAAATGGCTGTGGTCCAGGTAAG
AGGGTAGGTATTGTTGGCATCGGTGGTATTGGGCATATGGGGATTCTGTTGGCTAAAGCTATGGGAGCCGA
GGTTTATGCGTTTTCGCGAGGCCACTCCAAGCGGGAGGATTCTATGAAACTCGGTGCTGATCACTATATTGC
TATGTTGGAGGATAAAGGCTGGACAGAACAATACTCTAACGCTTTGGACCTTCTTGTCGTTTGCTCATCATCT
TTGTCGAAAGTTAATTTTGACAGTATCGTTAAGATTATGAAGATTGGAGGCTCCATCGTTTCAATTGCTGCTC
CTGAAGTTAATGAAAAGCTTGTTTTAAAACCGTTGGGCCTAATGGGAGTATCAATCTCAAGCAGTGCTATCG
GATCTAGGAAGGAAATCGAACAACTATTGAAATTAGTTTCCGAAAAGAATGTCAAAATATGGGTGGAAAAACT
TCCGATCAGCGAAGAAGGCGTCAGCCATGCCTTTACAAGGATGGAAAGCGGAGACGTCAAATACAGATTTA
CTTTGGTCGATTATGATAAGAAATTCCATAAATAG

SDR-B6

750 bp

ATGACCTCCACCCCAGCTATCTCCCGCCGCGCCGCGCTCGTCACCGGCGCCTCCCGCGGCATCGGCCGC
GCCATCGCACTGCGGCTGGCCGCCGACGGCTTCGACGTGGCCATTGGCTACGCCGGCAGCGCCGCCCGG
GCCGAAGAGACGGTGGCGGCGGCGCGCGAGGCCGGCAGCAATGCCATCGCCATCCAGGGCGATGTGGC
GCAGGCGCCAGACGTGGCACGCCTGTTCGACACCGCGCAGCAGGCCTTCGGCCGGCTCGACGTGGTCGT
CAACAGCGCCGGCATCATGCAGATGGCGTCGGTCGCGCCCGCCAGCCTAGACGCCTTCGACCAGACCATC
GCCACCAACCTGCGCGGCGCTTTCCTGGTGCTGGGCGAGGCCGCCGCACGGCTGGGCCAGGGCGGACG
CATCATCGCGCTGTCGACCAGCGTGATCGCGCGTTCCTTGCCCGGTTACGGTCCCTATATCGCGGCCAAGG
CAGGCGTGGAAGGGCTGGTGCGGGTCCTGGCCAACGAGCTGCGCGGGCGCGGCATCACCGCCAACGCG
GTGGCGCCGGGGCCGGTCGCGACCGAGCTGTTCCTCGATGGCAAATCGGAAGAGCAGGTGGCGCAGCTG
TCCAAAGTGGCGCCGCTGGAGCGGCTGGGCACGCCCGAGGACATTGCCGCGGCAGTGTCGTTCCTGGCC
GGGCCGGATGGGGCGTGGATCAATGCGCAGGTGGTGCGGGTGAACGGGGGCTTTGCCTGA

SDR-B3

765 bp

ATGGGACGTTTGTCTGGAAAAGTTGCCATCATTACCGGCGCCAGTGCCGGCATTGGCCGCGCCACCGCATT
GCTGTTTGCCGCCGAGGGCGCCAGGGTGGTAGTCGGTGCCCGCCGCCAGTCCGAACTGGACAGCCTGGT
GGCGCAGATCCGTGACGCCGGCGGCGACGCGGTGGCGCTCGCCGGCGATGTGCGGCGCGAGGAATACG
CCAGCGCGCTGGTGGCGCTGGCGGTCGAGCGCTATGGCCGCCTGGATATCGCCTTCAACAACGCCGGCA
CGCTCGGCGAGGGCGGGCCCAGCACCGGGGTTTCGGCAGACGGCTGGAACGACACCCTTGCCATCAATC
TCACCGGCGCATTCCTCGGCGCCAAGCACCAGCTTGCACAGATGCTGAAGGATGGCGGCGGTTCGGTGAT

CTTCACCTCGACCTTCGTTGGCTACACCGTCGCCTTTCCCGGCGTGGCCGCGTATGCGGCAAGCAAGTCCG
GCCTGATCGGCCTGACGCAGGCGCTGGCGGCCGAGTATGGGCCGCAGGGCATCCGCGTCAATGCGATCC
TGCCGGGCGCCGTGGACACGGACATGTATCGCACCATGAACGACACCGCGGAATCACAGGCGTTCATCAC
CAACCTGCATGCGCTCAAGCGCGTGGCCACGCCGGAAGAACTGGCGCGCTCGGTGCTGTACCTGGCATCG
GACGATTCGGCTTTCGTCACCGGCACGGCATCGCTGGTGGATGGCGGCGTCTCGATCACGCGCACCTGA

6-His-SDR-B3

807 bp

ATGTCGTACTACCATCACCATCACCATCACGATTACGACCATATGGGACGTTTGTCTGGAAAAGTTGCCATC
ATTACCGGCGCCAGTGCCGGCATTGGCCGCGCCACCGCATTGCTGTTTGCCGCCGAGGGCGCCAGGGTG
GTAGTCGGTGCCCGCCGCCAGTCCGAACTGGACAGCCTGGTGGCGCAGATCCGTGACGCCGGCGGCGAC
GCGGTGGCGCTCGCCGGCGATGTGCGGCGCGAGGAATACGCCAGCGCGCTGGTGGCGCTGGCGGTCGA
GCGCTATGGCCGCCTGGATATCGCCTTCAACAACGCCGGCACGCTCGGCGAGGGCGGGCCCAGCACCGG
GGTTTCGGCAGACGGCTGGAACGACACCCTTGCCATCAATCTCACCGGCGCATTCCTCGGCGCCAAGCAC
CAGCTTGCACAGATGCTGAAGGATGGCGGCGGTTCGGTGATCTTCACCTCGACCTTCGTTGGCTACACCGT
CGCCTTTCCCGGCGTGGCCGCGTATGCGGCAAGCAAGTCCGGCCTGATCGGCCTGACGCAGGCGCTGGC
GGCCGAGTATGGGCCGCAGGGCATCCGCGTCAATGCGATCCTGCCGGGCGCCGTGGACACGGACATGTA
TCGCACCATGAACGACACCGCGGAATCACAGGCGTTCATCACCAACCTGCATGCGCTCAAGCGCGTGGCC
ACGCCGGAAGAACTGGCGCGCTCGGTGCTGTACCTGGCATCGGACGATTCGGCTTTCGTCACCGGCACGG
CATCGCTGGTGGATGGCGGCGTCTCGATCACGCGCACCTGA

6-His-PDH_loopN

786 bp

ATGCATCATCATCATCATCATACCTCAACTGCTCAGATGCCCCACATCCTTGACCTCTTTCGTCTCGACGGAC
GCCACGCCCTGGTGACTGGCGGCGCGCAGGGGATCGGCTTCGAGATCGCGCGCGGACTGGCCCAGGCTG
GAGCGCGCGTGACCATCGCGAACCTGAACCCCGACGTGGGGGAGGGTGCGGCCCGCGAATTGGACGGGA
CCTTCGAGCGACTGAACGTCACCGACGCGGACGCCGTGGCGGACCTGGCCCGGCGCCTCCCCGATGTGG
ACGTGCTTGTGAACAACGCGGGAATTGTCCGCAACGCTCCCGCCGAGGACACCCCCGATGACGACTGGCG
GGCGGTGCTGAGCGTCAACCTGGACGGGGTGTTCTGGTGCTGCCGCGAGTTCGGCCGAACCATGCTGGCT
AGAGGCCGCGGCGCCATCGTCAGCACCGCCAGCATGAGCGGCCTGATCAGCAATCATCCGCAGCCGCAG
GCCGCCTACAACGCCTCCAAGGCCGCGGTCATTCACCTCACCCGCAGCCTCGCGGGCGAGTGGGCGAGC
CGGGGCGTGCGCGTGAACGCCGTCGCTCCCGGCTACACCGCTACAGAGATGACCCTGAAGATGCGGGAG
AGGCCCGAGTGGCGCGAAACCTGGCTGAAGGAAACGCCGCTGGGCCGCCTCGCCGAACCCCGCGAGATT
GCGCCCGCCGTGCTCTACCTCGCCAGCGACGCCGCCAGCTTCGTCACCGGGCATACGCTCGTGGTGGAC
GGTGGGTACACGGTGTGGTGA

ChnD-6-His

1092 bp

ATGCATTGTTACTGTGTGACCCATCATGGTCAGCCGCTGGAAGATGTTGAAAAAGAAATTCCGCAGCCGAAA
GGCACCGAAGTGCTGCTGCATGTTAAAGCAGCAGGTCTGTGCCATACCGATCTGCATCTGTGGGAAGGTTA
TTATGATCTGGGCGGCGGTAAACGTCTGAGCCTGGCAGATCGTGGCCTGAAACCGCCGCTGACCCTGAGT
CATGAAATTACCGGCCAGGTGGTTGCCGTTGGCCCGGATGCCGAAAGCGTGAAAGTTGGCATGGTGAGCC
TGGTGCATCCGTGGATTGGCTGTGGTGAATGCAATTATTGTAAACGCGGCGAAGAAAATCTGTGCGCAAAA
CCGCAGCAGCTGGGTATTGCAAAACCGGGTGGCTTCGCAGAATATATTATTGTTCCGCATCCGCGCTATCT
GGTGGATATTGCCGGTCTGGATCTGGCAGAAGCCGCACCGCTGGCCTGTGCAGGCGTGACAACCTATAGT
GCACTGAAAAAATTCGGCGATCTGATTCAGAGCGAACCGGTTGTGATTATTGGCGCCGGTGGCCTGGGCCT
GATGGCATTAGAACTGCTGAAAGCAATGCAGGCAAAAGGCGCAATTGTTGTTGATATTGATGATAGCAAACT
GGAAGCAGCCCGTGCAGCCGGTGCCCTGAGTGTGATTAATAGTCGCAGCGAAGATGCAGCCCAGCAGCTG
ATTCAGGCAACCGATGGTGGTGCCCGCCTGATTCTGGATCTGGTTGGTAGCAATCCGACCCTGAGTCTGGC
CCTGGCCAGCGCAGCCCGTGGTGGTCATATTGTGATCTGTGGTCTGATGGGCGGTGAAATTAAACTGAGTA
TTCCGGTTATTCCGATGCGCCCGCTGACCATTCAGGGTAGCTATGTTGGTACCGTTGAAGAACTGCGCGAA
CTGGTTGAACTGGTGAAAGAAACACATATGAGTGCAATTCCGGTTAAAAAACTGCCGATTAGCCAGATTAAT
AGCGCCTTCGGTGATCTGAAAGATGGTAATGTTATTGGCCGTATTGTGCTGATGCATGAAAATGCGGCCGCA
CTCGAGCACCACCACCACCACCACTGA

F. References

F.1. Cited Literature

1 Greg Hughes, J. C. L. Introduction: Biocatalysis in Industry. *Chem. Rev.* **118**, 1-3 (2018). https://doi.org:10.1021/acs.chemrev.7b00741
2 Bornscheuer, U. & Buchholz, K. Highlights in Biocatalysis - Historical Landmarks and Current Trends. *Eng. Life Sci.* **5**, 309-323 (2005). https://doi.org:10.1002/elsc.200520089
3 J. B. Sumner, K. M. *The Enzymes,* Vol. 1. *Academic Press, NY* (1950).
4 Bornscheuer, U. T. *et al.* Engineering the third wave of biocatalysis. *Nature* **485**, 185-194 (2012). https://doi.org:10.1038/nature11117
5 Bornscheuer, U. T. *et al.* Engineering the third wave of biocatalysis.
6 Pyser, J. B., Chakrabarty, S., Romero, E. O. & Narayan, A. R. H. State-of-the-Art Biocatalysis. *ACS Cent. Sci.* **7**, 1105-1116 (2021). https://doi.org:10.1021/acscentsci.1c00273
7 Abdelraheem, E. M. M., Busch, H., Hanefeld, U. & Tonin, F. Biocatalysis explained: from pharmaceutical to bulk chemical production. *Reaction Chemistry & Engineering* **4**, 1878-1894 (2019). https://doi.org:10.1039/C9RE00301K
8 Sheldon, R. A., Brady, D. & Bode, M. L. The Hitchhiker's guide to biocatalysis: recent advances in the use of enzymes in organic synthesis. *Chem. Sci.* **11**, 2587-2605 (2020). https://doi.org:10.1039/C9SC05746C
9 Bell, E. L. *et al.* Biocatalysis. *Nat. Rev. Methods Primers* **1**, 46 (2021). https://doi.org:10.1038/s43586-021-00044-z
10 Bornscheuer, U. T. The fourth wave of biocatalysis is approaching. *Philos. Trans. R. Soc., A* **376**, 20170063 (2017). https://doi.org:10.1098/rsta.2017.0063
11 Rosano, G. L. & Ceccarelli, E. A. Recombinant protein expression in microbial systems. *Front. Microbiol.* **5** (2014). https://doi.org:10.3389/fmicb.2014.00341
12 Morrow, J. F. *et al.* Replication and Transcription of Eukaryotic DNA in Esherichia coli. *Proc. Natl. Acad. Sci. U. S. A.* **71**, 1743-1747 (1974). https://doi.org:10.1073/pnas.71.5.1743
13 Ratzkin, B. & Carbon, J. Functional expression of cloned yeast DNA in Escherichia coli. *Proc. Natl. Acad. Sci. U. S. A.* **74**, 487-491 (1977). https://doi.org:10.1073/pnas.74.2.487
14 Sezonov, G., Joseleau-Petit, D. & D'Ari, R. Escherichia coli Physiology in Luria-Bertani Broth. *J. Bacteriol.* **189**, 8746-8749 (2007). https://doi.org:10.1128/JB.01368-07
15 Pope, B. & Kent, H. M. High Efficiency 5 Min Transformation of Escherichia Coli. *Nucleic Acids Res.* **24**, 536-537 (1996). https://doi.org:10.1093/nar/24.3.536
16 Rosano, G. L. & Ceccarelli, E. A. Recombinant protein expression in Escherichia coli: advances and challenges. *Front. Microbiol.* **5**, 172 (2014). https://doi.org:10.3389/fmicb.2014.00172
17 Bentley, W. E., Mirjalili, N., Andersen, D. C., Davis, R. H. & Kompala, D. S. Plasmid-encoded protein: The principal factor in the "metabolic burden" associated with recombinant bacteria. *Biotechnol. Bioeng.* **35**, 668-681 (1990). https://doi.org:https://doi.org/10.1002/bit.260350704
18 Del Solar, G. & Espinosa, M. Plasmid copy number control: an ever-growing story. *Mol. Microbiol.* **37**, 492-500 (2000). https://doi.org:https://doi.org/10.1046/j.1365-2958.2000.02005.x
19 Bolivar, F. *et al.* Construction and characterization of new cloning vehicle. II. A multipurpose cloning system. *Gene* **2**, 95-113 (1977). https://doi.org:https://doi.org/10.1016/0378-1119(77)90000-2
20 Minton, N. P. Improved plasmid vectors for the isolation of translational lac gene fusions. *Gene* **31**, 269-273 (1984). https://doi.org:https://doi.org/10.1016/0378-1119(84)90220-8
21 Baneyx, F. Recombinant protein expression in Escherichia coli. *Curr. Opin. Biotechnol.* **10**, 411-421 (1999). https://doi.org:https://doi.org/10.1016/S0958-1669(99)00003-8
22 Bayer, T., Milker, S., Wiesinger, T., Rudroff, F. & Mihovilovic, M. D. Designer Microorganisms for Optimized Redox Cascade Reactions – Challenges and Future Perspectives. *Adv. Synth. Catal.* **357**, 1587-1618 (2015). https://doi.org:https://doi.org/10.1002/adsc.201500202
23 Goldstein, M. A. & Doi, R. H. in *Biotechnol. Ann. Rev.* Vol. 1 (ed M. Raafat El-Gewely) 105-128 (Elsevier, 1995).
24 Müller-Hill, B. *The lac Operon*. (De Gruyter, 1996).
25 Studier, F. W. & Moffatt, B. A. Use of bacteriophage T7 RNA polymerase to direct selective high-level expression of cloned genes. *J. Mol. Biol.* **189**, 113-130 (1986). https://doi.org:https://doi.org/10.1016/0022-2836(86)90385-2
26 Goldstein, D. A. *et al.* Human safety and genetically modified plants: a review of antibiotic resistance markers and future transformation selection technologies. *J. Appl. Microbiol.* **99**, 7-23 (2005). https://doi.org:10.1111/j.1365-2672.2005.02595.x
27 Shaw, W. V. Chloramphenicol Acetyltransferase: Enzymology and Molecular Biology. *Crit. Rev. Biochem.* **14**, 1-46 (1983). https://doi.org:10.3109/10409238309102789
28 Roberts, M. C. Tetracycline resistance determinants: mechanisms of action, regulation of expression, genetic mobility, and distribution. *FEMS Microbiol. Rev.* **19**, 1-24 (1996). https://doi.org:10.1111/j.1574-6976.1996.tb00251.x
29 Peubez, I. *et al.* Antibiotic-free selection in E. coli: new considerations for optimal design and improved production. *Microb. Cell Fact.* **9**, 65 (2010). https://doi.org:10.1186/1475-2859-9-65
30 Nilsson, J., Ståhl S Fau - Lundeberg, J., Lundeberg J Fau - Uhlén, M., Uhlén M Fau - Nygren, P. A. & Nygren, P. A. Affinity fusion strategies for detection, purification, and immobilization of recombinant proteins. *Protein Expression Purif.* **11**, 1-16 (1997). https://doi.org:https://doi.org/10.1006/prep.1997.0767

31 Daegelen, P., Studier, F. W., Lenski, R. E., Cure, S. & Kim, J. F. Tracing Ancestors and Relatives of Escherichia coli B, and the Derivation of B Strains REL606 and BL21(DE3). *J. Mol. Biol.* **394**, 634-643 (2009). https://doi.org:https://doi.org/10.1016/j.jmb.2009.09.022

32 Gottesman, S. PROTEASES AND THEIR TARGETS IN ESCHERICHIA COLI. *Annu. Rev. Genet.* **30**, 465-506 (1996). https://doi.org:10.1146/annurev.genet.30.1.465

33 Torres Pazmiño, D. E., Dudek, H. M. & Fraaije, M. W. Baeyer–Villiger monooxygenases: recent advances and future challenges. *Curr. Opin. Chem. Biol.* **14**, 138-144 (2010). https://doi.org:https://doi.org/10.1016/j.cbpa.2009.11.017

34 de Gonzalo, G., Mihovilovic, M. D. & Fraaije, M. W. Recent Developments in the Application of Baeyer–Villiger Monooxygenases as Biocatalysts. *ChemBioChem* **11**, 2208-2231 (2010). https://doi.org:https://doi.org/10.1002/cbic.201000395

35 Fraaije, M. W. *et al.* Discovery of a thermostable Baeyer-Villiger monooxygenase by genome mining. *Appl. Microbiol. Biotechnol.* **66**, 393-400 (2005). https://doi.org:10.1007/s00253-004-1749-5

36 de Gonzalo, G. & Alcántara, A. R. Multienzymatic Processes Involving Baeyer–Villiger Monooxygenases. *Catalysts* **11** (2021).

37 Fürst, M. J. L. J., Gran-Scheuch, A., Aalbers, F. S. & Fraaije, M. W. Baeyer–Villiger Monooxygenases: Tunable Oxidative Biocatalysts. *ACS Catal.* **9**, 11207-11241 (2019). https://doi.org:10.1021/acscatal.9b03396

38 Snowden, M., Bermudez, A., Kelly, D. R. & Radkiewicz-Poutsma, J. L. The Preference for Anti over Gauche Migration in the Baeyer–Villiger Reaction. *J. Org. Chem.* **69**, 7148-7156 (2004). https://doi.org:10.1021/jo0491307

39 Goodman, R. M. & Kishi, Y. Experimental Support for the Primary Stereoelectronic Effect Governing Baeyer–Villiger Oxidation and Criegee Rearrangement. *J. Am. Chem. Soc.* **120**, 9392-9393 (1998). https://doi.org:10.1021/ja982188g

40 Li, G. *et al.* Overriding Traditional Electronic Effects in Biocatalytic Baeyer–Villiger Reactions by Directed Evolution. *J. Am. Chem. Soc.* **140**, 10464-10472 (2018). https://doi.org:10.1021/jacs.8b04742

41 Romano, D. *et al.* Esterases as stereoselective biocatalysts. *Biotechnol. Adv.* **33**, 547-565 (2015). https://doi.org:https://doi.org/10.1016/j.biotechadv.2015.01.006

42 Pleiss, J., Fischer, M. & Schmid, R. D. Anatomy of lipase binding sites: the scissile fatty acid binding site. *Chem. Phys. Lipids* **93**, 67-80 (1998). https://doi.org:https://doi.org/10.1016/S0009-3084(98)00030-9

43 Jones, J. B. Esterases in organic synthesis: present and future. *Pure Appl. Chem.* **62**, 1445-1448 (1990). https://doi.org:doi:10.1351/pac199062071445

44 Kazlauskas, R. J., Weissfloch, A. N. E., Rappaport, A. T. & Cuccia, L. A. A rule to predict which enantiomer of a secondary alcohol reacts faster in reactions catalyzed by cholesterol esterase, lipase from Pseudomonas cepacia, and lipase from Candida rugosa. *J. Org. Chem.* **56**, 2656-2665 (1991). https://doi.org:10.1021/jo00008a016

45 Rauwerdink, A. & Kazlauskas, R. J. How the Same Core Catalytic Machinery Catalyzes 17 Different Reactions: the Serine-Histidine-Aspartate Catalytic Triad of α/β-Hydrolase Fold Enzymes. *ACS Catal.* **5**, 6153-6176 (2015). https://doi.org:10.1021/acscatal.5b01539

46 Reid, M. F. & Fewson, C. A. Molecular Characterization of Microbial Alcohol Dehydrogenases. *Crit. Rev. Microbiol.* **20**, 13-56 (1994). https://doi.org:10.3109/10408419409113545

47 Kroutil, W., Mang, H., Edegger, K. & Faber, K. Biocatalytic Oxidation of Primary and Secondary Alcohols. *Adv. Synth. Catal.* **346**, 125-142 (2004). https://doi.org:10.1002/adsc.200303177

48 de Miranda, A. S., Milagre, C. D. F. & Hollmann, F. Alcohol Dehydrogenases as Catalysts in Organic Synthesis. *Front. Catal* **2** (2022).

49 Keinan, E., Hafeli, E. K., Seth, K. K. & Lamed, R. Thermostable enzymes in organic synthesis. 2. Asymmetric reduction of ketones with alcohol dehydrogenase from Thermoanaerobium brockii. *J. Am. Chem. Soc.* **108**, 162-169 (1986). https://doi.org:10.1021/ja00261a026

50 Pham, V. T. & Phillips, R. S. Effects of substrate structure and temperature on the stereospecificity of secondary alcohol dehydrogenase from Thermoanaerobacter ethanolicus. *J. Am. Chem. Soc.* **112**, 3629-3632 (1990). https://doi.org:10.1021/ja00165a057

51 Muschiol, J. *et al.* Cascade catalysis – strategies and challenges en route to preparative synthetic biology. *Chem. Commun.* **51**, 5798-5811 (2015). https://doi.org:10.1039/C4CC08752F

52 Schrittwieser, J. H., Velikogne, S., Hall, M. & Kroutil, W. Artificial Biocatalytic Linear Cascades for Preparation of Organic Molecules. *Chem. Rev.* **118**, 270-348 (2018). https://doi.org:10.1021/acs.chemrev.7b00033

53 Schmidt-Dannert, C. & Lopez-Gallego, F. A roadmap for biocatalysis – functional and spatial orchestration of enzyme cascades. *Microb. Biotechnol.* **9**, 601-609 (2016). https://doi.org:https://doi.org/10.1111/1751-7915.12386

54 de Carvalho, C. C. Whole cell biocatalysts: essential workers from Nature to the industry. (2016).

55 Lin, B. & Tao, Y. Whole-cell biocatalysts by design. *Microb. Cell Fact.* **16**, 106 (2017). https://doi.org:10.1186/s12934-017-0724-7

56 Lopez-Gallego, F. & Schmidt-Dannert, C. Multi-enzymatic synthesis. *Curr. Opin. Chem. Biol.* **14**, 174-183 (2010). https://doi.org:https://doi.org/10.1016/j.cbpa.2009.11.023

57 Kosjek, B. *et al.* Purification and characterization of a chemotolerant alcohol dehydrogenase applicable to coupled redox reactions. *Biotechnol. Bioeng.* **86**, 55-62 (2004). https://doi.org:10.1002/bit.20004

58 Sperl, J. M. & Sieber, V. Multienzyme Cascade Reactions—Status and Recent Advances. *ACS Catal.* **8**, 2385-2396 (2018). https://doi.org:10.1021/acscatal.7b03440

59 Staudt, S., Bornscheuer, U. T., Menyes, U., Hummel, W. & Groger, H. Direct biocatalytic one-pot-transformation of

cyclohexanol with molecular oxygen into varepsilon-caprolactone. *Enzyme Microb. Technol.* **53**, 288-292 (2013). https://doi.org:10.1016/j.enzmictec.2013.03.011
60 Rudroff, F. Whole-cell based synthetic enzyme cascades-light and shadow of a promising technology. *Curr. Opin. Chem. Biol.* **49**, 84-90 (2019). https://doi.org:10.1016/j.cbpa.2018.10.016
61 Schmidt, S. *et al.* An enzyme cascade synthesis of epsilon-caprolactone and its oligomers. *Angew. Chem. Int. Ed. Engl.* **54**, 2784-2787 (2015). https://doi.org:10.1002/anie.201410633
62 Hummel, W. & Groger, H. Strategies for regeneration of nicotinamide coenzymes emphasizing self-sufficient closed-loop recycling systems. *J. Biotechnol.* **191**, 22-31 (2014). https://doi.org:10.1016/j.jbiotec.2014.07.449
63 Huang, L. *et al.* Convergent Cascade Catalyzed by Monooxygenase-Alcohol Dehydrogenase Fusion Applied in Organic Media. *ChemBioChem* **20**, 1653-1658 (2019). https://doi.org:10.1002/cbic.201800814
64 Huang, L. *et al.* Nicotinamide Adenine Dinucleotide-Dependent Redox-Neutral Convergent Cascade for Lactonizations with Type II Flavin-Containing Monooxygenase. *Adv. Synth. Catal.* **359**, 2142-2148 (2017). https://doi.org:10.1002/adsc.201700401
65 Olson, L. P., Luo, J., Almarsson, Ö. & Bruice, T. C. Mechanism of Aldehyde Oxidation Catalyzed by Horse Liver Alcohol Dehydrogenase. *Biochem* **35**, 9782-9791 (1996). https://doi.org:10.1021/bi952020x
66 Bayer, T. *et al.* In Vivo Synthesis of Polyhydroxylated Compounds from a "Hidden Reservoir" of Toxic Aldehyde Species. *ChemCatChem* **9**, 2919-2923 (2017). https://doi.org:https://doi.org/10.1002/cctc.201700469
67 Suchy, L. *Enzymatic cascades in Escherichia Coli based on the equilibration of reactive Aldehyde intermediates*, (2021).
68 Krebsfänger, N., Zocher, F., Altenbuchner, J. & Bornscheuer, U. T. Characterization and enantioselectivity of a recombinant esterase from Pseudomonas fluorescens. *Enzyme Microb. Technol.* **22**, 641-646 (1998). https://doi.org:https://doi.org/10.1016/S0141-0229(98)00004-0
69 Theorell, H. & McKinley McKee, J. S. Mechanism of Action of Liver Alcohol Dehydrogenase. *Nature* **192**, 47-50 (1961). https://doi.org:10.1038/192047a0
70 Delneri, D., Gardner, D. C. J. & Oliver, S. G. Analysis of the Seven-Member AAD Gene Set Demonstrates That Genetic Redundancy in Yeast May Be More Apparent Than Real. *Genetics* **153**, 1591-1600 (1999). https://doi.org:10.1093/genetics/153.4.1591
71 LARROY, C., FERNÁNDEZ, M. R., GONZÁLEZ, E., PARÉS, X. & BIOSCA, J. A. Characterization of the Saccharomyces cerevisiae YMR318C (ADH6) gene product as a broad specificity NADPH-dependent alcohol dehydrogenase: relevance in aldehyde reduction. *Biochem. J.* **361**, 163-172 (2001). https://doi.org:10.1042/bj3610163
72 Larroy, C., Pares, X. & Biosca, J. A. Characterization of a Saccharomyces cerevisiae NADP(H)-dependent alcohol dehydrogenase (ADHVII), a member of the cinnamyl alcohol dehydrogenase family. *Eur. J. Biochem.* **269**, 5738-5745 (2002). https://doi.org:10.1046/j.1432-1033.2002.03296.x
73 Pohlmann, A. *et al.* Genome sequence of the bioplastic-producing "Knallgas" bacterium Ralstonia eutropha H16. *Nat. Biotechnol.* **24**, 1257-1262 (2006). https://doi.org:10.1038/nbt1244
74 Wulf, H., Mallin, H. & Bornscheuer, U. T. Protein engineering of a thermostable polyol dehydrogenase. *Enzyme Microb. Technol.* **51**, 217-224 (2012). https://doi.org:https://doi.org/10.1016/j.enzmictec.2012.06.006
75 Cheng, Q., Thomas Stuart, M., Kostichka, K., Valentine James, R. & Nagarajan, V. Genetic Analysis of a Gene Cluster for Cyclohexanol Oxidation in Acinetobacter sp. Strain SE19 by In Vitro Transposition. *J. Bacteriol.* **182**, 4744-4751 (2000). https://doi.org:10.1128/JB.182.17.4744-4751.2000
76 Huang, L., Bittner, J. P., Domínguez de María, P., Jakobtorweihen, S. & Kara, S. Modeling Alcohol Dehydrogenase Catalysis in Deep Eutectic Solvent/Water Mixtures. *ChemBioChem* **21**, 817 (2020). https://doi.org:10.1002/cbic.201900624
77 Ramaswamy, S., Eklund, H. & Plapp, B. V. Structures of Horse Liver Alcohol Dehydrogenase Complexed with NAD+ and Substituted Benzyl Alcohols. *Biochem* **33**, 5230-5237 (1994). https://doi.org:10.1021/bi00183a028
78 Orski-Ritchie, D. T. Q.-R. D. T. *Evaluation of an enzyme library of reductases for application in bioactive compound synthesis*, Wien, Techn. Univ., Diss., 2009, (2009).
79 Magomedova, Z. *Homologous and heterologous expression of oxidoreductases of R. eutropha H1*, (2015).
80 Magomedova, Z., Grecu, A., Sensen, C. W., Schwab, H. & Heidinger, P. Characterization of two novel alcohol short-chain dehydrogenases/reductases from Ralstonia eutropha H16 capable of stereoselective conversion of bulky substrates. *J. Biotechnol.* **221**, 78-90 (2016). https://doi.org:10.1016/j.jbiotec.2016.01.030
81 Wu, S., Zhou, Y., Gerngross, D., Jeschek, M. & Ward, T. R. Chemo-enzymatic cascades to produce cycloalkenes from bio-based resources. *Nat Commun* **10**, 5060 (2019). https://doi.org:10.1038/s41467-019-13071-y
82 Cha, H.-J. *et al.* Simultaneous Enzyme/Whole-Cell Biotransformation of C18 Ricinoleic Acid into (R)-3-Hydroxynonanoic Acid, 9-Hydroxynonanoic Acid, and 1,9-Nonanedioic Acid. *Adv. Synth. Catal.* **360**, 696-703 (2018). https://doi.org:10.1002/adsc.201701029
83 Schubert, T., Hummel, W. & Müller, M. Highly Enantioselective Preparation of Multifunctionalized Propargylic Building Blocks. *Angew. Chem.* **114**, 656-659 (2002). https://doi.org:10.1002/1521-3757(20020215)114:4<656::Aid-ange656>3.0.Co;2-z
84 Daniel, E. T. P. Kinetic Mechanism of Phenylacetone Monooxygenase from Thermobifida fusca. *Biochem* **47**, 4093 (2008). https://doi.org:10.1021/bi702296k
info:doi/10.1021/bi702296k
85 Cheeseman, J. D., Tocilj, A., Park, S., Schrag, J. D. & Kazlauskas, R. J. Structure of an aryl esterase from Pseudomonas fluorescens. *Acta Crystallogr. D* **60**, 1237-1243 (2004). https://doi.org:doi:10.1107/S0907444904010522
86 Giparakis, S. *Development of novel chemoenzymatic one-pot reactions for the synthesis of fragrance aldehydes*, Wien, (2022).

87 González-Martínez, D., Gotor, V. & Gotor-Fernández, V. Stereoselective Synthesis of 1-Arylpropan-2-amines from Allylbenzenes through a Wacker-Tsuji Oxidation-Biotransamination Sequential Process. *Adv. Synth. Catal.* (2019). https://doi.org:10.1002/adsc.201900179

88 Rodney A. Fernandes, G. V. R., Venkati Bethi. MnO2 as a terminal oxidant in Wacker oxidation of homoallyl alcohols and terminal olefins. *Org. Biomol. Chem.* **18** (2020). https://doi.org:10.1039/d0ob01344g

89 Gierer, J., Petterson, I. & Smedman, L.-A. The Reactions of Lignin During Sulphate Pulping. Part XII. Reactions of Intermediary o,p'-Dihydroxy-stilbene Structures. *Acta Chem. Scand.* **26** (1972). https://doi.org:10.3891/acta.chem.scand.26-3366